UCLouvain

epl

École polytechnique de Louvain

Modelling active distribution grids in power systems frequency stability studies

Author: **Christophe Rogiest**
Supervisors: **Emmanuel de Jaeger, Cyril Cousein**
Readers: **Emmanuel de Jaeger, Cyril Cousein, Bruno Dehez**
Academic year 2021–2022
Master [120] in Electrical Engineering

Contents

Abstract

Due to the urgency of the energy transition, a lot of changes are made on the grid. The main goal is to keep stable and reliable energy provisioning while reducing its carbon footprint. While renewable generators like PV panels are more and more connected to the grid, the stability of the latter is impacted. In order to improve that stability, battery energy storage system (BESS) are connected onto the grid. The objective of this work is to propose a simplified model which has the same behavior in case of frequency deviations, than a real grid with active components.

First, the BESS and its connection to the grid as well as its control will be explained. Then, an equivalent model of a distribution grid with active components (PV panel and BESS) is designed, using the Monte-Carlo methodology on a "grey box" approach.

The main elements leading to the equivalent model will be analysed and described. Among others, a partial tripping is added to the equivalent active components in order to react to the variance of tolerance to frequency deviation of the different active components present on the distribution grid. Analysis demonstrates that the best calculation error in the methodology corresponds to the mean of the absolute value. It is also shown that the parameters with a small influence on the power response as well as the ones for which the initial value is fairly accurate can be discarded from the methodology, in order to decrease the computation time by approx. 38 %. It's also noticed that the voltage stays inside acceptable range even if some powers are exchanged between active components and the grid, so there is no need to control it. Finally, the suggested equivalent model continues to work well against more complex distribution grids and associated models as well as with load's dependency to frequency.

As a result of this work, we obtain a methodology that can design the equivalent model to active distribution grids, so that they all have the same reaction to frequency issues.

Acknowledgements

I wish to thank my family and my friends for their support and advises. Thanks also to my father that helped me in the structure and in the writing of my thesis.

I wish also to thank my professor Emmanuel de Jaeger who supported me and guided me throughout this work, as a professor but also as a supervisor. Finally, I thank the assistant supervisor Cyril Cousein for his availability, advises, feedbacks and help with the software. He was a crucial support in the progress of this master thesis.

Introduction

Today, the importance of the energy transition has become a fact for everyone. However, this is a very complex and long objective, and a lot of challenges must be resolved. One of the most important ones is to keep the energy system stable and reliable for everyone, while reducing the carbon footprint of the energy system, by reducing the amount of CO_2 emitting generators. The solution requires to use renewable generators like wind turbines, dams, PV panels, etc.

In Belgium and globally in Europe, the renewable energy that has been developed the most is the one associated to the PV panels [1], thanks to the decrease of their price during the last few years. Moreover, PV panels are distributed all around the grid, since we can have many of them on simple houses and public buildings. Therefore, this work will be focused on PV panels as renewable source.

PV panels can perform well, but they depend on external parameters, like the weather, the time of day, the location, etc. Such dependency makes their energy production very fluctuating and quite hard to anticipate [2]. This variable energy may cause some problems of stability on the grid, therefore appropriate measures need to be taken to guarantee the stability and security of the grid [3].

One way to improve the grid stability is to keep synchronous generators connected to the grid, because they are controllable and can provide inertia, which is the ability of a generator to modify its operation point in case of variation on the grid [4] [5]. However, most of those generators are non-renewable, so keeping them operational is not realistic considering the energy transition. Another way to improve the stability of the grid is to use battery energy storage systems (BESS) that will react to disturbances in the grid. An additional advantage of these systems is that they can charge at times when there is excess power and discharge at times of power deficit, improving the adequacy of the power grid. The main problem with batteries is that they are quite expensive and that their capacity is quite small. In consequence, grid-dedicated batteries are not very profitable and efficient.

To circumvent those disadvantages, an idea is to use batteries that are already in use and wouldn't need to be installed just for the purpose of grid stability. An example is to use the batteries which lie inside the electric vehicles (EV) [6]. Indeed, EVs are most of the time connected to their charge station, and so by adding a controller at this station, we can use the power stored in the batteries of EVs to respond to deviations that can occur on the grid, like voltage and frequency deviations. Doing so allows to help the stability of the grid while becoming less dependent on synchronous generators.

Today, the number of EV is not significant, but this number is going to increase in the next decade due to the reduction of their price and the upcoming restriction of the countries on classical vehicles. Currently, in France there are 300 000 electric vehicles [7]. Assuming that all the EV have a battery capacity of 50 kWh [8], that means that, should we use all the EV available, and knowing that there is 2935 MV grids in France [9], one would have 5400 kWh of batteries available for one MV grid. In 2040, the amount of EV in France will grow to 15.6 million [10], which will give a capacity of 268 MWh of capacity for one MV grid: that becomes very interesting and meaningful as a resource to stabilise the grid.

With the significant increase of new components connected to the grid, it becomes more and more complex to model it entirely. Indeed, before the arrival of active components like PV panel and BESS, the distribution grids were only composed of elements that were characterized by passive loads [11], so it was easy to calculate the equivalent load of a LV or a MV grid with electrical laws such as Kirchhoff. However, with the vast deployment of active components, the behaviour of the LV grids has changed and consequently, modelling them as a simple load becomes inappropriate.

In France, for each of the 2935 MV grids spread around the country, there are 316 LV grids associated to them while for each LV grid, there are 38 households, where possibly PV panels and/or EV vehicles can be connected. In total, there are 35 million households [12] in France, for 927 753 LV [13] grids spread on the 2935 MV grid. Because of this, the computational load of simulating the entire grid would be too high without specialized equipment.

One practical way to perform simulations it is to work with simplified models that fairly represent real-case LV grids but with only one equivalent line, one equivalent passive load and one equivalent active component. That is, the simulated grid becomes less complex and it's possible to model it. Such simplified model, designed with a "grey-box" approach and simulated with the Monte-Carlo methodology [14]

[15], shall have the same behaviour as the entire LV grid.

The main goal of this work is to design an equivalent model that will have the same behaviour, in terms of reaction to frequency issues, than a real distribution grid with active components.

This work is decomposed in different chapters. Chapter 1 explains the state of the art concerning the actual evolution of grids and of battery energy storage systems (BESS), as well as how to generally simplify distribution grids. The chapter 2 gives a detailed model of a BESS, which, as mentioned above, may be based on grid-dedicated batteries or on EV batteries. In chapter 3 the simplified models of BESS and of PV panel are elaborated. The chapter 4 will explain how to develop an equivalent model of a complex distribution grid with active components such as BESS and PV panels. Finally, the chapter 5 will analyse several cases, models and results based on the equivalent model developed, in order to assess its accuracy and representativity vis-à-vis frequency deviation issues. Note that all models are herein computed on Simulink (MATLAB extension) with the Simscape's library.

Chapter 1

State of the Art

This chapter will set the actual current situation about the different subjects addressed in this work. First, the global evolution of the grid and its consequences will be explained. Then we'll describe how the Battery Energy Storage System (BESS) and the PV panel controllers can today be used to help the stability of the grid. Information about how to develop BESS are then given, before closing with explanation about state-of-the-art creation of an equivalent grid model from a detailed model.

1.1 Evolution of the grid and its stability

In order to decrease the global warming, there is an increase of non-synchronous generation like renewable sources that are connected to the grid, as shown on figure 1.1.

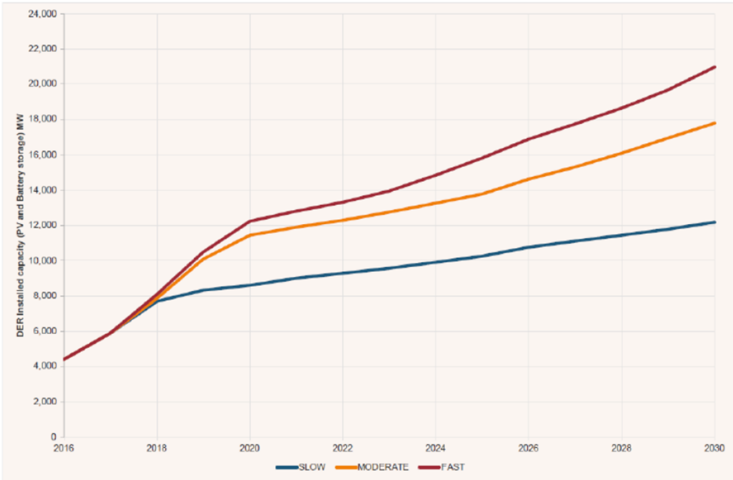

Figure 1.1: Increase of PV panels and batteries installation [15]

The problem with renewable that are connected with power electronics [16] is that the power production has a stochastic nature and has difficulties to respond to the variable energy demand [17]. This causes a reduction of the available inertia of the grid in response to voltage or frequency deviation, which is a problem for the grid operator in terms of overall power management and interaction with the other grids, especially when the power systems are quite small [18]. Even if some renewables are synchronous generators like hydraulic units, alone they are not capable of stabilizing the frequency [19]. So, today, classical energy sources still have a critical role to maintain such stability of the grid. To progressively replace them, there is a need of integrating dynamic elements, distributed on the network, in order to keep a relative agility and flexibility of the grid [20]. Furthermore, the increase of renewable on distribution grids makes them more complex, more sensitive to the dynamic of the *transmission* grid which also influence further the dynamic of this *distribution* grid [21]. The distributions grids become more active, as it is shown on figure 1.2.

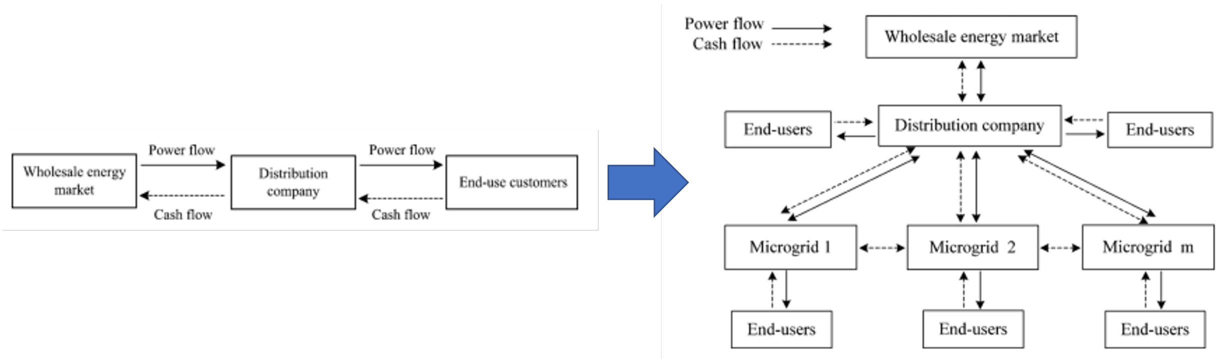

Figure 1.2: Evolution of the grid to a more active behaviour [11]

So, to help the grid in terms of this reduction of grid's inertia, new technologies have been developed. The first technology used is the BESS, which fast dynamic response can counterbalance the decrease of inertia of the grid and help to regulate it [19]. In BESS, the controller is divided between inertia and primary control in order to be more efficient [18]. A big advantage of BESS is that, when well controlled, it can provide or absorb a large amount of energy in a short amount of time [20], so it can help to manage both under- or over- deviations, thereby enhancing the efficiency, the reliability and the stability of the grid [22] and counter-measuring any cascade of failures [23]. A good way to connect a large amount of BESS systems to the grid is to use the batteries of the Electric Vehicles (EV). Indeed, with a proper controller, EVs can absorb the excess of grid power in their batteries and use it for driving or inject it later in the grid [6]. To connect the BESS to the grid, a voltage source converter (VSC) shall be used and shall be connected with a grid-following control in order to support the grid, i.e. to limit the frequency's decrease and damp the frequency oscillations [16]. Regarding PV panels, they can only help in case on over-frequency deviation by decreasing the injected power into the grid [2], but in case of under-frequency deviation they cannot give more power, since the maximal power in determined by external parameters like weather, moment of the day, localisation, etc. Even if a PV panel is less flexible than BESS, a frequency controller still helps to improve the overall frequency reliability and stability of the grid [24].

1.2 BESS model

Concerning the BESS model, the battery has first to be connected to the grid. As explained before, a VSC is used for such connection and the control of the battery will be made through it [25] [26] [27]. After the VSC, in order to have a proper sinusoidal signal for the voltage and the current, a LCL filter is added between the BESS and the grid. This filter damps the different harmonics present on the output voltage and current of the VSC, so as to have a cleaner signal [28] [29]. For the controller, the first thing to do is to measure the frequency, which is done by implementing a phase locked loop (PLL) [30]. The parameters inside the PLL influence the measure of the frequency and its oscillations, in order to have a clean value for the frequency controller of the BESS [31]. This controller calculates the power variation of the BESS in function of the frequency deviation and the rate of change of frequency (ROCOF) [19]. A dead band is added on the frequency deviation controller in order to regulate the power in case of small variations [32]. When the power deviation is set, there is still to control the switches of the VSC to be applied to the battery. For that purpose, a PQ control is used, which as output gives the modulation index of the VSC, converted into switch's signals with a pulse width modulation [22]. The global BESS model is shown on figure 1.3.

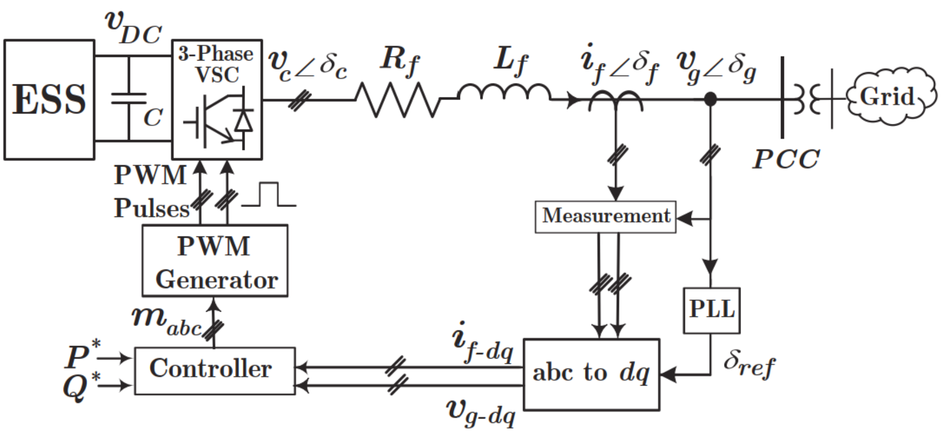

Figure 1.3: Global BESS scheme [22]

1.3 Equivalent model

With the large increase of elements connected to the grid, especially with active components like PV panels and BESS, the distribution grids are becoming more complex and simulating them can lead to computational burden. In order to decrease the complexity of modelling while keeping the same behaviour, an equivalent model of distribution grid has been developed. The ideas and the procedure mainly come from the works of Gilles CHASPIERRE [14] [15] [21] [33] [34] [35].

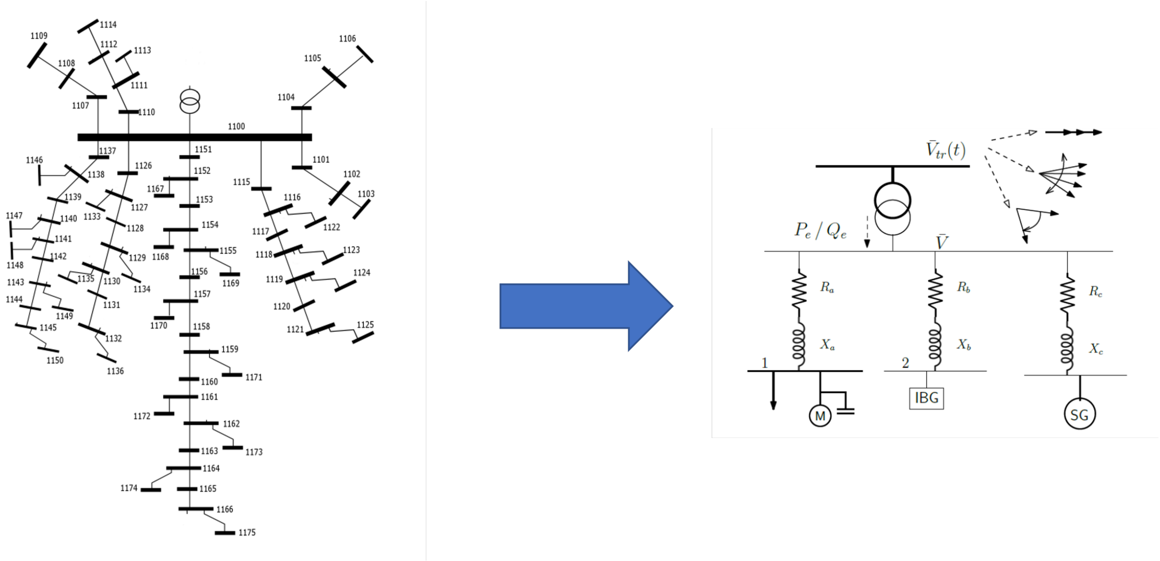

Figure 1.4: Equivalent of a distribution grid [21]

To achieve the objective of decreasing complexity, the loads, the lines and the actives components must have an equivalent. The methodology used to find the equivalent parameters of all the parts of the equivalent model is through Monte-Carlo simulations. The different parameters are adjusted in order to match the behaviour of the detailed model as closely as possible. This method is called "grey box", since the parameters and their physical relations are known but not their values, that shall be found through simulations. The advantage of using a "grey box" approach is that it combines the advantage of the "white box" and the "black box" [33] [34]. In the "white box" all the physical relations and the detailed components are known, but the calculations to find the appropriate values are too complex, while in the "black box" neither the structure nor the parameter's value has to be known, but it requires large data sets to find an accurate model. To have a quite robust equivalent, large disturbance simulations are used to tune the equivalent. First, the equivalent is initialised with standard values, then for one disturbance, the model is trained, which means that all the parameter values are chosen to have the most accurate equivalent model. Then, to be sure that the model is working, it is tested with other disturbances. If the equivalent model is not accurate enough, another frequency deviation can be added to the training until the test gives appropriate results. Gilles CHASPIERRE calls it a recursive procedure. In this work, his methodology has been adapted to frequency deviations.

To minimize the number of the studied parameters during the equivalent's training, their influence on the model is analysed, and the parameters which have a negligible impact are discarded. Furthermore, a partial tripping must be added to the equivalent active components in order to correctly model the various tolerances to disturbance of the active components.

1.4 Conclusion

So, current's state-of-the-art shows that BESS model has been developed, as well as equivalent model of detailed distribution grids in order to analyse voltage deviations. The work of this master thesis will be first to understand how a BESS model is made, and how they are controlled in case of frequency deviation, in order to make a simpler model of it. Then an equivalent model of a distribution grid with active components will be developed and analysed in case of frequency deviations.

Chapter 2

Detailed model of BESS

The Battery Energy Storage System (BESS) model is separated in 2 main parts, i.e. the physical part which encompasses the different components used in reality to construct a BESS, and the controller part that uses the different data coming from the components to control the input of those components in order to bring or to absorb power to/from the grid when there is a frequency variation on it. The system comes from the different sources: [22], [25], [30] and [31].

Figure 2.1 shows the overall BESS system, where the battery is represented by the DC source, complemented by the VSC, the LCL filter and the 3 phase transformers. The resistance R_{grid}, the inductance L_{grid} and the programmable 3 phase sources represent the grid.
Those components are linked to the controller that gives the pulses for the VSC to control the power exchanged between the battery and the grid.

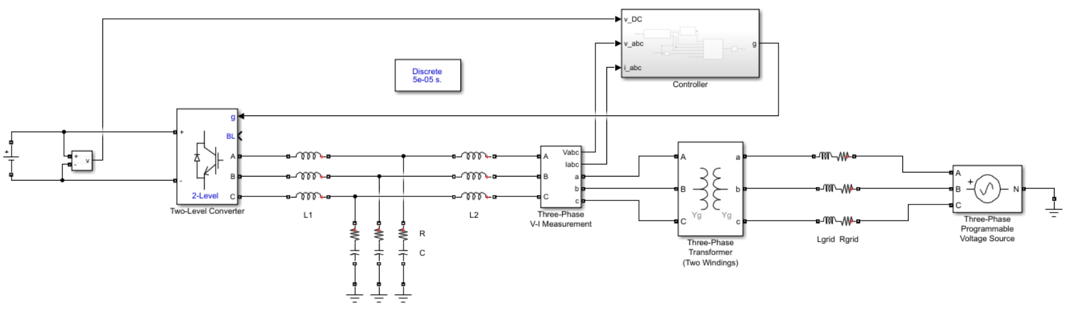

Figure 2.1: Overall BESS system

2.1 BESS components

2.1.1 Battery

The first part is the supply battery that can bring or absorb power from/to the grid. It is represented with a simple DC voltage source, as the battery is considered ideal. The State of Charge (SoC) is calculated in the controller and will be explained in section 2.2.3. The voltage of the source is set to the maximum voltage of the considered AC voltage. As the low voltage grid in Belgium is equal to 400 V, the voltage of the battery will be:

$$V_{BESS} = \sqrt{2} \cdot V_{LV,grid} = 567.7V \tag{2.1}$$

Which is an acceptable range for a standard battery. To stay also in an acceptable range in term of power, the nominal power of the battery $P_{nom,BESS}$ is set to 5000 W [25] [31].
Those values can be modified depending on the kind of battery we wish to represent.

2.1.2 Voltage Source Converter (VSC)

To convert DC voltage to AC voltage, a 2-level voltage source converter is used, as represented in figure 2.2. The used block is coming from the Simscape library [36].

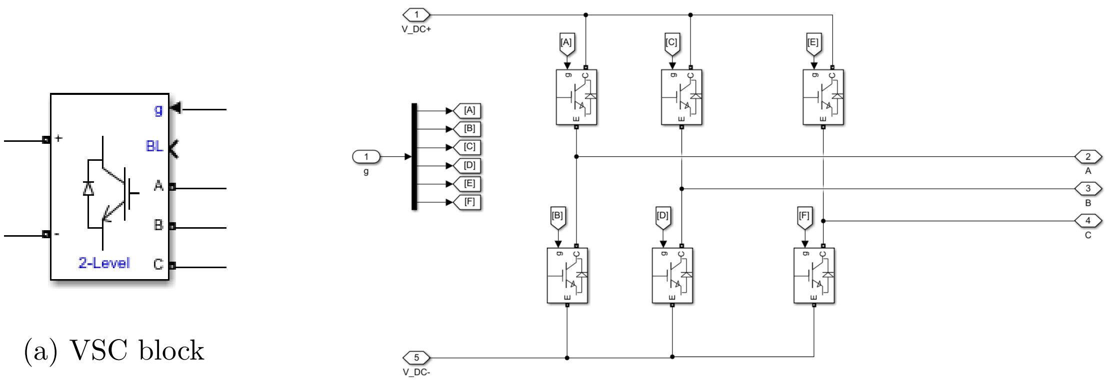

(a) VSC block

(b) VSC circuit

Figure 2.2: 2-level Voltage Source Converter

The switches are controlled to be opened or closed over time in order to create step voltages of varying width that can produce a sine wave after filtering. It is called the Pulse Width Modulation (PWM) and is represented in figure 2.3.

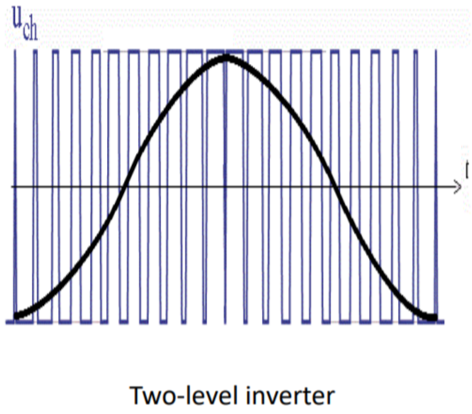

Figure 2.3: Pulse Width Modulation [37]

The obtained voltage is calculated with the equation 2.2 ([38]) and is shown on figure 2.4.

$$\begin{pmatrix} v_a \\ v_b \\ v_c \end{pmatrix} = \frac{V_{BESS}}{3} \cdot \begin{pmatrix} 2 & -1 & -1 \\ -1 & 2 & -1 \\ -1 & -1 & 2 \end{pmatrix} \cdot \begin{pmatrix} f_a \\ f_b \\ f_c \end{pmatrix} \tag{2.2}$$

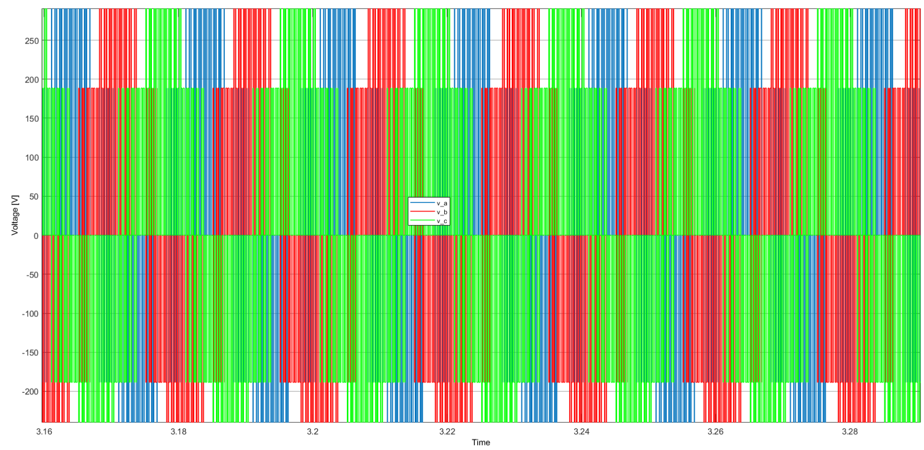

Figure 2.4: AC voltage at the output of the VSC

Since the VSC is quite simple, there are many harmonics distortions in the AC voltage, as seen on figure 2.4. We shall add a filter to decrease those oscillations.

2.1.3 LCL filter

The idea is to filter the output AC voltage of the VSC by using RLC components. The concept of the LCL filter comes from [28] and [29].

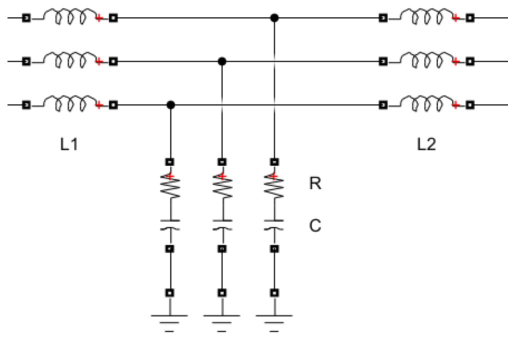

Figure 2.5: LCL filter

The LCL filter is a good comprising tool to handle filter effect on the voltage and on the current. Indeed, the filters equations are:

$$\begin{aligned} \frac{v_{out}}{v_{in}}(s) &= \frac{sRC+1}{s^2L_1C+sRC+1} \\ \frac{i_{out}}{i_{in}}(s) &= \frac{sRC+1}{s^2L_2C+sRC+1} \end{aligned} \tag{2.3}$$

The values of the different components are generally chosen to have:

- a low cut-off frequency
- a good phase margin
- a acceptable overshoot

At the end, the following different values for the components of the filter are:

L_1	L_2	C	R
100 [mH]	100 [mH]	50 [μF]	20 [Ω]

Table 2.1: Components' value of the LCL filter

The corresponding Bode diagram is presented on figure 2.6.

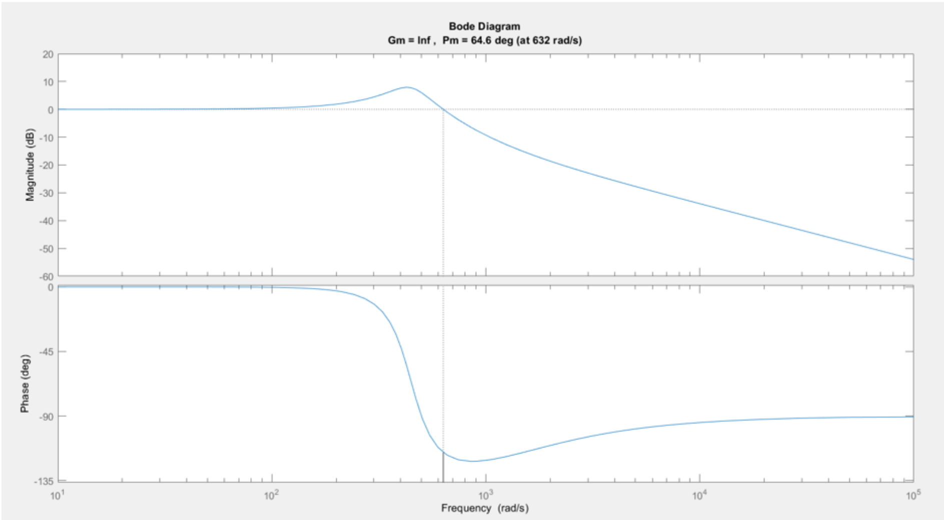

Figure 2.6: Bode diagram of LCL filter

As expected, the filter respects the required specifications. Indeed, by measuring the voltage at the output of the filter (figure 2.7), there is a great improvement of the sinusoidal aspect, when compared with figure 2.4.

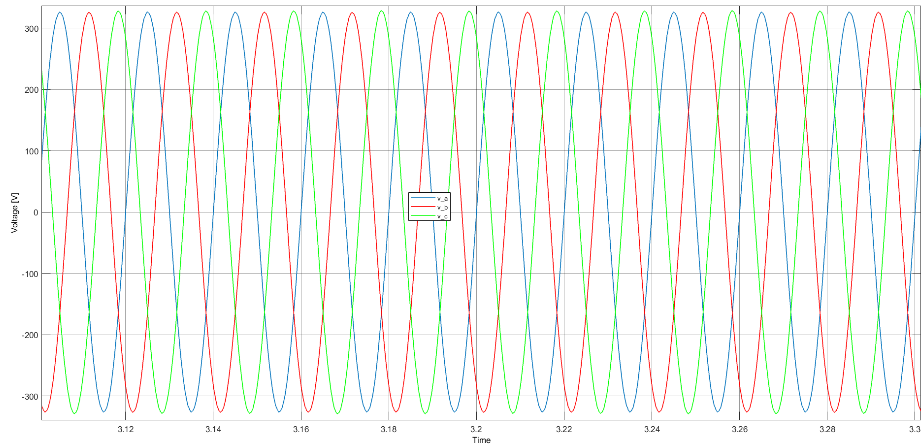

Figure 2.7: AC voltage at the output of the LCL filter

2.1.4 Three-Phase Transformer

To connect the BESS to the grid, the output voltage has to be adapted with the grid voltage. For that, a 3-phase transformer is used [39], as shown on figure 2.8. The low voltage part is set to the LV voltage of the grid in Belgium, while the high voltage part will be set to the MV voltage of the grid. The nominal power is set to be the same as the nominal power of the battery $P_{nom,BESS}$. So we do have:

$V_{LV,grid}$	$V_{MV,grid}$	$P_{nom,AC-AC}$
400 [V]	20 [kV]	5000 [W]

Table 2.2: Components' value of the 3-phase transformer

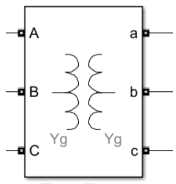

Figure 2.8: 3-phase Transformer

2.2 BESS Controller

As shown on figure 2.9, the controller is composed of multiple segments. First the Phase-Locked Loop (PLL), which measures the frequency. Then the frequency controller which gives the power setpoint of the battery, i.e. the power that the battery has to give or take to/from the grid. Then there is the battery limits, that verify if there is enough energy in the battery to give that amount of power. Finally stands the active and reactive power control that gives the modulation index, to be used in the PWM generator to have the different pulses that will be imposed into the VSC.

To improve the simulation time, the model is made in discrete timing, so discrete calculation's blocks are used in the controller. Note however that it has the same behaviour as a simple continuous time transfer function, that we will use for the analysis.

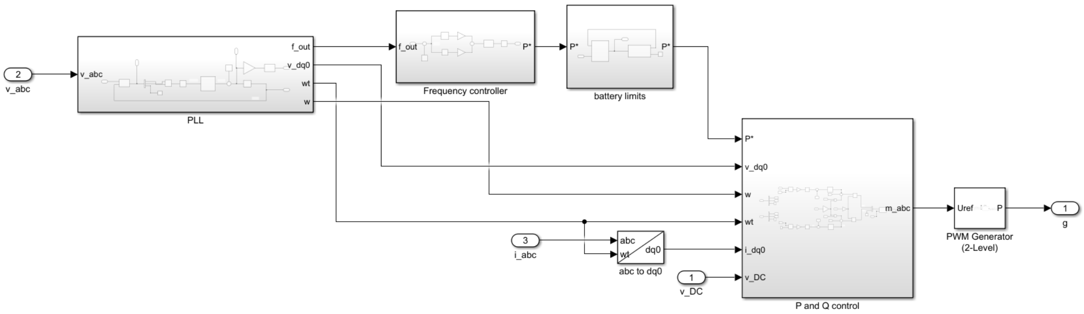

Figure 2.9: Controller of BESS

2.2.1 Phase-Locked Loop (PLL)

The PLL has 2 mains goals [40]. Its calculates both the frequency of the system as well as the phase angle ϕ_{out} $(= \omega t)$ which is useful to convert the voltage or the current from the abc reference frame to the synchronous reference frame dq0.

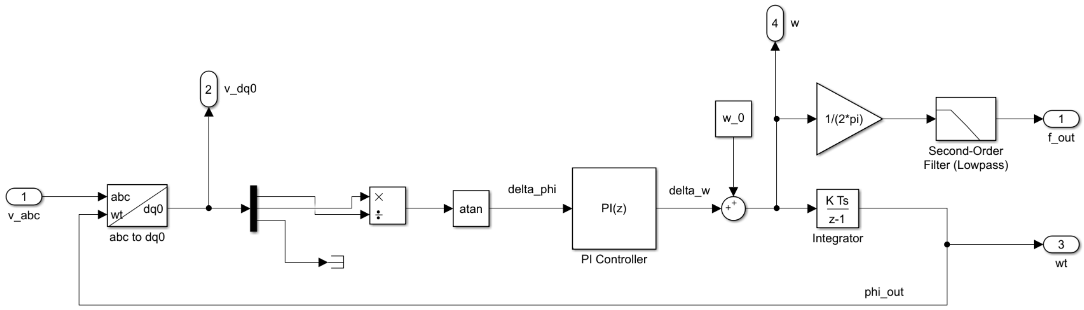

Figure 2.10: PLL block of the controller

The first block inside the PLL transforms the voltage into the synchronous reference frame with a Park's transformation [41]:

$$\begin{pmatrix} v_d \\ v_q \\ v_0 \end{pmatrix} = \frac{2}{3} \cdot \begin{pmatrix} \sin(\omega t) & \sin(\omega t - \frac{2\pi}{3}) & \sin(\omega t + \frac{2\pi}{3}) \\ \cos(\omega t) & \cos(\omega t - \frac{2\pi}{3}) & \cos(\omega t + \frac{2\pi}{3}) \\ \frac{1}{2} & \frac{1}{2} & \frac{1}{2} \end{pmatrix} \cdot \begin{pmatrix} v_a \\ v_b \\ v_c \end{pmatrix} \tag{2.4}$$

With this transformation, the voltage does not vary over time anymore, which is much easier for the calculations.
The phase deviation between the direct and the quadrature component is calculated as:

$$\Delta\phi = \arctan(\frac{v_q}{v_d}) \tag{2.5}$$

Then a PI controller is used to adjust the measurement of the deviation of the angular velocity $\Delta\omega$ as a function of the phase deviation $\Delta\phi$. The PI equation is:

$$H_{PLL}(s) = \frac{k_p s + k_i}{k_p s} \tag{2.6}$$

The 2 parameters in that equation have a big influence on the resulting $\Delta\omega$ and thus on the frequency:

- k_i : the frequency of the frequency-oscillations is proportional to it, but if k_i is too small the oscillations do not decrease.
- k_p : the amplitude of the frequency-oscillations will decrease faster when k_p is higher but the maximum amplitude will be higher at the beginning.

For both parameters, we have to do a trade-off between the different effects. Acceptable values are:

k_i	k_p
900 $[s^{-1}]$	90 $[s^{-1}]$

Table 2.3: Components' value of the PI controller of the PLL

The parameters' value can be modified in order to change the BESS characteristics.

Then the nominal angular velocity ω_0 is introduced into the PLL block to have the actual angular velocity ω. In one branch, the latter gets integrated to find the phase angle ϕ_{out} used in the Park's transformation. In the other branch ω is divided by 2π to find the frequency, that is filtered with a Butterworth low pass filter to cancel harmonics that might appear in the voltage measurement or in the Park's transformation. The cut-off frequency ω_c has to be low enough to reduce the effects of harmonics but cannot be too low since the PLL would then be useless to detect disturbance. The equation of the filter is:

$$F_{PLL}(s) = \frac{\omega_c^2}{s^2 + \sqrt{2}\omega_c s + \omega_c^2} \tag{2.7}$$

A good value for the cut-off frequency can be :

ω_c
20π [rad/s]

Table 2.4: Components' value of the Butterworth filter of the PLL

As a result, we get the output frequency f_{out}.

2.2.2 Frequency controller

Depending on the output frequency of the PLL, the frequency controller provides the amount of power that the battery will have to exchange with the grid [25] [30] [31].

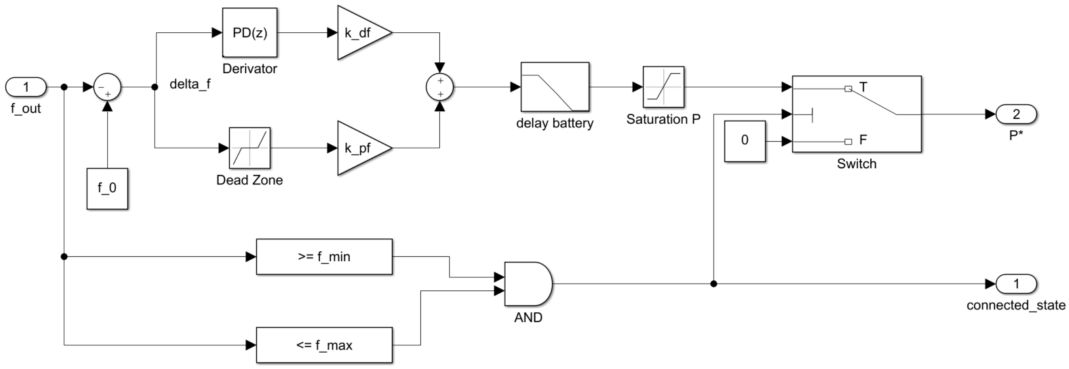

Figure 2.11: frequency controller block of the controller

The first thing is to protect the battery from too large frequency deviation from the grid. The difference between the output frequency f_{out} and the nominal frequency f_0 provides the frequency deviation Δf. The protection logic is represented as follows:

$$P^* = \begin{cases} P^* & \text{if } |\Delta f| < \Delta f_{max,BESS} \text{ (connected)} \\ 0 & \text{else (disconnected)} \end{cases} \tag{2.8}$$

So, the battery is disconnected when the frequency deviation is too large.
Then, based on the latter, we separate in 2 branches.
In the upper branch the frequency deviation is derived in order to find the Rate of Change of Frequency (RoCoF), which is multiplied by the derivative factor k_{df}, in order to react properly to a fast frequency deviation, i.e. a high RoCoF.
In the lower branch we add a dead zone block that puts the frequency deviation Δf in this branch to 0 if:

$$|\Delta f| < \Delta f_{min,BESS} = f_{s,BESS} \tag{2.9}$$

Note that this is how Frequency Containment Reserve (FCR) is regulated in real life [42].
The proportional factor k_{pf} influences the power setpoint as a function of Δf.
Both parameters k_{df} and k_{pf} have a big influence on the power setpoint P^* and therefore on the frequency regulation. As we can assume that a frequency deviation of 1 Hz is very big, for such Δf, all the power the battery can exchange with the

grid shall be required, i.e. the nominal power of the battery shall be exchanged through the proportional factor. By increasing k_{pf}, the big frequency variations are decreased, but it can lead to oscillations at the equilibrium because the too big values of k_{pf} prevent a good stabilization of the frequency.
Concerning the derivative factor, we know that a frequency deviation can be almost instantaneous, so the derivative can be high. If k_{df} is too high, it will lead to oscillations on P^* that can cause instability. On the other, if too low, the derivative part would not have enough influence on P^* and oscillations on the frequency would be less damped.

As illustrated in Figure 2.11, we then sum the rate of power resulting from the proportional and the derivative parts, and add a first order filter that represents the intrinsic delay response of the battery. If the delay T_B is too big, it will cause instability problem because the power takes too much time to be injected/absorbed to/from the grid. If it is too low, the following P and Q control will not have the time to operate because the power setpoint given by the frequency controller would change before the PQ controller has the time to give the information needed by the VSC.

At the end of the Frequency Controller diagram, and before giving the power setpoint to the P and Q control, a saturation block is added in order to keep P^* between $\pm P_{nom,BESS}$. Indeed, the power setpoint cannot exceed the nominal power of the battery, since the battery will not have the capacity to exchange it with the grid.

Standard values for the different parameters of the frequency controller have herein been selected to be as follows:

$\Delta f_{min,BESS}$	$f_{s,BESS}$	k_{df}	k_{pf}	T_B	$P_{nom,BESS}$
0.5 [Hz]	0.05 [Hz]	100 [sW/Hz]	5000 [W/Hz]	0.1 [s]	5000 [W]

Table 2.5: Components' value of the frequency controller

Those are only standard assumptions, and the factors can of course be changed depending on the BESS we want to characterize.
At the end of Figure 2.11, we end up with the power setpoint P^* we wish to exchange with the grid.

2.2.3 Battery limits

The Battery Limits block calculates the stage of charge (SoC) of the battery, by taking into account the efficiency of the battery and its initial energy capacity, then the block verifies that the power requested by the Frequency Controller is possible to be exchanged, i.e. whether there is not too much or too less energy in the battery. The concept comes from the battery block in [43].

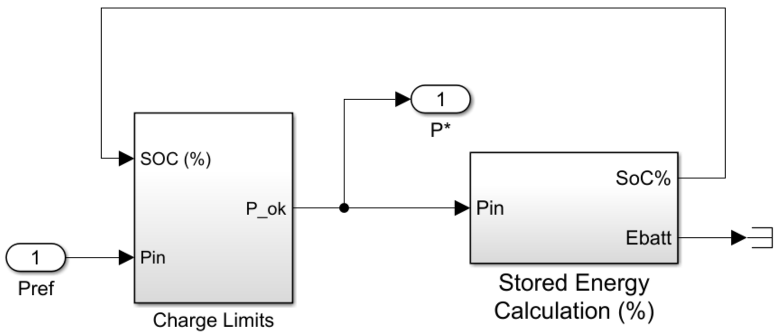

Figure 2.12: Battery Limits block of the controller

The first block in figure 2.12 verifies that it's possible to exchange the required power. The following logic is applied:

In case of injected power of the battery to the grid (discharge)

$$P^* = \begin{cases} 0 & \text{if } P^* > 0 \text{ and } SoC < p_{min,BESS} \\ P^* & \text{else} \end{cases} \tag{2.10}$$

In case of absorbed power of the battery from the grid (charge)

$$P^* = \begin{cases} 0 & \text{if } P^* < 0 \text{ and } SoC > p_{max,BESS} \\ P^* & \text{else} \end{cases} \tag{2.11}$$

Where $p_{min,BESS}$ and $p_{max,BESS}$ are the lower and upper limits of charge of the battery, respectively.

The second block in Figure 2.12 calculates the State of Charge:

$$SoC = \frac{1}{E_{nom,BESS}} \cdot \left(SoC_0 \cdot E_{nom,BESS} - \int_0^t P_{BESS}\, dt \right) [\%] \tag{2.12}$$

Where $E_{nom,BESS}$ is the nominal energy capacity of the battery, SoC_0 is the initial state of charge, and P_{BESS} the power of the battery exchanged with the grid, calculated like:

$$P_{BESS} = \begin{cases} \frac{P^*}{\eta_{BESS}} & \text{if } P^* > 0 \text{ (discharge)} \\ P^* \cdot \eta_{BESS} & \text{if } P^* < 0 \text{ (charge)} \end{cases} \tag{2.13}$$

Standard values for the different parameters of the battery limits can be:

$p_{min,BESS}$	$p_{max,BESS}$	$E_{nom,BESS}$	SoC_0	η_{BESS}
10 [%]	90 [%]	50 [kWh]	50 [%]	96 [%]

Table 2.6: Components' value of the battery limits

Those are only typical values, and they can, as for the other parameters, vary as a function of the BESS we want to characterize.
Note that after some simulations, typical frequency deviation does not require a large amount of power, so the energy capacity of the battery, E_{BESS} is always in an acceptable range. This block is therefore not mandatory in the design of the controller.

2.2.4 P and Q control

The goal of the P and Q control is to control the modulation index m_{abc} in function of the desired active (and reactive) power. The ideas come from the articles [19] and [23]. The block diagram is shown in Figure 2.13.

Since we only analyse frequency deviation in this work, and so only exchange of active power between the battery and the grid, the reactive power setpoint Q^* is always set to 0.

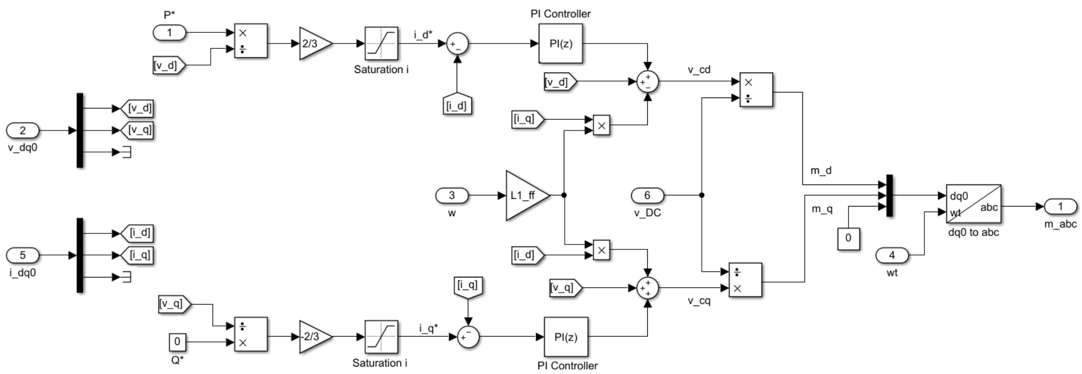

Figure 2.13: P and Q control block of the controller

The first step is to calculate the current setpoint i^* depending on the P^*:

$$
\begin{aligned}
i_d^* &= \frac{2P^*}{3v_d} \\
i_q^* &= \frac{-2Q^*}{3v_q}
\end{aligned}
\tag{2.14}
$$

Then we impose that i^* shall be below the nominal current of the battery, with $i_{nom,BESS} = \frac{P_{nom,BESS}}{V_{BESS}}$.

The internal voltage v_c is then determined. For simplicity, even if the output of the VSC block of this work (LCL filter) is different from the output of the VSC block in article [19] (RL line), the same Kirchhoff's Voltage Law as in the article is used and so the same equations to calculate v_c. The PI controller's parameter applied to $(i_d^* - i_d)$ has the equation :

$$H_{PQ}(s) = \frac{k_p s + k_i}{k_p s} \tag{2.15}$$

Both k_p and k_i have an influence on the applied power:

- k_p: influences the amplitude of the oscillations of the applied power. If it is too high, there is a lot of oscillations, which can cause instability. But it must be higher than 0 to still have a proportional term. The influence of k_p is quite small compared to k_i.
- k_i: influences the proportion of power given/taken by the battery to/from the grid during the stabilisation time. If k_i is too small, the stabilisation time is too big. On the other hand, if k_p is too small, the maximum amplitude of the exchanged power is too big; a trade-off has to be found between the 2.

Following on the block diagram, the modulation terms are finally calculated by dividing the internal voltages by the battery voltage:

$$\begin{aligned} m_d &= \frac{v_{c,d}}{V_{BESS}} \\ m_q &= \frac{v_{c,q}}{V_{BESS}} \end{aligned} \tag{2.16}$$

Then the parameters that are in the synchronous reference frame dq0 (m_0 is set to 0 because it has no influence on the power) are transformed to the reference frame abc with the block [41]. The equation is:

$$\begin{pmatrix} m_a \\ m_b \\ m_c \end{pmatrix} = \begin{pmatrix} \cos(\omega t) & -\sin(\omega t) & 1 \\ \cos(\omega t - \frac{2\pi}{3}) & -\sin(\omega t - \frac{2\pi}{3}) & 1 \\ \cos(\omega t + \frac{2\pi}{3}) & -\sin(\omega t + \frac{2\pi}{3}) & 1 \end{pmatrix} \cdot \begin{pmatrix} m_d \\ m_q \\ m_0 \end{pmatrix} \tag{2.17}$$

where ω is the radial frequency.
Standard values for the different parameters of the P and Q controller can be:

k_p	k_i
50 [V/A]	1000 [Vs^{-1}/A]

Table 2.7: Components' value of the P and Q controller

Those values are generally acceptable, but they can be adapted depending on the BESS to be characterized.
The output of the P and Q control is the modulation index m_{abc}.

2.2.5 PWM generator

The PWM generator block [44] transforms the modulation index m_{abc} into pulses that will control the switches of the VSC. In order to have a good accuracy between m_{abc} and the output AC voltage of the VSC, the switching frequency f_{switch} of the PWM generator much higher than the frequency of the voltage. However, a too high f_{switch} will lead to big simulation time. A good compromise is:

$$f_{switch} = 27 \cdot f_0 \quad \text{(default value of the block)} \tag{2.18}$$

All in all, we finally obtain the pulses used to control the VSC as a function of the frequency deviation, as per Figure 2.9.

2.3 Conclusion

In this chapter, all the details of the model have been described, corresponding to the real model implemented when we want to connect a battery to the grid. Into the controller, only the frequency deviation is analysed but other features, such as voltage regulation, could also be modelled. In the physical part there is the battery, then a voltage source converter, a LCL filter and a 3-phase transformer in order to connect the battery to the grid. The controlled block is the VSC and it is controlled by the pulses applied to it. The controller part calculates first the output frequency with the phase-lock loop block, then the power setpoint is calculated in the frequency controller block, while the modulation index is obtained with the P and Q control block. All in all, we finally get the pulses with the PWM generator block.

Chapter 3

Simplified model

The purpose of simplified models is to represent the same behaviour as the detailed components model, but by using other tools in order to decrease the simulation time. The simplified model will be less close to reality but should still have the same characteristics as the detailed model for the timescale we are considering for simulations (seconds). In addition of the simplified models of the BESS, the ones of the Photovoltaic (PV) generator will also be modelled and analysed.

3.1 BESS

3.1.1 Model

The main difference between the detailed and the simplified models of the BESS is that a DC source with a VSC and a LCL filter is not used anymore, but we use a 3-phase dynamic load [45] used as a simple battery inverter. The idea comes from the model [43]. As for the detailed model, the grid is represented with the programmable 3-phase source.

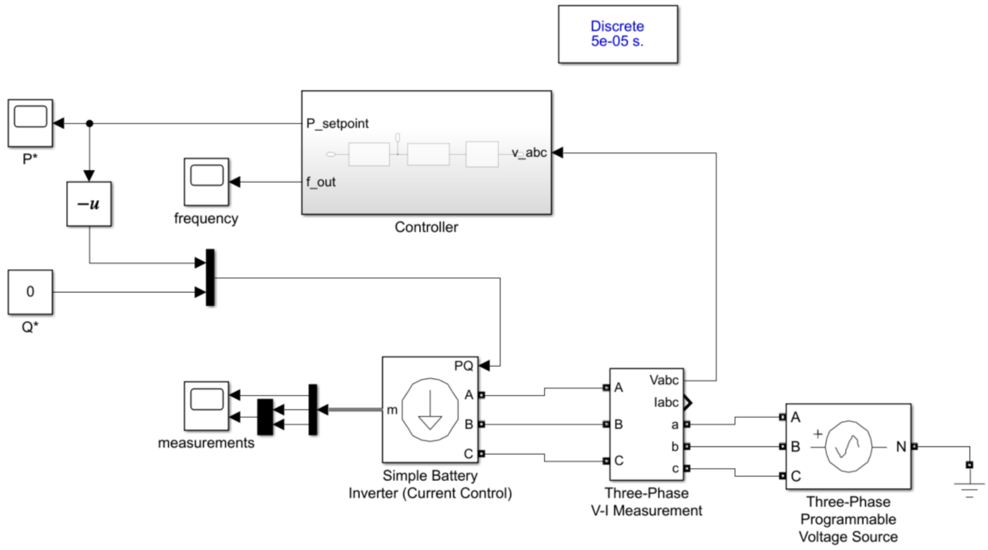

Figure 3.1: Simplified model of BESS

The battery inverter has the following characteristics, as a function of the battery to be modelled:

- A nominal AC voltage which is equal to the AC voltage on the low voltage side of the grid in the detailed model 2.2.
- A nominal frequency, the same as the grid one.
- A nominal power which is the same as the nominal power of the battery in the detailed model 2.1.1.
- An external P and Q control. Note that Q^* is again always set to 0 because we only consider frequency deviation; to simulate the battery injecting power instead of consuming power, the opposite of the power P^* is asked to the block.

Hence, to have the same behaviour as the detailed model, the following various values are used:

$V_{LV,grid}$	f_0	$P_{nom,BESS}$
400 [V]	50 [Hz]	5000 [W]

Table 3.1: Components' value of the simple battery inverter for BESS

The BESS controller is similar to the detailed model 2.2, except that the 2 last blocks, the P and Q control block and the PWM generator block are removed because there are not needed anymore. So, there is only the PLL block which calculates the frequency, together with the frequency controller block that sets the power setpoint, as well as the battery limits block that verifies if the required power is possible to be exchanged with the grid.

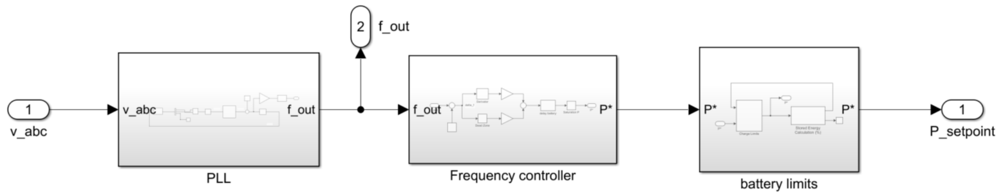

Figure 3.2: Simplified controller of BESS

3.1.2 Analysis

To analyse the accuracy of the simplified model, a frequency disturbance is simulated on the grid size with the 3-phase programmable voltage source, then we look at the measured frequency f_{out} after the PLL block and at the power setpoint P^*. All the parameters are set to the same value. For simplicity of simulation and to be like in the simplified model, the 3-phase transformer, the resistance R_{grid} and the inductance L_{grid} are removed from the detailed model. On the figure 3.3, the upper graph shows the frequency measure from the detailed and simplified model of the BESS and the lower graph shows the error between the 2 measures.

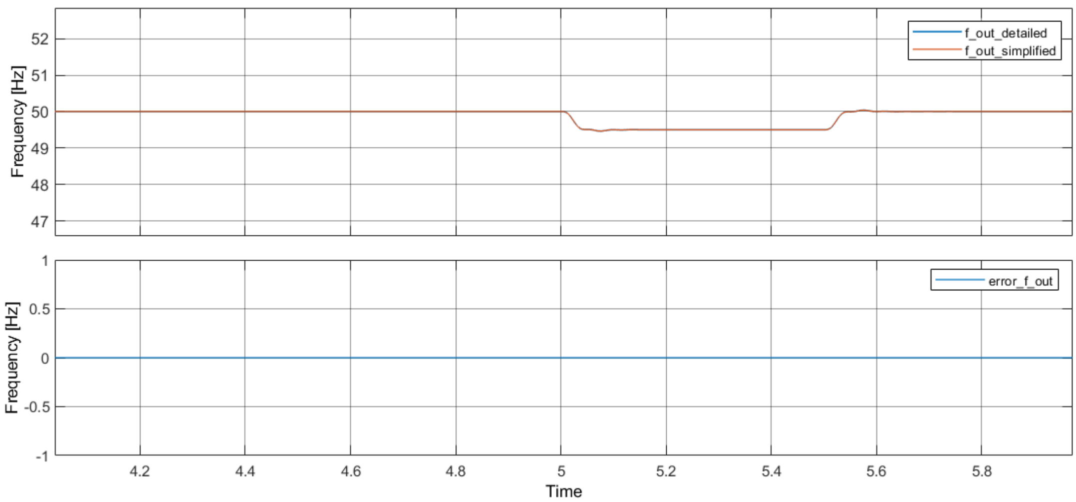

Figure 3.3: Accuracy of the frequency measurement between the detailed and the simplified models of a BESS.

The figure 3.4 shows on the upper graph the power response to the frequency deviation of the detailed and simplified BESS model, and the lower graph shows the error between the 2 measures.

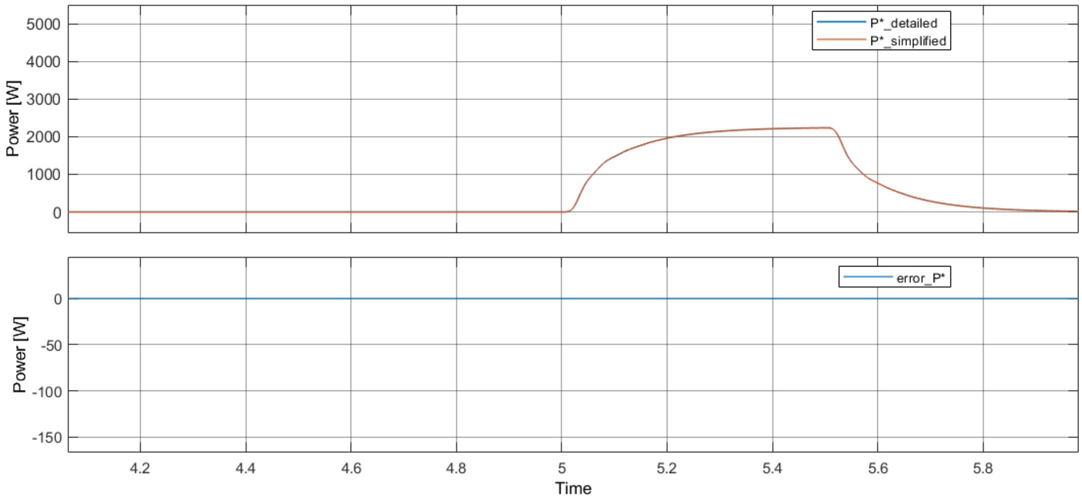

Figure 3.4: Accuracy of the power setpoint between the detailed and the simplified model of a BESS

By looking at the figures 3.3 and 3.4, we can say that the model is accurate, since the error for the frequency measure and for the power response is 0.

3.2 PV generator

3.2.1 Model

The model of a PV generator is based on the same principle of the model of the BESS, but the controller changes. Naturally, the PV panel cannot give more power to the grid in case of an under-frequency event, but it can decrease its produced power in case of an over-frequency event. As for the BESS, the block that models the PV panel itself is a 3-phase dynamic load [45]. The following concept and model came from different papers: [2], [21] and [24].

The input power P_{ext} represents the power that the PV panel can produce as a function of the sun power. As we perform a frequency analysis, we are focused on small periods of time, so it can be assumed that P_{ext} stays constant during the simulation.

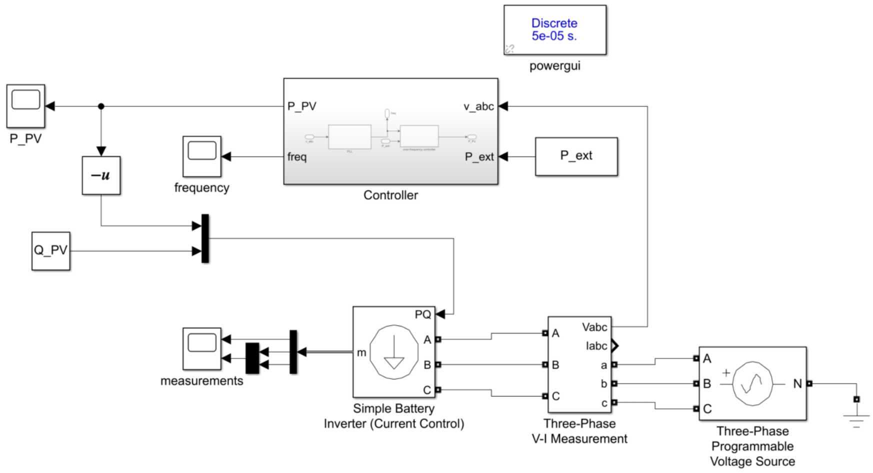

Figure 3.5: PV model

The parameters of the PV model depend on the wanted type of installation, but in this work, private decentralized installations on the roof of houses are considered. So, the power will be mainly on the same order of magnitude. Standard values can be:

$V_{LV,grid}$	f_0	$P_{nom,PV}$	P_{ext}
400 [V]	50 [Hz]	13 000 [W]	10 000 [W]

Table 3.2: Components' value of the simple PV generator

3.2.2 Over-frequency controller

As for the BESS, first the frequency has to be measured: the same PLL as for the BESS (2.2.1) is used. The over-frequency block decreases the power that the PV panel will inject to the grid as a function of the frequency deviation.

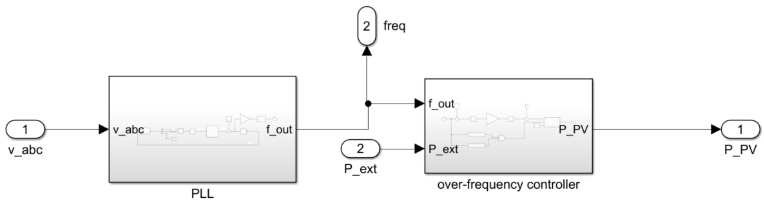

Figure 3.6: Controller of the PV

As for the BESS, there is a protection of the PV, such that, if the frequency deviation is too high, the PV is disconnected from the grid. As illustrated in Figure 3.7, the frequency deviation Δf is calculated:

$$P^* = \begin{cases} P^* & \text{if } |\Delta f| < \Delta f_{max,PV} \text{ (connected)} \\ 0 & \text{else (disconnected)} \end{cases} \tag{3.1}$$

Then, a dead zone block is added in order to not take it into account the deviation if it is too low. So, Δf is equal to 0 if:

$$|\Delta f| < \Delta f_{min,PV} = f_{s,PV} \tag{3.2}$$

As a function of the deviation, the amount of power ΔP_f to remove from the power production of the PV panel is chosen. For that, the power factor p_F which acts as a fraction of the nominal power of the PV $P_{nom,PV}$ is used, then ΔP_f is removed from P_{ext}.

$$\Delta P_f = p_F \cdot \Delta f \cdot P_{nom,PV} \tag{3.3}$$

Then the saturation block limits the value of ΔP_f between 0 and P_{ext}. Indeed ΔP_f cannot be negative, because it would mean that more power is asked from the PV panel, which is not possible. Also ΔP_f cannot be higher than P_{ext} because it would mean that the PV would behave like a load, which is also not possible.
At the end me remove the power deviation from the input power to find the appropriate power setpoint P^*.

$$P^* = P_{ext} - \Delta P_f \tag{3.4}$$

Standard values for the different parameters of the over-frequency controller can be:

$\Delta f_{max,PV}$	$f_{s,PV}$	p_F
0.9 [Hz]	0.2 [Hz]	40 [%]

Table 3.3: Components' value of the frequency controller

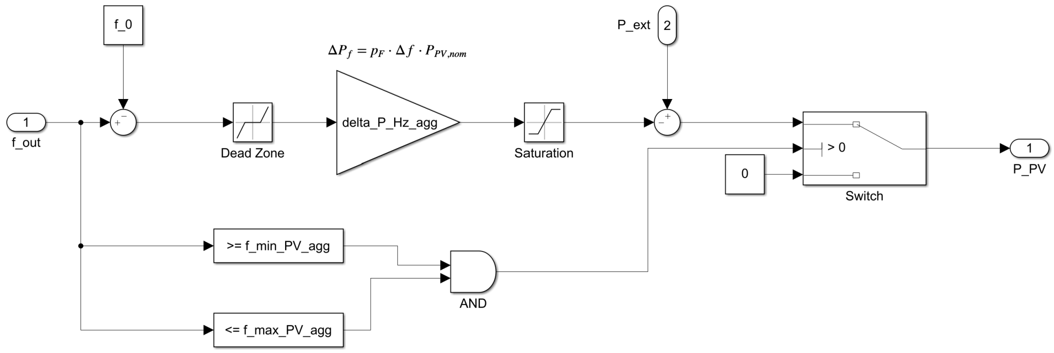

Figure 3.7: Over-frequency controller of the PV

3.3 Conclusion

The simplified model of a BESS and of a PV generator have been established. We've seen that for the accuracy of the BESS behaviour between the detailed and the simplified models is very good. Those models will be useful to simulate active components on a distribution grid as they will allow it to be more active. This is what will be analysed in the next sections.

Chapter 4

Research of an equivalent model

This chapter explains the methodology to design an equivalent model of a distribution grid. For this work, we will consider a CIGRE distribution grid but only as an example. The methodology is not designed for one particular grid but for all kinds of distribution grid.

4.1 Detailed model

4.1.1 Studied benchmark

As reference for modelling a complex detailed grid, the CIGRE TF C6.04.02 network [46] that simulates a low voltage European microgrid network will be used. The grid has 2 voltage levels. The first one is the MV side which is at 20 kV, while the second one is in the LV side at 400 V and composes the majority of the grid. The connection between the 2 voltage levels is done with a 3-phase transformer with a nominal power up to 1 MVA and a delta-star connection. The main lines are overhead lines, but the grid also has underground lines and service connection between the main grid and the different loads. Concerning the loads, there are 2 single residential consumers, 2 types of apartment buildings and 1 group of 4 residences for a total power of 116.4 kVA. More information about the network and the loads' and lines' values are given in [46].

As it stands, the CIGRE TF C6.04.02 benchmark has only passive components (loads); hence, to make the distribution grid active, PV panels and batteries are added into some lines.

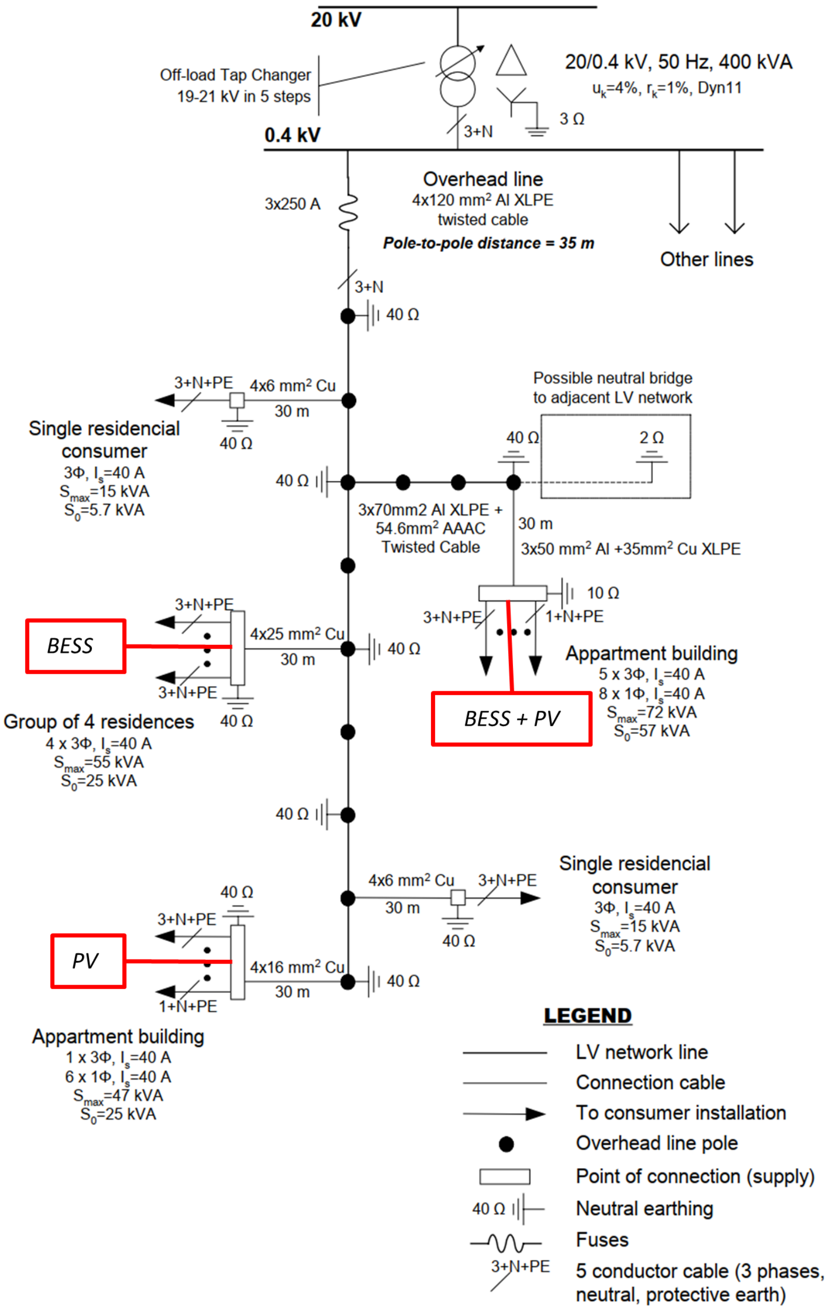

Figure 4.1: CIGRE TF C6.04.02 with active components

Then the whole grid is modelled on Simulink and shown on figure 4.2. A bigger representation of the detailed model is shown on appendix A 6.1. For that, some simplifications have nevertheless been made. First, the MV transmission grid is modelled with a variable 3-phase source at 20 kV as in [46]. It is on that block that a frequency deviation will be applied to look at the behaviour of LV distribution grid. Second, all the loads are active components which means that they have no reactive part. Furthermore, the loads in Simulink are implemented as constant impedance, where the power is equal to the set power if the voltage is equal to the nominal voltage [47]. Third, the different kinds of lines in the network are modelled with simple 3-phase RL lines where only the phase resistance and inductance are considered. Fourth, the loads are implemented as balanced which is not the case in the paper of the benchmark [46]. Fifth, the earthing is not implemented.

As a result of the above assumptions, a simpler LV grid is obtained but still representing the reality in case of frequency deviation. Indeed, the reactive components are more influenced by voltage deviations than by frequency ones. Furthermore, in European grid, we can assume the grid to be balanced, even if the residential consumers are considered as 1-phase loads.

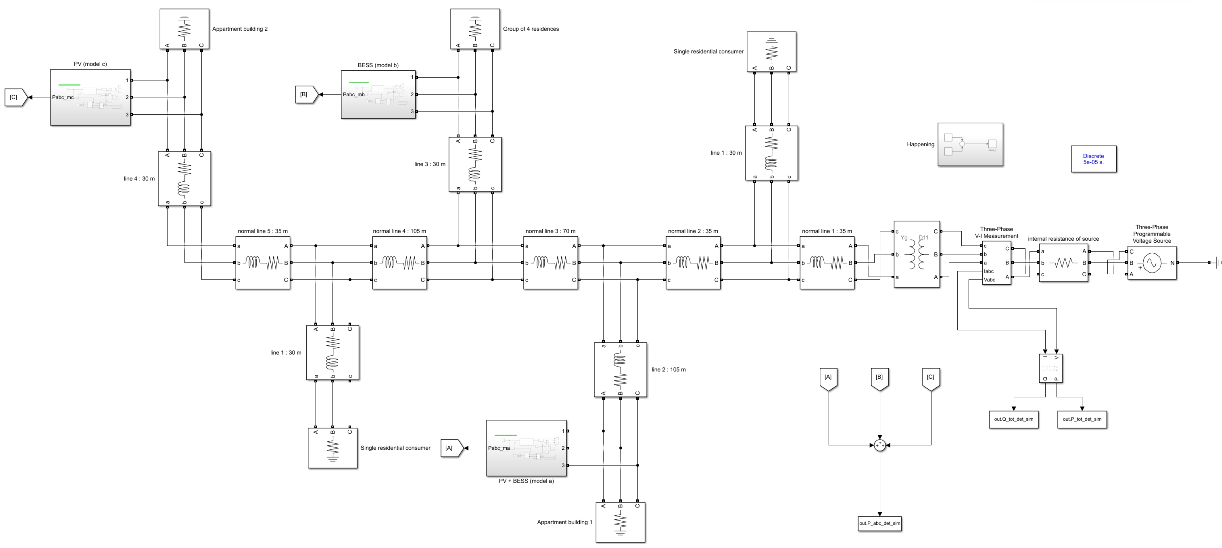

Figure 4.2: CIGRE TF C6.04.02 with active components on Simulink

4.1.2 Active components

For this analysis, 3 different active components will be placed on the grid. First, at the node of the apartment building 2, a PV panel is placed (model c). Then at the node of the group of 4 residences, a BESS is implemented (model b). Finally, on the nodes with the apartment building 1 on figure 4.2, to model the PV panel and the BESS at the same place, only one block of 3-phase dynamic load [45] is used and add the power setpoint given by the BESS controller 3.2 and by the PV controller 3.6 (model a).

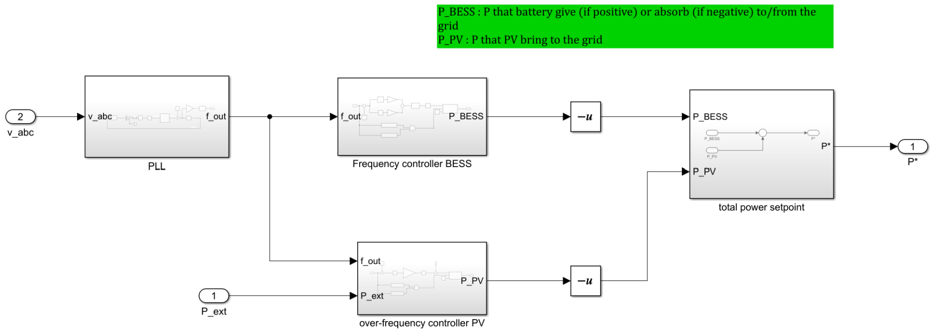

Figure 4.3: Controller of PV and BESS

The values of all parameters of those active components can be randomized inside a certain range. This range is defined around typical values coming from different sources [2] [18] [19] [24] [25] [31] [48]. However, to be sure that comparisons can be made when analyses are being done, the parameters will be chosen inside their range and stay constant between the different analyses. All the parameters' values of all active components in the detailed models and their usual respective range are given in the table 4.1.

block	parameter	range	model a	model b	model c	unit
PLL	k_p	[60,120]	90	110	100	[1/s]
	k_i	[600,1200]	800	700	800	[1/s]
	w_c	[10 π,20 π]	14π	10 π	17 π	[rad/s]
BESS	$P_{nom,BESS}$	[3000,8000]	5000	8000	/	[W]
	k_{pf}	[1000,8000]	3000	6000	/	[W/Hz]
	k_{df}	[100,1000]	700	400	/	[sW/Hz]
	T_B	[0.05,0.15]	0.09	0.1	/	[s]
	$f_{s,BESS}$	[0.01,0.1]	0.04	0.08	/	[Hz]
	$\Delta f_{max,BESS}$	[0.1,1]	0.7	0.5	/	[Hz]
PV	$P_{nom,PV}$	[3000,8000]	7000	/	4000	[W]
	p_F	[30,60]	50	/	40	[%]
	$f_{s,PV}$	[0.05,0.25]	0.12	/	0.17	[Hz]
	$\Delta f_{max,PV}$	[0.1,1]	0.7	/	0.3	[Hz]
	P_{ext}	[2000,8000]	4000	/	5000	[W]

Table 4.1: Parameters' value of the the different active components in the detailed model

4.2 Aggregate model

The aggregate model is much simpler than the detailed one. Indeed, the purpose of an equivalent model is to have similar behaviour as a complex detailed model but with much less complexity. For the aggregated model there will be only one equivalent line, one equivalent load and one active component that assemble BESS and PV behaviour, as shown in Figure 4.3 and explained just in the previous section for the apartment building 1. However the frequency controllers of BESS and PV will be different, this part is explained in the subsection 4.2.2. The aggregated model is shown on figure 4.4. Note that this design of aggregated model works for all kinds of distribution grids.

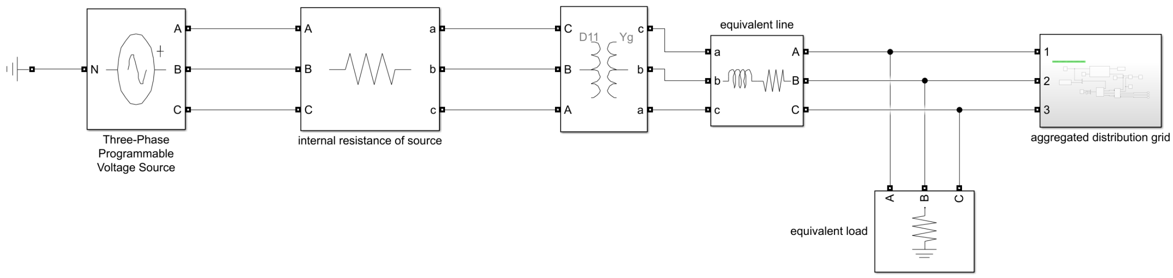

Figure 4.4: Aggregated model on Simulink

The 3-phase source, the internal resistance and the transformer are the same as in the detailed model. The calculation of the equivalent line's and load's value are explained in the following subsection 4.2.1.

4.2.1 Equivalent line and load

For the equivalent line's and load's values, we can focus on the detailed and the aggregated grid without considering any active components, since the study of the equivalent of such active components will be made in the next session. The idea of the equivalent load and line are coming from [21] but the methodology herein is different.

First let's calculate the equivalent load. By looking at all the loads on the detailed model, it can be assumed that they all have the same voltage at their terminals since the voltage is almost constant on the grid if the small voltage influence of the lines is neglected. So, we can calculate the equivalent load by putting all the loads in parallel. Note that the impedance for each load is obtained with:

$$Z_{load,i} = \frac{V_{LV}^2}{S_{load,i}} \tag{4.1}$$

With this distribution grid, the equivalent load impedance and load power are calculated with:

$$\begin{aligned} Z_{equ,load} &= Z_{src}//Z_{ap1}//Z_{go4r}//Z_{src}//Z_{ab2} = 1.3514\Omega \\ P_{equ,load} &= \frac{V_{LV}^2}{Z_{equ,load}} = 118.4kW \end{aligned} \tag{4.2}$$

Where src means single residential consumer, $ap1$ and $ap2$ apartment building 1 and 2, and $go4r$ group of 4 residences. The values of the different powers are coming from [46] where the nominal values are taken (S_0).

Next the equivalent line impedance can be calculated by using the following relation:

$$\overline{Z_{equ,line}} = \overline{Z_{equ,tot}} - Z_{equ,load} \tag{4.3}$$

Where $\overline{Z_{equ,tot}}$ is the total equivalent impedance of the grid. This equation allows to separate between the loads and the resulting line of system simplification while being sure that total equivalence impedance is linked to the transformer. The total equivalent impedance is obtained with the following relations, starting from the end of the grid for this distribution grid:

$$\begin{aligned} \overline{Z_{equ,3}} &= (Z_{ap2} + \overline{Z_{l,4}} + \overline{Z_{l,n,5}})//(\overline{Z_{l,1}} + Z_{src}) \\ \overline{Z_{equ,2}} &= (\overline{Z_{equ,3}} + \overline{Z_{l,n,4}})//(\overline{Z_{l,3}} + Z_{go4r}) \\ \overline{Z_{equ,1}} &= (\overline{Z_{equ,2}} + \overline{Z_{l,n,3}})//(\overline{Z_{l,2}} + Z_{ap1}) \\ \overline{Z_{equ,tot}} &= (\overline{Z_{equ,1}} + \overline{Z_{l,n,2}})//(\overline{Z_{l,1}} + Z_{src}) + \overline{Z_{l,n,1}} = 1.38465 + 0.00844i\Omega \end{aligned} \tag{4.4}$$

Where $\overline{Z_{l,i}}$ are specified kind of lines and $\overline{Z_{l,n,i}}$ are the same overhead lines with different lengths. More information are given in [46].

Then the equivalent line impedance can be obtained and so the following line resistance and inductance:

$$\begin{aligned} \overline{Z_{equ,line}} &= \overline{Z_{equ,tot}} - Z_{equ,load} = 0.03330 + 0.00844i\Omega \\ R_{equ,line} &= \mathbb{R}(\overline{Z_{equ,line}}) = 0.03330\Omega \\ L_{equ,line} &= \frac{\mathbb{I}(\overline{Z_{equ,line}})}{2\pi f_0} = \frac{0.00844}{100\pi} = 26.865\mu H \end{aligned} \tag{4.5}$$

In function of the distribution grid studied, the equations to obtain $\overline{Z_{equ,line}}$ and $Z_{equ,load}$ will be different but the methodology to find them works for other grids.

Now that the equivalent load and line are found, we can focus on the active components.

4.2.2 Partial tripping of frequency controllers for equivalent BESS and PV

As seen on table 4.1 of active components, the latter have a different tolerance to frequency deviation. Indeed, some are disconnected if the frequency deviation is over 0.3 Hz while certain can resist to up to 0.7 Hz of frequency deviation.

For the equivalent model, we could set a parameter that would be a global disconnection parameter but that would mean that if the frequency deviation is higher that the equivalent maximum frequency deviation $\Delta f_{max,equ}$, the equivalent would not provide any power even if some components are still connected in the detailed model. That would lead to several errors.

To tackle this problem, a partial tripping of the components is modelled inside the frequency controller of the equivalent BESS and the equivalent PV. That means that, when the frequency deviation is between the minimum $\Delta f_{max,min}$ and the maximum $\Delta f_{max,max}$ tolerance of the components of the detailed model, it will be taken into account in the equivalent model by taking a fraction of the initial power setpoint given by the controller. Note that for this process, the BESS and the PV are independent and that the tolerance to frequency deviation is the same in case of over- or under-frequency.

The partial tripping model can be explained with the following equations:

$$P^* = \begin{cases} P_0^* & \text{if } |\Delta f| < |\Delta f_{max,min}| \\ F_f \cdot P_0^* = \frac{|\Delta f_{max,max}| - |\Delta f|}{|\Delta f_{max,max}| - |\Delta f_{max,min}|} \cdot P_0^* & \text{if } |\Delta f_{max,min}| < |\Delta f| < |\Delta f_{max,max}| \\ 0 & \text{if } |\Delta f| > |\Delta f_{max,max}| \end{cases} \tag{4.6}$$

The equations are graphically shown on figure 4.5.

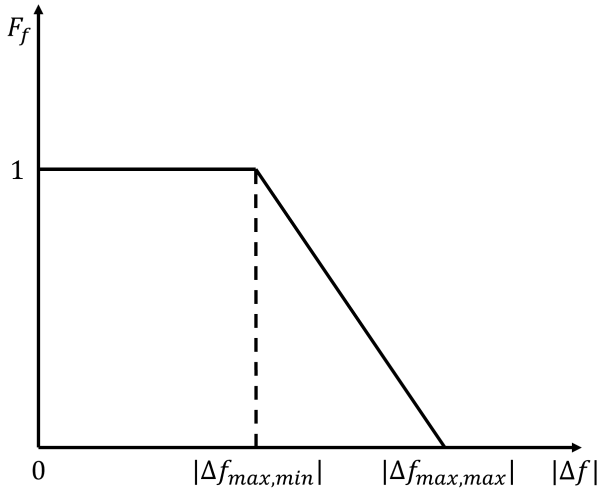

Figure 4.5: Partial tripping of the frequency controller

The figures 4.6 and 4.7 show the Simulink implementation of the new frequency controller of BESS and PV.

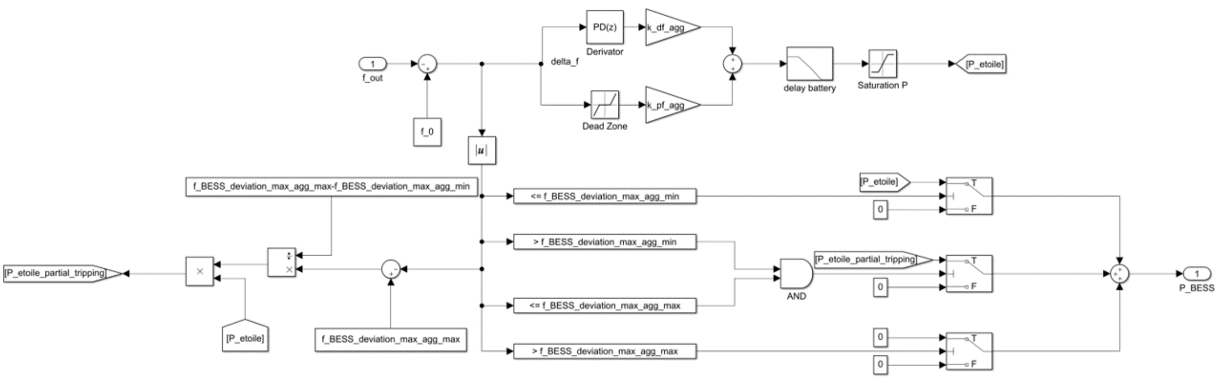

Figure 4.6: Frequency controller of BESS with partial tripping

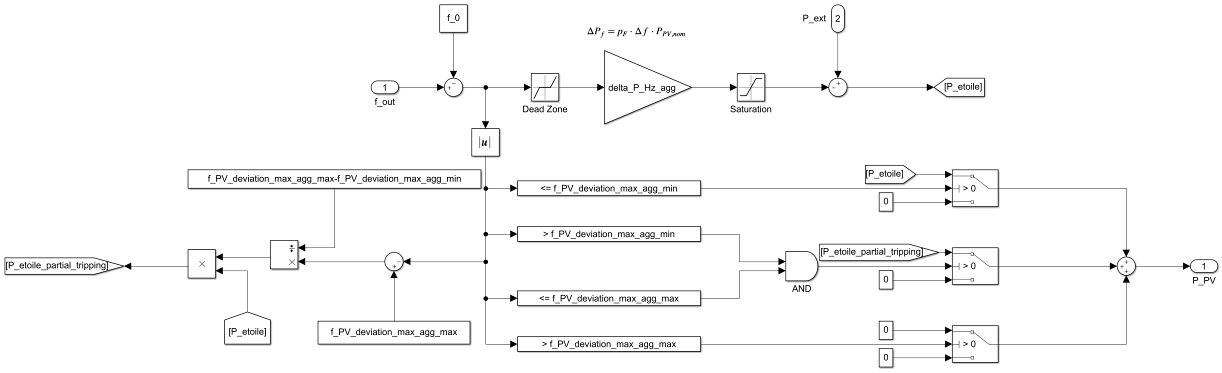

Figure 4.7: Frequency controller of PV with partial tripping

4.3 Methodology of the research for the equivalent of active components

4.3.1 Global methodology

The methodology used to find the best values for all parameters of the equivalent active components is based on a Monte-Carlo simulation [21]. The methodology is divided in multiple steps.

The first step is to initialise the equivalent model. For that, the range of all parameter's value must be set as well as their initial value.

Then the second step is to choose the different frequency deviations that will be used.

The next step 3 is called the training step. It stands when one deviation is chosen and then, one parameter at a time, we calculate the error between the detailed and the aggregated models obtained for each parameter's value inside the corresponding range. Then the parameter's value for which the error is minimum is selected. During this research of the best value of one parameter, the other ones keep a constant value. If they have already been studied, they have their best value, otherwise they have their initial value. At the end of the training step, one ends up with all the parameter's values which give the best equivalent model.

The last step is to test the equivalent model. For that, all the frequency deviations chosen in step 2 are applied on the obtained model as well on the detailed model, and the error obtained as a function of the different deviations is calculated. If small errors are obtained for all the other frequency deviations, the equivalent model is deemed good. On the contrary if the errors are too big, that means that the model does not work correctly. To improve such situation, one can go back to the training step (step 3) but with adding 1 deviation at the time to choose the best parameter's value. The methodology continues until one reaches an acceptable working model if possible. If not, the Monte-Carlo methodology fails.

4.3.2 Step 1 : Initialisation of the equivalent

For the initialisation of the equivalent model, the range of all the different parameters must be set. For some parameters like the nominal power or the proportional factor, the range is equal to a value from the minimum of the range's value of the detailed model to the maximum of such range, multiplied by the number of components present on the detailed grid. Indeed, the equivalent model have to give the sum of the power given by all the components of the grid. For those parameters the initial value will be the sum of all the values of the components of the detailed model.

On the other hand, some parameters like the delay, the range of the equivalent model is the same as the range of the detailed model, since there is no sense to increase those kinds of parameters. For those parameters, the initial value is the mean of the values from the detailed model.
The different range and initial values of all parameters are given in the table 4.2.

block	parameter	range	initial value	unit
PLL	k_p	[60,120]	100	[1/s]
	k_i	[600,1200]	767	[1/s]
	w_c	[10 π,20 π]	13.7π	[rad/s]
BESS	$P_{nom,BESS}$	[3000,16000]	13000	[W]
	k_{pf}	[1000,16000]	9000	[W/Hz]
	k_{df}	[100,2000]	1100	[sW/Hz]
	T_B	[0.05,0.15]	0.095	[s]
	$f_{s,BESS}$	[0.01,0.1]	0.06	[Hz]
PV	$P_{nom,PV}$	[3000,16000]	11000	[W]
	p_f	[30,100]	50	[%]
	$f_{s,PV}$	[0.05,0.25]	0.145	[Hz]
	P_{ext}	[2000,16000]	9000	[W]

Table 4.2: Parameters' range and initial value in the equivalent model

Note that in the table 4.2, the maximum frequency deviation Δf_{max} is not there because it is already taken into account on the partial tripping.

4.3.3 Step 2 : Choice of the different frequency deviation

In order to train and to test the equivalent model, we must choose some frequency deviations. One or more will be use for the training step and the other for the test step.

On a grid, the frequency must be as constant as possible, and a small deviation can lead to several problems. Usually, a frequency deviation of 1 Hz is already huge, and a lot of components disconnect themselves to avoid damage. So, for the choice of the different deviations the 10 deviations present in the table 4.3 will be used.

deviation	1	2	3	4	5	6	7	8	9	10
Δf [Hz]	0.2	0.4	0.6	0.8	1	-0.2	-0.4	-0.6	-0.8	-1

Table 4.3: All frequency deviations for training and test

Note that positive Δf means an over-frequency deviation, while a negative one means an under-frequency deviation.

4.3.4 Step 3 : Training test of the equivalent

When the equivalent model has been initialised as well as the frequency deviations are set for the training and the test, the training step can start. The "training" means that for each parameter of the equivalent active components, we will find the value that minimizes the error. The used error formula is the mean of the absolute values of the differences between the power given by all the components present in the detailed model and the power given by the active component in the equivalent model, and can be written as:

$$e = \frac{\sum_{i=0}^{N} |P_{det,i} - P_{equ,i}|}{N} \tag{4.7}$$

Since the parameters are studied one by one, the order of them influences the final equivalent model. The influence of each parameter and their utility on the research will be analysed in the analysis chapter 5.2. The order of the parameters' study, their best trained values and the error at each step are given in the table 4.4 for a training deviation of 0.8 Hz. The step error in percentage is defined as:

$$error\ [\%] = \frac{error\ [W]}{P_{nom,BESS} + P_{nom,PV}} \tag{4.8}$$

order	studied parameter	best value	step error [W]	step error [%]
1	k_p of PLL	60	90	0.69
2	T_B of BESS	0.1	87.5	0.67
3	$P_{nom,PV}$ of PV	10000	87.4	0.67
4	k_i of PLL	600	84.6	0.65
5	$P_{nom,BESS}$ of BESS	3000	83.8	0.64
6	w_c of PLL	14 π	81.7	0.63
7	P_{ext} of PV	9000	81.7	0.63
8	$f_{s,BESS}$ of BESS	0.04	80.9	0.62
9	p_F of PV	50	79.7	0.61
10	k_{pf} of BESS	9000	79.7	0.61
11	k_{df} of BESS	1100	79.7	0.61
12	$f_{s,PV}$ of PV	0.14	79.7	0.61

Table 4.4: parameter study list and step error

We see that the error is decreasing during the training steps, even if the starting point is already quite good. That means that the ideas of the initial values are coherent. Also, some parameters do not seem to decrease the error. They may be discarded because of their lack of influence in the process. This will be analysed in the analysis chapter 5.2.

4.3.5 Step 4 : Test of the obtained equivalent

For now, the equivalent model works for a frequency deviation of 0.8 Hz, but we do not know if it works for other frequency deviations. To verify that the equivalent model is working, which means that it has the same behaviour as the detailed model for different type of frequency deviations, the equivalent will be tested with the different frequency deviations chosen at step 2. The different errors for each test deviation are shown on table 4.5. The type of error formula used is the same as in the training step (equation 4.7).

deviation	Δf [Hz]	error [W]	error [%]
1	0.2	158	1.22
2	0.4	432	3.32
3	0.6	287	2.21
4	0.8	80	0.62
5	1	89	0.68
6	-0.2	67	0.52
7	-0.4	629	4.84
8	-0.6	665	5.12
9	-0.8	133	1.02
10	-1	111	0.85

Table 4.5: Error value for the test frequency deviation

By looking at the values on the table 4.5, the error for the different deviations seams acceptable (<10 %), and so the methodology successfully stops here. There is no need to add a frequency deviation for the training.

4.4 Accuracy between detailed and aggregated models

Since the aggregated model is working, let's look more in details into the accuracy between the detailed and the equivalent models. For that we will look at all the graphs of the power given by active components in both models (same parameter used for the calculation of the error). All the plots are in the appendix A 6.1.1.

For the small over-frequency deviation (0.2-0.4 Hz), the equivalent model follows quite correctly the detailed model. The behaviour of the curve is similar, but a small offset is remaining due to a difference with the proportional coefficients. To have a better accuracy a smaller training deviation can be used.

For the other over-frequency deviation (0.6-1 Hz), the equivalent model is following the detailed model with a good accuracy. This is because those deviations are close to the training deviation. For the bigger deviation (0.8-1 Hz), the behaviour is easier to follow because the components are disconnected.

Regarding the under-frequency events, the results are less good. For the small deviations, there is an offset, but it stays reasonable.

For the big under-frequency deviation (0.8-1 Hz), as for the over-frequency deviations, the behaviour is easy to follow due to the disconnection of the components.

For frequency deviation where partial tripping happens (0.4-0.6 Hz), the offset is important, due to a wrong reduction of the nominal power arising from the partial tripping. This is due to a big variation of the tolerance to frequency deviation of the active components present on the detailed model. Note that if the tolerance of all the active components are the same, the accuracy of the model for all the variation of frequency becomes very good, as shown on the graphs in the appendix A 6.1.2. The influence of this tolerance will be developed in section 5.2.4.

4.5 Conclusion

Thanks to the Monte-Carlo methodology, it has been possible to model an equivalent aggregated model of a detailed model that contains active components. The accuracy between the detailed and the equivalent models is good enough to only use one frequency deviation for the training step. However, due to the different tolerances to frequency deviation of the different components, a partial tripping model has been added to the active components of the equivalent model. For frequency deviations inside such tolerance range and if the tolerance is too big, the equivalent model follows less correctly the detailed model.

Chapter 5

Analysis

5.1 Error calculation

For the training and the test steps of the research of the equivalent above, the type of error used was the mean of the absolute value of the error between the power given by the detailed model and that given by the equivalent model. However, using other types of error can change the result of the equivalent. For this analysis, we will study the influence of 3 different types of errors on the equivalent model and its resulting accuracy. The 3 types of error are the mean of the absolute value error, the root mean square error and the maximum error. The types of error are written in 5.1.

mean of absolute value error	root mean square error	maximum error
$e = \frac{\sum_{i=0}^{N} \lvert P_{det,i} - P_{equ,i} \rvert}{N}$	$e = \sqrt{\frac{\sum_{i=0}^{N} (P_{det,i} - P_{equ,i})^2}{N}}$	$e = max(\lvert P_{det,i} - P_{equ,i} \rvert) \; \forall i \in N$

Table 5.1: Different types of error

The 3 types of error are used in the training and test steps. The other characteristics of the simulations are the same as in the chapter 4, i.e. a training frequency deviation of 0.8 Hz. The best values of the different parameters found during the training step for each type of error are shown on table 5.2.

parameter	mean of absolute value error	root mean square error	maximum error
k_p of PLL	60	60	60
T_B of BESS	0.1	0.09	0.05
$P_{nom,PV}$ of PV	10000	8000	/
k_i of PLL	600	600	1100
$P_{nom,BESS}$ of BESS	3000	7000	9000
w_c of PLL	14 π	15 π	14 π
P_{ext} of PV	9000	9000	9000
$f_{s,BESS}$ of BESS	0.04	0.01	0.02
p_F of PV	50	70	30
k_{pf} of BESS	9000	9000	10000
k_{df} of BESS	1100	1100	1100
$f_{s,PV}$ of PV	0.14	0.05	0.16

Table 5.2: Parameters' value for different types of error

By looking at the different parameters as a function of the type of error used, we see that the values are often similar. For the maximum error, the nominal power of the PV panel is not studied because the results gives 0 as the best value, which does not make a lot of physical sense; so $P_{nom,PV}$ stays to its initial value. The nominal power of the BESS increases to compensate the decrease of $P_{PV,nom}$ in the different types of errors. For the maximum error, k_i of PLL is much bigger to compensate the big amplitudes at the start of the frequency deviation, even it that causes more oscillations on the measurement of the frequency. Since the influence of the PV is less important for the RMSE and the maximum error, the proportional factor p_F is also less important. The minimal value for the activation of the controller $f_{s,BESS}$ and $f_{s,PV}$ also have different values, but the difference does not have a big influence since the studied variations are bigger.

5.1.1 Accuracy of the detailed model for different types of error

Since the way to calculate the error is different, there is no sense to analyse the error's value. But we can look at the different graphs obtained for each frequency deviation, for each type of error. The graphs for the mean of absolute value error are shown in appendix A 6.1.1, while the graphs for the root mean square error and the maximum error are shown in appendix B 6.2.1 and 6.2.2 respectively.

For big frequency deviations, when all the components are disconnected, the behaviour of the aggregate model is quite similar, even if the accuracy is best for the mean of absolute value error, then for the root mean square, and then for the maximum value error. For frequency deviations inside the different tolerances of the active components of the detailed model, the accuracy is less good for all types of error, but usually the best error type corresponds to the mean of the absolute value, since the offset between the detailed and the equivalent model is there less important than for the other types of error. However, for some frequency deviations, the other type of error gives the best equivalent model. The following table shows for each deviation, which type of error gives the best equivalent model. The types of error are classified from the best (1) to the worst (3).

deviation	mean of absolute value error	root mean square error	maximum error
1	2	3	1
2	1	2	3
3	2	3	1
4	1	2	3
5	1	2	3
6	1	2	3
7	1	3	2
8	3	1	2
9	1	2	3
10	1	2	3

Table 5.3: Ranking of the types of error in function of the frequency deviation

The table clearly shows that usually, this is the mean of absolute value that gives the best equivalent error.

5.2 Analysis of the parameters of the active components

If we look at the simulation time needed to find the equivalent model and to test it, it takes 26 minutes in average, which is quite long. An idea to reduce this time is to look at the parameters' utility and influence. The utility's analysis is about the difference between the initial value and the best value of one parameter, to see if the value's research for this parameter is useful. The influence's analysis is the dependence of the given power by the active components as a function of the value of one parameter.

If some parameters are not useful or do not have any influence, they could be discarded in order to reduce the computation time.

5.2.1 Utility in the research

To assess whether a parameter is useful, we will look at the initial value and at the best value for 2 different training deviations (Δf = 0.4, 0.8 Hz) in order to have one case where all the parameters are used in the frequency deviation, and one other where the active components are disconnected. The best parameters' value for those 2 training deviations are shown on table 5.4.

parameter	initial value	best value for Δf = 0.4 Hz	best value for Δf = 0.8 Hz
k_p of PLL	100	60	60
T_B of BESS	0.095	0.09	0.1
k_i of PLL	767	700	600
$P_{nom,PV}$ of PV	11000	16000	16000
$P_{nom,BESS}$ of BESS	13000	16000	4000
w_c of PLL	13.7 π	14 π	14 π
P_{ext} of PV	9000	9000	9000
$f_{s,BESS}$ of BESS	0.06	0.01	0.04
p_F of PV	50	100	50
k_{pf} of BESS	9000	9000	9000
k_{df} of BESS	1100	1200	1100
$f_{s,PV}$ of PV	0.145	0.13	0.12

Table 5.4: Parameters' utility analysis : parameter's best value

Furthermore, when there is almost no difference between the initial and the best value, as expected, the step error does not decrease a lot. The step errors for the 2 training deviations are shown on table 5.5.

parameter	step error [W] for $\Delta f = 0.4$ Hz	step error [W] for $\Delta f = 0.8$ Hz
k_p of PLL	669	93
T_B of BESS	667	89.8
k_i of PLL	667	88.1
$P_{nom,PV}$ of PV	567	85.2
$P_{nom,BESS}$ of BESS	567	84.7
w_c of PLL	567	83.8
P_{ext} of PV	567	83.8
$f_{s,BESS}$ of BESS	473	82.5
p_F of PV	98	82.2
k_{pf} of BESS	98	82.2
k_{df} of BESS	95	82.2
$f_{s,PV}$ of PV	87	81.8

Table 5.5: Parameters' utility analysis : step error

By looking at the 2 tables 5.4 and 5.5, we see that for some parameters, the best value is almost similar to the initial value and that the step error does not decrease after the value's research of those parameters. This is the case for T_B, w_c, P_{ext}, k_{pf} and k_{df}. To reduce the computation effort, those parameters will be removed from the training step, except if they have a big influence on the given power. That will be analysed in the next section 5.2.2.

5.2.2 Influence of the parameters

The influence of a parameter is shown by the impact the different values of their range have on the given power of the active components. This impact can be an offset, a delay or a variation in the peaks' amplitude depending on their function in the controller. To look at the importance of all parameters, a training frequency deviation of 0.4 Hz is used so that all the parameters can have an influence since most of the active components are still connected.

First, we will look at the impact of the parameters of the PLL, i.e. k_p, k_i and w_c.

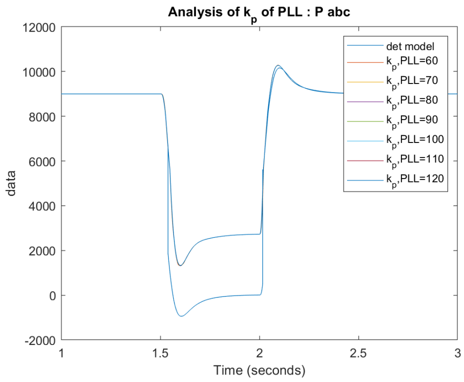

(a) Influence of k_p of PLL

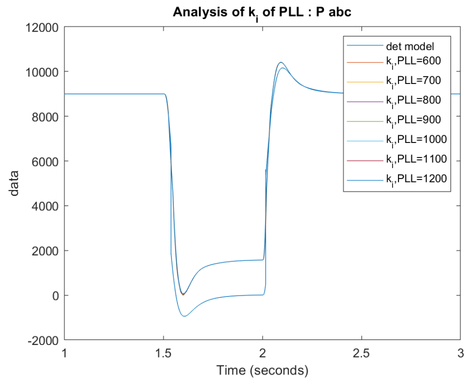

(b) Influence of k_i of PLL

Figure 5.1

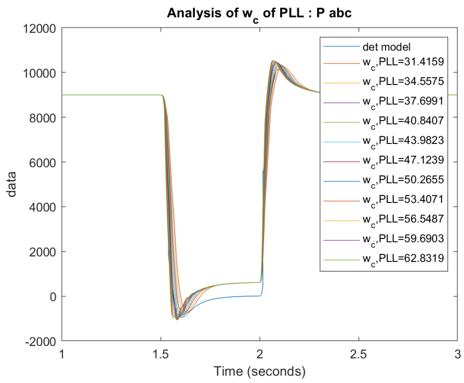

Figure 5.2: Influence of w_c of PLL

By looking at the figure 5.1a, 5.1b and 5.2, we see that the different parameters of the PLL have a negligible impact on the power given. So, in order to decrease the computation time, those parameters will be removed from the training step and will stay at their initial value.

Second the BESS parameter are analysed, which correspond to $P_{nom,BESS}$, k_{pf}, k_{df}, $f_{s,BESS}$ and T_B.

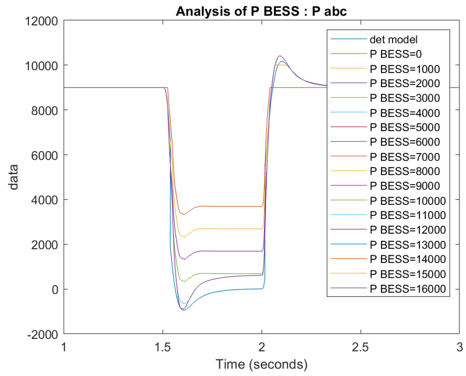

Figure 5.3: Influence of $P_{nom,BESS}$ of BESS

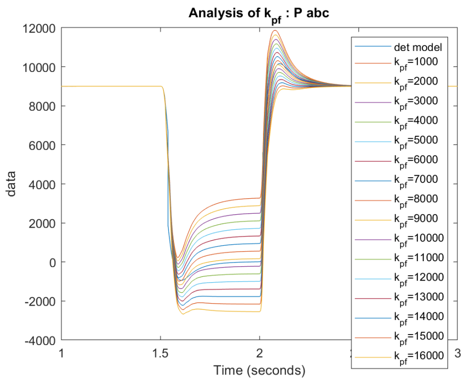

(a) Influence of k_{pf} of BESS

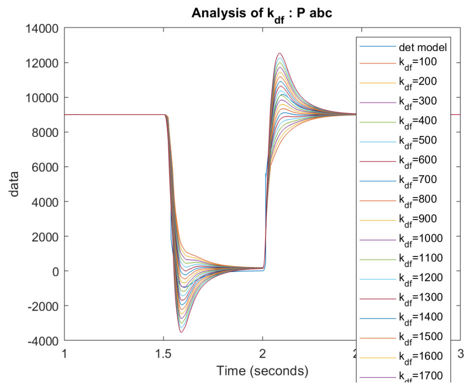

(b) Influence of k_{df} of BESS

Figure 5.4

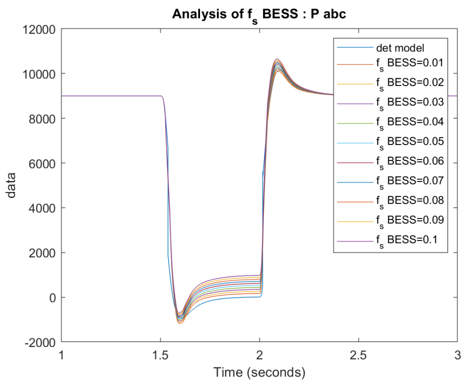

(a) Influence of $f_{s,BESS}$ of BESS

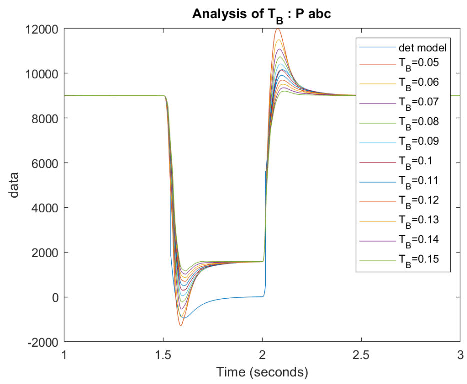

(b) Influence of T_B of BESS

Figure 5.5

The parameters have a different impact. $P_{nom,BESS}$, k_{pf} and $f_{s,BESS}$ create an offset of the power given during the frequency deviation. However, the offset's amplitude is different depending on the parameter studied. $P_{nom,BESS}$ have a very big impact, so it is needed to be kept in the training step. $f_{s,BESS}$ will also be kept because even if the influence is smaller, it impacts the resulting error as we can see on the table 5.5. However, for k_{pf}, even if it has an impact on the power given, the fact that the initial and the best value are similar makes the research of the best value useless, so it will be removed from the training step. The 2 other parameters, k_{df} and T_B have more an impact on the peaks' amplitude. For both parameters, the initial value is already very good, so they will also be discarded from the training step for computation time reasons.

Third the parameters of the PV panel are analysed, which means $P_{nom,PV}$, P_{ext}, p_F and $f_{s,PV}$.

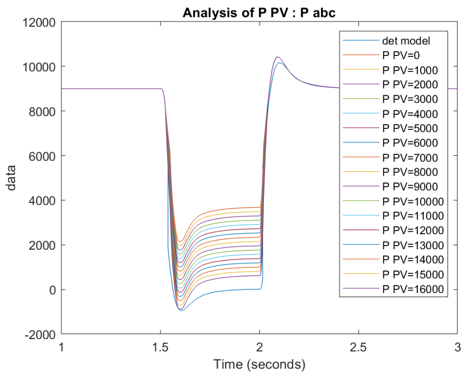

(a) Influence of $P_{nom,PV}$ of PV

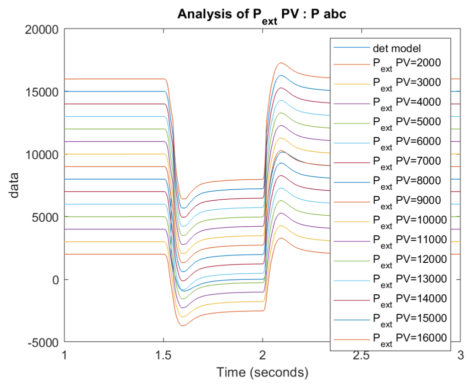

(b) Influence of P_{ext} of PV

Figure 5.6

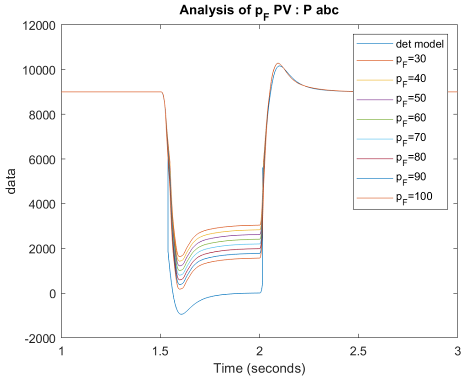

(a) Influence of p_F of PV

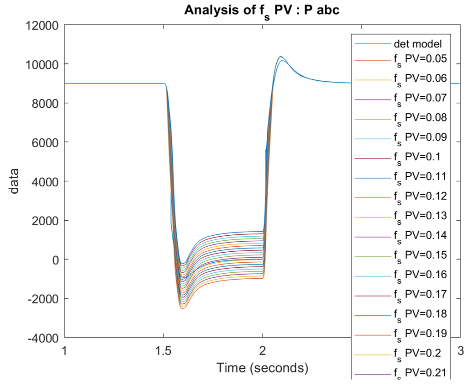

(b) Influence of $f_{s,PV}$ of PV

Figure 5.7

Contrary to the BESS, all the parameters of the PV have an offset influence during the frequency deviation, but for P_{ext} it also influences the power given at f_0, which makes it an important parameter and so even if the initial and the best values are the same, it will be kept in the training step. $P_{nom,PV}$ and p_F will also be kept, since their influence is not negligible and the relative step error is quite large 5.5. For $f_{s,PV}$ since the relative influence is quite small and the relative step error is quite small due to the fact that is the last parameter analysed, it can be removed from the training step without altering the equivalent model.

5.2.3 Test of equivalent model with useless parameters discarded

If we look at the more useful parameters to be studied, there are only 5 of them, i.e. $P_{nom,BESS}$, $f_{s,BESS}$, $P_{nom,PV}$, P_{ext} and p_F. As in the parameter influence analysis, a training frequency deviation of 0.4 Hz will be used. The results of the other frequency deviation are given on the table 5.6. To have a good comparison, the first 2 columns of error will be when all the parameters are present in the training step, while the 2 right-most error columns will be when only the 5 more useful parameters are taken in the training step.

deviation	Δf [Hz]	error [W]	error [%]	error [W]	error [%]
1	0.2	324	1.01	266	0.83
2	0.4	87	0.27	112	0.35
3	0.6	671	2.1	630	1.97
4	0.8	128	0.4	98	0.31
5	1	150	0.47	101	0.32
6	-0.2	139	0.43	139	0.43
7	-0.4	834	2.61	817	2.54
8	-0.6	396	1.24	385	1.23
9	-0.8	172	0.54	122	0.38
10	-1	159	0.5	100	0.31

Table 5.6: Error value for the test frequency deviation with all parameters and with only the important ones

Note that for both cases, the best value of $P_{nom,BESS}$ and $P_{nom,PV}$ are 16 000 W and 16 000 W, respectively.

By looking at the errors, the training step with only the 5 useful parameters is working as good as when all the parameters are studied. For some deviations, it even seems that it is better to do only the training for those parameters and not for all. It is because the initial value of some parameters is equal to the mean of the parameters of the detailed model, so the mean value can be different values that the ones studied, and those mean values are better.

By looking at the graphs of the power for the different deviation in appendix C 6.3.1 for the results with the training with all the parameters and in appendix C 6.3.2 for the results with the training with the useful parameters, and by comparing the different graphs, the behaviour seams very similar. We can conclude that the equivalent model with only useful parameters trained works fine.

With 5 parameters for the training step, the simulation time decreases to 16 minutes, which is 62 % of the initial computation time and therefore constitutes a good improvement.

With only 5 parameters, it seems possible to find a better optimisation by studying multiple parameters at the same time. So, the 3 PV's parameters and the 2 BESS's parameters have been trained at the same time, which means all the possible configurations with their values inside their range have been tested, while before only one parameter was tested while the others were set to constant values (initial or best). This method takes much more time (2 hours) since more possibilities have to be tested. However, the resulting parameters' value are the same as when the parameters are studied one at a time. Consequently, the results are not better with this methodology, which will then not be reused since it only increases the computation time.

5.2.4 Influence of the tolerance to frequency deviation of active components

In the section 4.3, we saw that the tolerance to frequency deviation has a big impact on the accuracy of the equivalent model and if this tolerance is different for the active components, the model does not work correctly at some frequency deviations.

By making simulation test and model analysis, 2 main points stand out. The first one is that when tolerance is equal to tested frequency deviations, the associate component oscillates between connected and disconnected, which creates big variation on the given power, and reduces the accuracy of the model.

The second one is that because the PV panel controller has only a primary factor and not an inertia factor, the PV panel is more influenced by the variance of its tolerance. On the other hand, the BESS model, which has a primary and an inertia factor, allows the tolerance's variance of the BESS to be bigger. By trials and errors, an acceptable range of tolerance for PV and BESS can be found. For the PV panels the tolerance to frequency deviation must be between 0.42 and 0.58 Hz and for the BESS between 0.42 and 0.68 Hz.

The results with those extreme values are shown on appendix C 6.3.3, trained with a frequency deviation of 0.4 Hz. By looking at all the graphs we see that the model is much more accurate in this case than the one in 4.3. So, even if the model works better when all the components have the same tolerance, a variance in the tolerance to frequency deviation is still acceptable.

5.3 Voltage analysis

As explained since the beginning, when a frequency deviation occurs, the BESS and the PV panel respond to bring or to absorb more/less power in order to help the transmission grid to tackle this frequency problem. However, this variation of active power modifies the voltage level of the distribution grid. If this variation is too big, it could lead to problems on the grid and to disconnections of loads or components present on the grid. To be sure that the model stays realistic, a voltage analysis must be performed as a function of the response of the active components to frequency deviation.

First, let's look at the voltage at the MV level of the grid in case of frequency deviation, for the detailed and equivalent models. The voltage's graph is shown on figure 5.8.

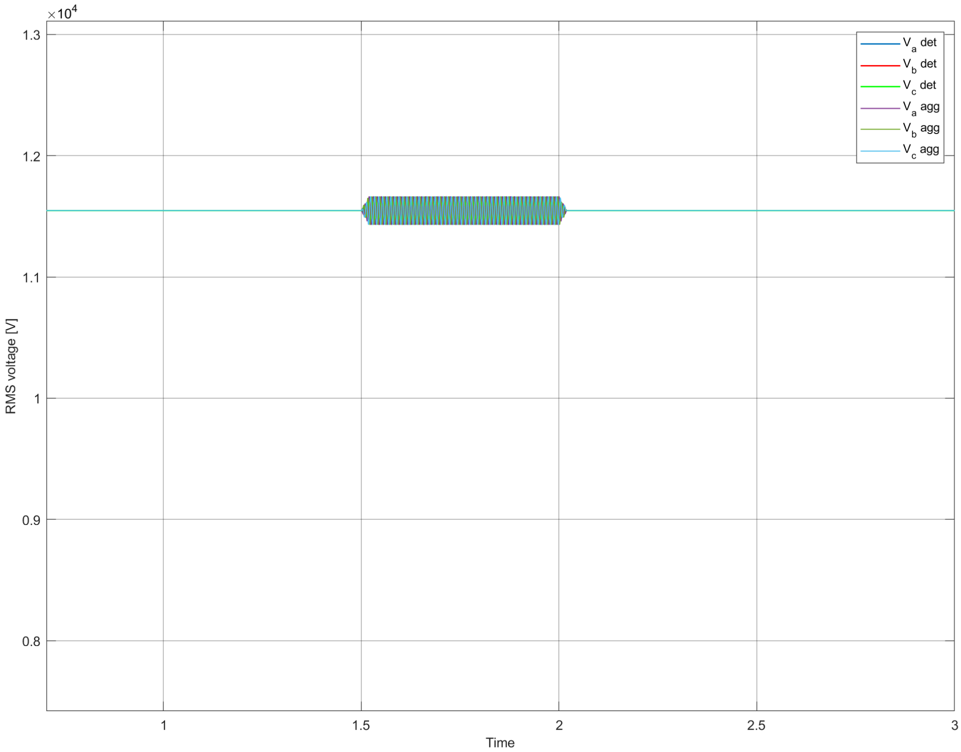

Figure 5.8: Voltage at MV level

We see that the voltage variation is very small (0.0101 pu), so there shall not be issue on the MV side.
For assessing the voltages on the LV side, the voltage just near the active's components in the detailed model are analysed, because this corresponds to the nearest point of the variation of active power. For the equivalent model, the voltage will also be measured at the output of the active components. The different voltage graphs are shown on the following figures.

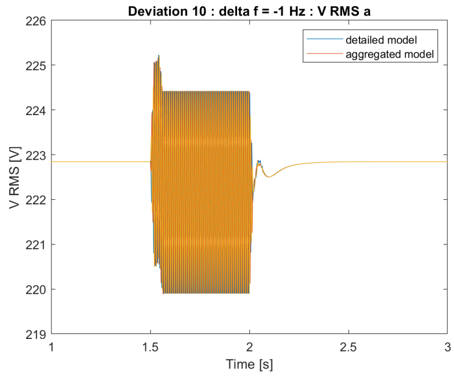

Voltage at the output of the active component A

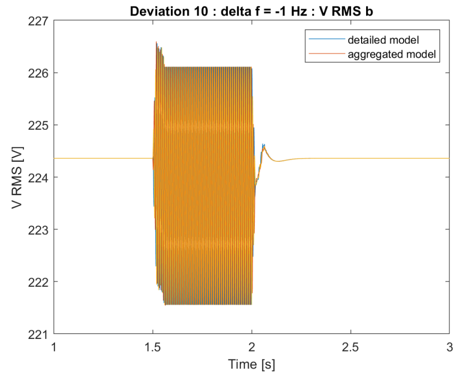

Voltage at the output of the active component B

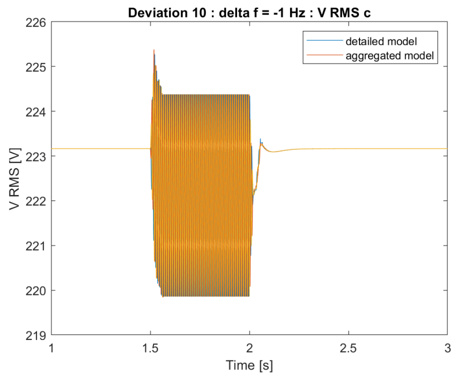

Voltage at the output of the active component C

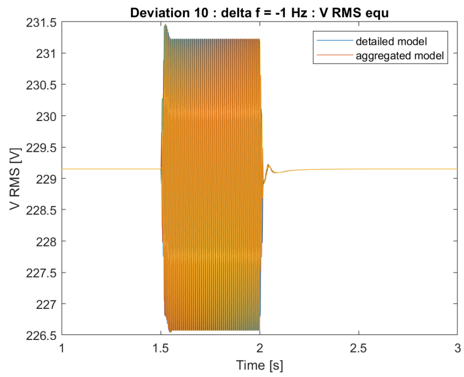

Voltage at the output of the equivalent active components

For all the different voltages, the maximum voltage deviation is 3 V, which correspond to 0.014 pu. It can be assumed that the active components have a negligible impact on the voltage level, and so that we shall not be afraid of voltage problems.

5.4 Dynamic load

Until now, the different loads present on the grid were only passive loads, which means that they are not influenced by the frequency deviation. To be more realistic, a load dependency on the frequency has to be implemented. The relation between the load's power and the frequency can be written as in the following equation [21].

$$P_{load} = P_{load,0}(1 + D_p \frac{\Delta f}{f_0}) \tag{5.1}$$

Where $P_{load,0}$ is the load's power at nominal frequency f_0, and D_p is the damping factor, i.e. the proportion of the load's power that is influenced by Δf. The damping factor varies as a function of the distribution grid we want to model, but the range of magnitude is of the order of 0.01 [pu/Hz] [49] [50].

To implement the frequency dependency, for each load, a 3-phase dynamic load [45] is added in parallel to the passive load, and it shall model the dependent part of the load. The representation of the detailed model is shown on figure 5.11. A bigger representation of the model is shown on appendix D 6.4.

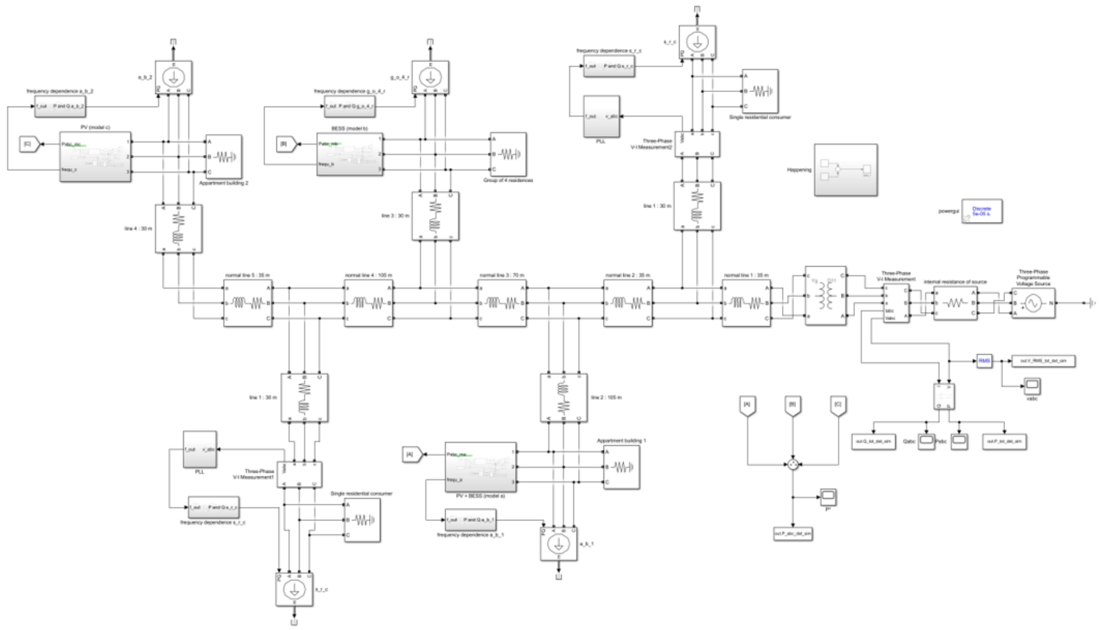

Figure 5.11: Detailed grid with dynamic loads

To be coherent, the equivalent load on the aggregated model have also been implemented in this work, with a dynamic load in parallel to a passive load, as in the detailed model.
In order to perform a meaningful comparative analysis, the same training frequency as in section 4.3 (0.8 Hz) is considered. The results of the test of the equivalent are shown on table 5.7 and the graphs of the power are in the appendix D 6.4.1.

deviation	Δf [Hz]	error [W]	error [%]	error from 4.3 [%]
1	0.2	140	0.7	1.22
2	0.4	475	2.38	3.32
3	0.6	300	1.5	2.21
4	0.8	82	0.41	0.62
5	1	90	0.45	0.68
6	-0.2	67	0.34	0.52
7	-0.4	737	3.69	4.84
8	-0.6	562	2.81	5.12
9	-0.8	135	0.68	1.02
10	-1	114	0.57	0.85

Table 5.7: Error value for the test frequency deviation with dynamic loads

Note that the nominal values of the active components in this test are different than the ones in 4.3. Indeed, in this test $P_{nom,PV} = 16000$ W and $P_{nom,BESS} = 4000$ W. This is why the errors in percentage for the model with dynamics loads are smaller than in 4.3.

By looking at the errors and the figure shown on the appendix D, the equivalent model stays accurate even if the loads have a dynamic dependency on frequency. The behaviours of the power given by the active components as a function of the frequency deviation are the same as in the test section 4.3 for which the graphs are in appendix A 6.1.1. In consequence, the dynamic dependency of the load has a small impact on the equivalent model and so we can neglect it.

5.5 Complexity of the grid

The actual benchmark herein studied as complex reality model, remains nevertheless quite simple, since it only encompasses 5 different loads, a few lines and 2 active components of each type. This section will show that, should the equivalent model methodology also work for more complex models, which would require much higher computation time, even more interest would be assigned to having an equivalent model that reduces such computation time.

The more complex grid considered has 9 PV panel and 9 BESS for the active components, and 15 single residential consumers, 6 groups of 4 residences and 12 apartment buildings for the passive loads. All those components are spread on 3 similar grids connected to the transmission grid trough a transformer. This grid is shown on the figure 5.12. A bigger representation of the detailed grid is shown on appendix E 6.5.

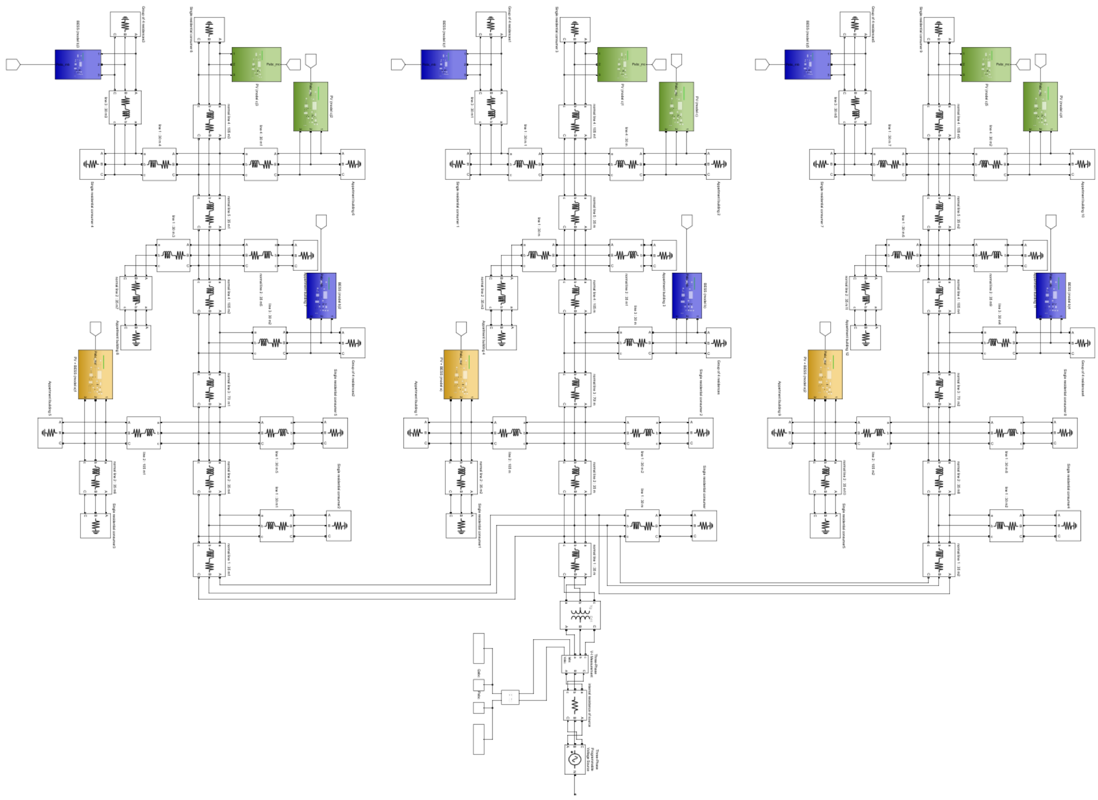

Figure 5.12: More complex grid

As for the other analysis, the same training frequency as in 4.3 will be be used, to be coherent. The results of the test with other deviations are given on the table 5.8.

deviation	Δf [Hz]	error [W]	error [%]	error from 4.3 [%]
1	0.2	1029	1.21	1.22
2	0.4	2802	3.3	3.32
3	0.6	1531	1.8	2.21
4	0.8	418	0.49	0.62
5	1	487	0.57	0.68
6	-0.2	811	0.95	0.52
7	-0.4	4825	5.68	4.84
8	-0.6	1155	1.36	5.12
9	-0.8	661	0.78	1.02
10	-1	587	0.69	0.85

Table 5.8: Error value for the test frequency deviation with a more complex grid

By looking at the error in watts, the equivalent model seams to not work, but it is because the power given by the active components is much higher since there are many more PVs and BESS. Indeed $P_{nom,PV} = 70000$ W and $P_{nom,BESS} = 15000$ W. By looking at the error in term of percentage, the results of the more complex grid are very similar to the ones of the simple grid.

To be more consistent, we can further look at the different graphs of the given power, illustrated in appendix E 6.5.1. By observing all the graphs, the different behaviours are very similar to the ones obtained in 4.3 and presented in appendix A 6.1.1. For both tests, the model has more difficulties to be accurate for deviation 7 and 8, due to the difference of the tolerance to frequency deviation.

If all the different active components of the grid have the same frequency tolerance, as for the simpler detailed model 6.1.2, the accuracy becomes very good, as shown in the figures presented in the appendix E 6.5.2.

We can conclude that at this stage, the complexity of the model does not have a big impact on the equivalent model's accuracy. So, this methodology can be used to model more complex grids, i.e. to model a lot of detailed models through their equivalent model in order to reduce the computation time.

5.6 Conclusion

The methodology used to find an equivalent model has been studied on multiple aspects. First the type of error used is studied, which reveal that the best one is the mean of the absolute error. Then the influence and the utility of each parameter of the active components has been analysed. This shows that some parameters have a negligible impact of the resulting power, and that some others do not have to be studied since their initial value is already the best. Those parameters can be removed from the training step to decrease the computation time. After, the voltage variation is studied: with a frequency deviation and the associated response of the active component, the voltage variation by the amplitude is so small that we do not have to be worried about the voltage deviation. To be more realistic, a dependency on frequency of the loads have been added, but it does not seem to have a big influence on the equivalent model's methodology. This is the same conclusion for more complex grids, i.e. grids with more active components, more lines and more loads.

Conclusion

In this work, the reaction and the control of active components, like BESS and PV panels present on a distribution grid, in case of frequency variations have been studied. Following proper understanding of real BESS model, simpler models of BESS and PV panel have been implemented. Then an equivalent model of a distribution grid with active components that will have the same behaviour to frequency issues has been developed and analysed.

Understanding of the components and the controller of the BESS corresponding to real model has constituted an important initial step in the process of this work. A DC battery is connected to the AC voltage with a VSC and then a LCL filter to have a better signal. The amount of power given/absorbed by the battery is controlled by the pulses of the VSC. In the controller, a PLL first measures the frequency, then the related power setpoint is given by the frequency controller which takes care of the frequency deviation and of the RoCoF. At the end the pulses are obtained with a PQ control and a PWM generator.

Based on the above, a simplified model of BESS and PV generator has been proposed and implemented in order to place active components on a distribution grid. The accuracy between the real BESS model and the simplified one has been verified.

The work then proceeded to distribution grid modelling. In order to obtain an equivalent model of a reference distribution grid, the Monte-Carlo methodology has been used with a "grey-box" approach of the parameters. The accuracy of the equivalent model developed, is proven to be good and robust. There is nevertheless an exception when the variance tolerance to frequency deviation of the different active components present on the grid is too high: in this case, even with the partial tripping added to the equivalent active components, the behaviour of the equivalent model is less accurate.

Multiple aspects of the equivalent model have been studied. First the type of error calculation used during the research of the equivalent model has been analysed, showing that the mean of the absolute value appears to be the best type of error. Then the influence and the utility of the different parameters of the active components have been studied in order to discard the few useless ones, and thereby to have a better simulation time while maintaining the same accuracy of the model. The voltage has then been addressed, and the resulting voltage deviations due to the behaviour of the active components are minimal; the voltage therefore does not need to be controlled. Finally, a frequency dependency of the loads spread on the grid has been added, but it has not a real impact neither on the equivalent model, nor on more complex distribution grids. Therefore, the equivalent model can be used for more complex distribution grids with load frequency dependency.

Globally, the methodology aiming at having an equivalent model of an active distribution grid that would exhibit the same reaction to frequency variations works. The accuracy of the equivalent model mainly depends on the variance of the tolerance to frequency issues. If this variance is too high, the equivalent model has difficulties to correctly follows the behaviour of the detailed grid, although remaining within an acceptable range of the variance is generally affordable.

However, the variance of the tolerance to frequency deviation of the different active components present on the grid remains the main influencing parameter of the equivalent model. Even if it has been studied in the work and considered with a linear partial tripping. One way to improve the model could be to improve the partial tripping with a non-linear relationship between the frequency deviation and the power setpoint fraction F_f (see section 4.2.2).

Also, looking forward, some hypothesis taken might be challenged and/or improved, such as the symmetry tolerance to frequency deviation of the active components, the loads that are only resistive and non-reactive, the non-grounded lines, the MV level modelled has a perfect 3-phase sources, etc. One has to keep in mind that the models presented in this work are quite ideal ones, and that several neglected characteristics could have an influence on the model.

By hypothesis, only LV distribution grids have been analysed in this work. Further works could be performed to tune the equivalent model methodology in order to be able to model equivalent MV distribution grid connected to one HV transmission grid, and to decrease further the complexity of the associated model.

Bibliography

[1] De Jeager E. Photovoltaic systems. *LENVI2007*, Solar Energy:6, 2021.

[2] Eckehard Troester. New german grid codes for connecting pv systems to the medium voltage power grid. pages 1–4, 2009.

[3] De Jeager E. Electrical interfaces associated with pv modules. *LENVI2007*, Solar Energy, 2021.

[4] De Jeager E. Wind energy conversion. *LENVI2007*, Wind Energy, 2021.

[5] De Jeager E. Dynamic modelling of synchronous machines. *LELEC2595*, Generators, 2022.

[6] Kristien Clement-Nyns, Edwin Haesen, and Johan Driesen. The impact of vehicle-to-grid on the distribution grid. *Electric Power Systems Research*, 81(1):185–192, 2011.

[7] Model Sport. Nombre de voitures électriques en france en 2021. `https://model-sport.com/blogs/news/nombre-voitures-electriques-france-2021`, May 2022.

[8] Moba. Tout sur la batterie tesla. `https://get-moba.com/tout-sur-la-batterie-tesla/`, May 2022.

[9] ENEDIS. Postes source et postes de répartition hta/hta. `https://data.enedis.fr/explore/dataset/poste-source/map/?location=3,49.5368,3.69141&basemap=jawg.streets`, May 2022.

[10] Selectra. En 2040, le réseau pourra-t-il tenir la consommation des véhicules électriques ? `https://selectra.info/energie/actualites/insolite/consommation-vehicules-electriques-france-2040`, May 2022.

[11] Amin Kargarian Marvasti, Yong Fu, Saber DorMohammadi, and Masoud Rais-Rohani. Optimal operation of active distribution grids: A system of systems framework. *IEEE Transactions on Smart Grid*, 5(3):1228–1237, 2014.

[12] Wikipedia. Enedis. https://fr.wikipedia.org/wiki/Enedis#cite_note-7, May 2022.

[13] Enedis. Postes de distribution publique (postes hta/bt). https://data.enedis.fr/explore/dataset/poste-electrique/map/?location=3,31.80289,-40.16602&basemap=jawg.streets, May 2022.

[14] Chaspierre G., Panciatici P., and Van Cutsem T. Aggregated dynamic equivalent of a distribution system hosting inverter-based generators. *Proc. 20th PSCC conference*, Dublin (Ireland), 2018.

[15] Chaspierre G, Ghazavi Dozein M., Denis G., Panciatici P., and Van Cutsem T. Dynamic equivalent of a real distribution grid hosting photovoltaic and synchronous generators. *CIGRE Science and Engineering*, 2021.

[16] Yihui Zuo, Mario Paolone, and Fabrizio Sossan. Effect of voltage source converters with electrochemical storage systems on dynamics of reduced-inertia bulk power grids. *Electric Power Systems Research*, 189:106766, 2020.

[17] Jiefeng Hu, Yinghao Shan, Josep M. Guerrero, Adrian Ioinovici, Ka Wing Chan, and Jose Rodriguez. Model predictive control of microgrids – an overview. *Renewable and Sustainable Energy Reviews*, 136:110422, 2021.

[18] Arrigo F. Mazza A. Bompard E. Carpaneto E. Chicco G. Mosca, C. and P. Cuccia. Mitigation of frequency stability issues in low inertia power systems using synchronous compensators and battery energy storage systems. *IET Generation, Transmission and Distribution*, 13(17):3951–3959, 2019.

[19] Lucian Toma, Mihai Sanduleac, Stefan Andrei Baltac, Francesco Arrigo, Andrea Mazza, Ettore Bompard, Aysar Musa, and Antonello Monti. On the virtual inertia provision by bess in low inertia power systems. pages 1–6, 2018.

[20] Giorgio Graditi, Roberto Ciavarella, and Maria Valenti. An innovative bess management for dynamic frequency restoration. pages 1–5, 2017.

[21] G. Chaspierre. Reduced-order modelling of active distribution networks for large-disturbance simulations. *Ph.D. dissertation, University of Liege (Belgium)*, October, 2020.

[22] Ahvand Jalali and Mohammad Aldeen. Dynamic voltage stability procurement of power systems using energy storage devices. pages 1–6, 2017.

[23] Ahvand Jalali, Mehdi Ghazavi Dozein, and Pierluigi Mancarella. Frequency stability provision from battery energy storage system considering cascading failure s with applications to separation events in australia. pages 1–6, 2019.

[24] Youngsang Bae, Trung-Kien Vu, and Rae-Young Kim. Implemental control strategy for grid stabilization of grid-connected pv system based on german grid code in symmetrical low-to-medium voltage network. *IEEE Transactions on Energy Conversion*, 28(3):619–631, 2013.

[25] Ioan Serban and Corneliu Marinescu. Control strategy of three-phase battery energy storage systems for frequency support in microgrids and with uninterrupted supply of local loads. *IEEE Transactions on Power Electronics*, 29(9):5010–5020, 2014.

[26] Deepak Pullaguram, Sukumar Mishra, Nilanjan Senroy, and Monish Mukherjee. Design and tuning of robust fractional order controller for autonomous microgrid vsc system. *IEEE Transactions on Industry Applications*, 54(1):91–101, 2018.

[27] Thai-Thanh Nguyen, Hyeong-Jun Yoo, and Hak-Man Kim. Application of model predictive control to bess for microgrid control. *Energies*, 8(8):8798–8813, 2015.

[28] Jon San-Sebastian, Ion Etxeberria-Otadui, Alejandro Rujas, Jon Andoni Barrena, and Pedro Rodriguez. Optimized lcl filter design methodology applied to mv grid-connected multimegawatt vsc. pages 2506–2512, 2012.

[29] Mohamed Azab. Multi-objective design approach of passive filters for single-phase distributed energy grid integration systems using particle swarm optimization. *Energy Reports*, 6:157–172, 2020.

[30] Marinescu C. Serban, I. and R. Teodorescu. Energy storage systems impact on the short-term frequency stability of distributed autonomous microgrids, an analysis using aggregate models. *IET Renewable Power Generation*, 7(5):531–539, 2013.

[31] I. Serban and C. Marinescu. Battery energy storage system for frequency support in microgrids and with enhanced control features for uninterruptible supply of local loads. *International Journal of Electrical Power and Energy Systems*, 54:432–441, 2014.

[32] Francisco Sánchez and Francisco Gonzalez-Longatt. Optimization of frequency controller parameters of a bess by considering rate of change constraints. pages 1–6, 2019.

[33] P. Panciatici G. Chaspierre and T. Van Cutsem. Dynamic equivalent of a distribution grid hosting dispersed photovoltaic unit. *Proc. IREP'17 Symposium*, Espinho (Portugal), 2017.

[34] Gilles Chaspierre, Guillaume Denis, Patrick Panciatici, and Thierry Van Cutsem. An active distribution network equivalent derived from large-disturbance simulations with uncertainty. *IEEE Transactions on Smart Grid*, 11(6):4749–4759, 2020.

[35] Gilles Chaspierre, Guillaume Denis, Patrick Panciatici, and Thierry Van Cutsem. Dynamic equivalent of an active distribution network taking into account model uncertainties. pages 1–6, 2019.

[36] MathWorks. Two-level converter. `https://nl.mathworks.com/help/physmod/sps/powersys/ref/twolevelconverter.html`, January 2022.

[37] De Jeager E. Pv installations: electrical interfaces and control. *LENVI2007*, Solar Energy:10, 2021.

[38] Bekemans M. Dc to ac converter. *LELEC2660*, 2020.

[39] MathWorks. Three-phase transformer (two windings). `https://nl.mathworks.com/help/physmod/sps/powersys/ref/threephasetransformertwowindings.html?s_tid=doc_ta`, January 2022.

[40] S. Canevese, A. Gatti, E. Micolano, L. Pellegrino, and M. Rapizza. Battery energy storage systems for frequency regulation: Simplified aging evaluation. pages 291–297, 2017.

[41] MathWorks. abc to dq0, dq0 to abc. `https://nl.mathworks.com/help/physmod/sps/powersys/ref/abctodq0dq0toabc.html?s_tid=doc_ta`, January 2022.

[42] Next. When and how is the fcr activated? `https://www.next-kraftwerke.com/knowledge/frequency-containment-reserve-fcr#when-and-how-is-the-fcr-activated`, June 2022.

[43] MathWorks. Active distribution system with distributed generation. `https://nl.mathworks.com/matlabcentral/fileexchange/71534-active-distribution-system-with-distributed-generation?s_tid=srchtitle`, January 2022.

[44] MathWorks. Pwm generator (2-level). `https://nl.mathworks.com/help/physmod/sps/powersys/ref/pwmgenerator2level.html?s_tid=doc_ta`, January 2022.

[45] MathWorks. Three-phase dynamic load. https://nl.mathworks.com/help/physmod/sps/powersys/ref/threephasedynamicload.html?s_tid=doc_ta, January 2022.

[46] Stavros Papathanassiou, Nikos Hatziargyriou, Kai Strunz, et al. A benchmark low voltage microgrid network. pages 1–8, 2005.

[47] MathWorks. Three-phase series rlc load. https://nl.mathworks.com/help/physmod/sps/powersys/ref/threephaseseriesrlcload.html, April 2022.

[48] Butagaz. Production électrique annuelle des panneaux solaires : quel calcul ? en hiver ? https://solaire.butagaz.fr/faq/calcul-production-electrique-annuelle-panneau-solaire, June 2022.

[49] Shuo Liang, Weidong Chen, Liwen Qin, Yuchuan Qin, and Lingfeng Wen. Adaptive damping factor control strategy of inverter interfaced distributed generators based on virtual synchronous generator technology. pages 4202–4207, 2018.

[50] Raza Haider Muhammad Omer Khan Chul-Hwan Kim MUHAMMAD SAEED UZ ZAMAN, Syed Basit Ali Bukhari. Effects of modified inertia constant and damping coefficient on power system frequency response. Gazi University.

Chapter 6

Appendix

6.1 Appendix A

Detailed model of the grid

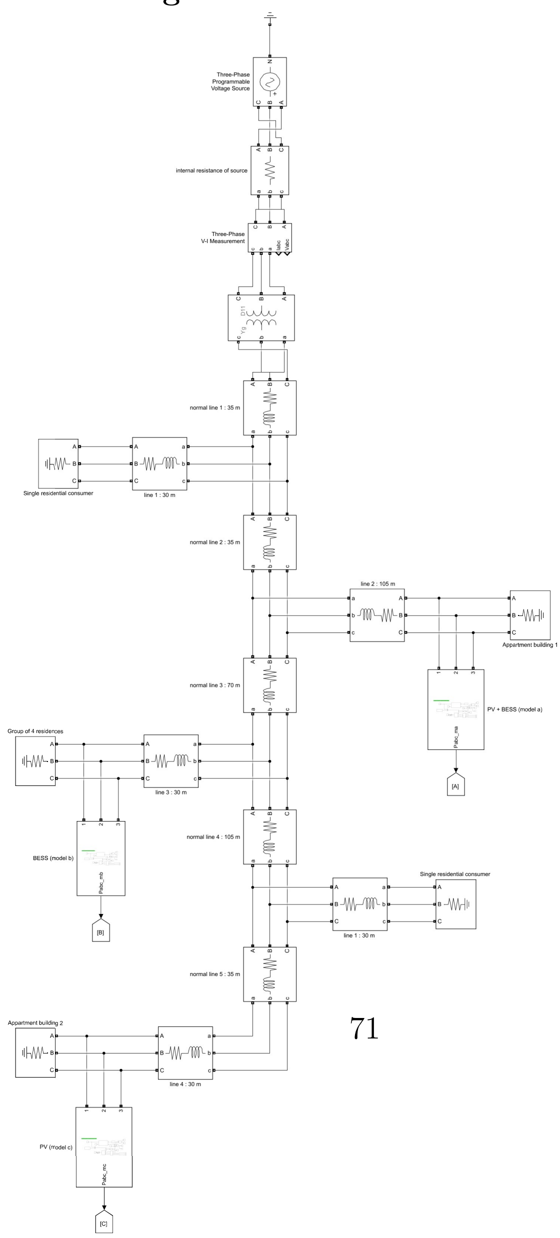

6.1.1 Results of chapter 4

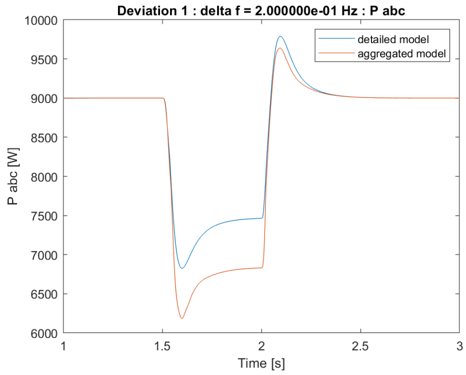

Power given for frequency deviation number 1

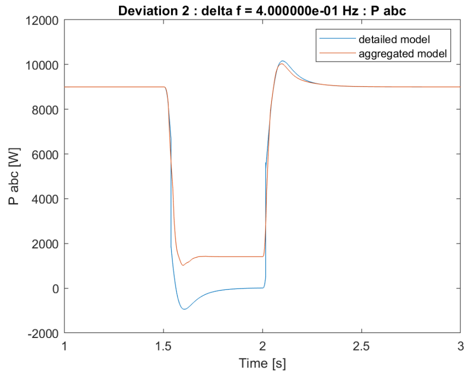

Power given for frequency deviation number 2

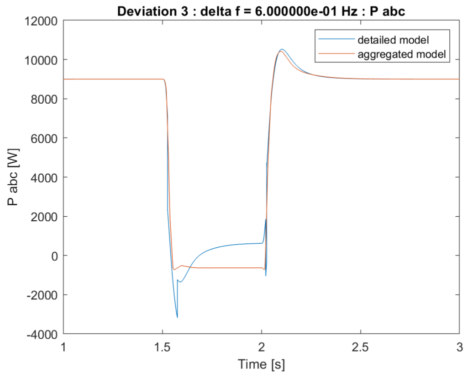

Power given for frequency deviation number 3

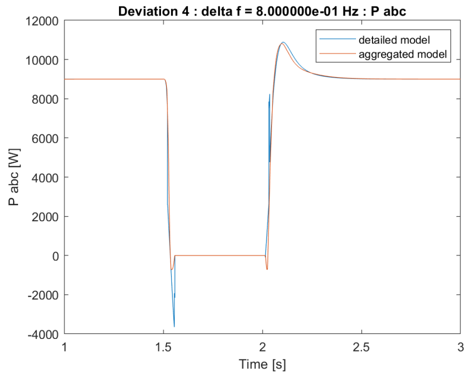

Power given for frequency deviation number 4

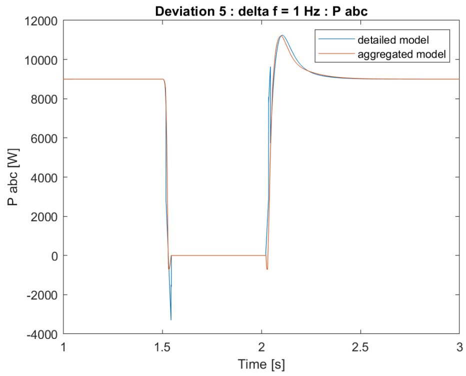

Power given for frequency deviation number 5

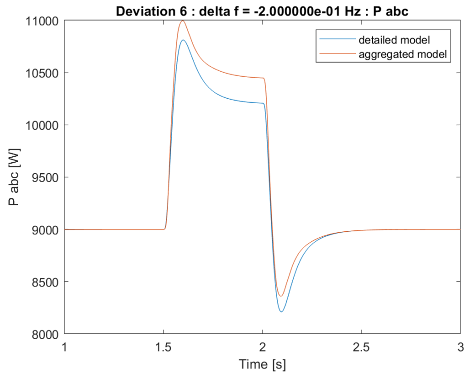

Power given for frequency deviation number 6

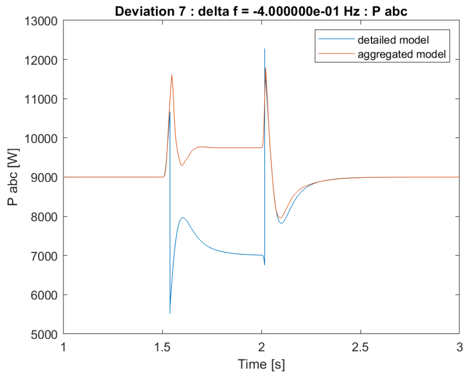

Power given for frequency deviation number 7

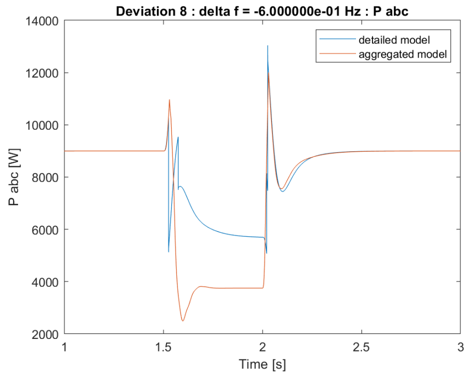

Power given for frequency deviation number 8

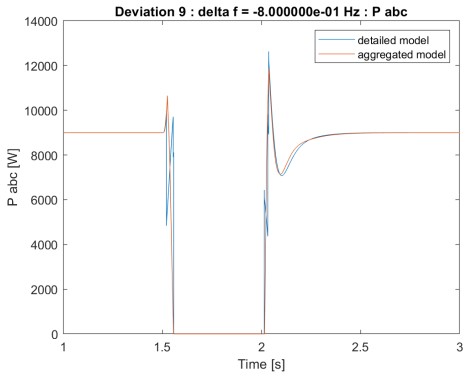

Power given for frequency deviation number 9

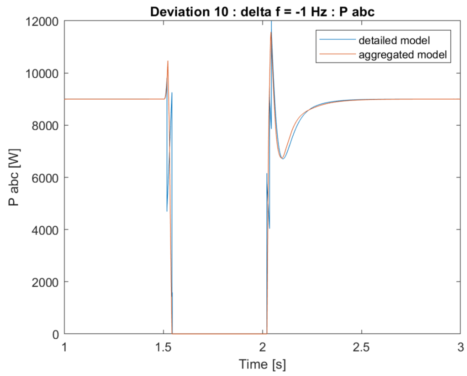

Power given for frequency deviation number 10

6.1.2 Results if all active components have the same frequency tolerance

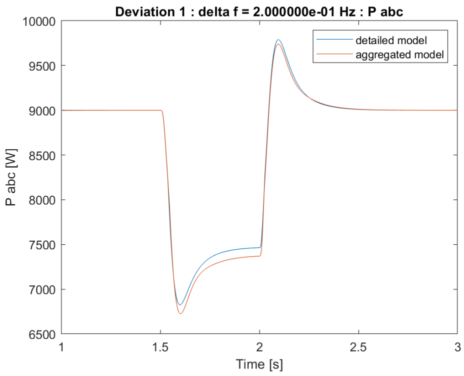

Power given for frequency deviation number 1

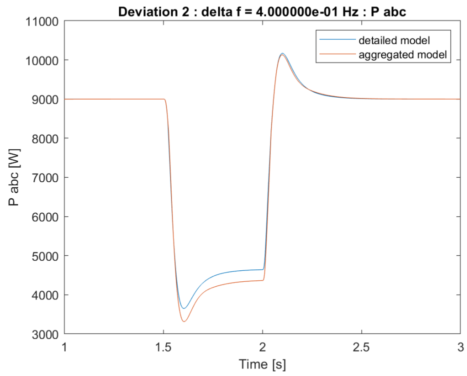

Power given for frequency deviation number 2

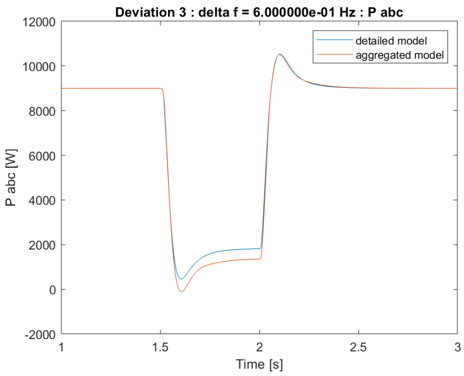

Power given for frequency deviation number 3

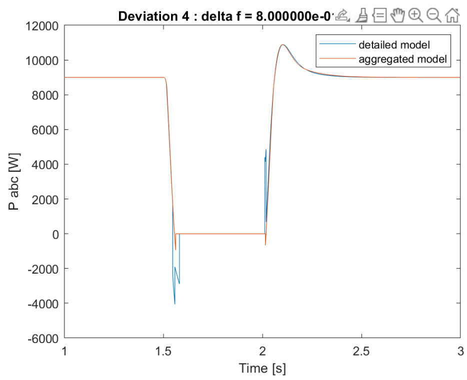

Power given for frequency deviation number 4

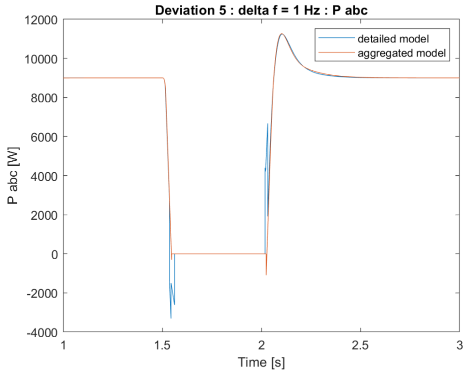

Power given for frequency deviation number 5

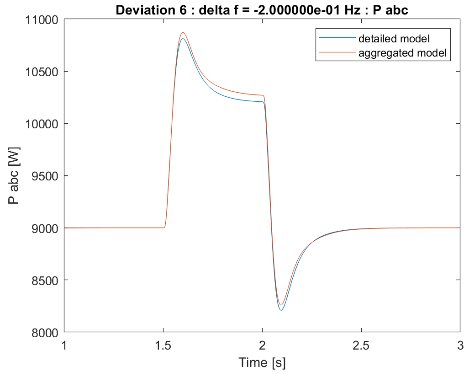

Power given for frequency deviation number 6

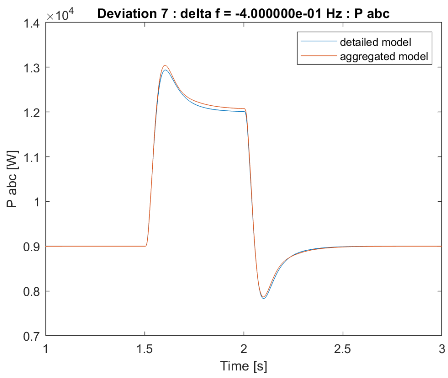

Power given for frequency deviation number 7

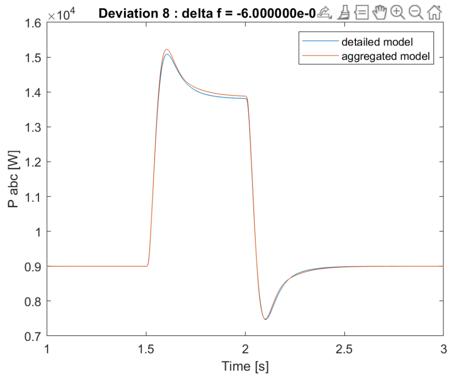

Power given for frequency deviation number 8

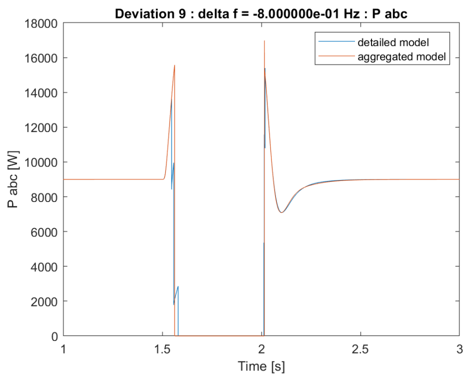

Power given for frequency deviation number 9

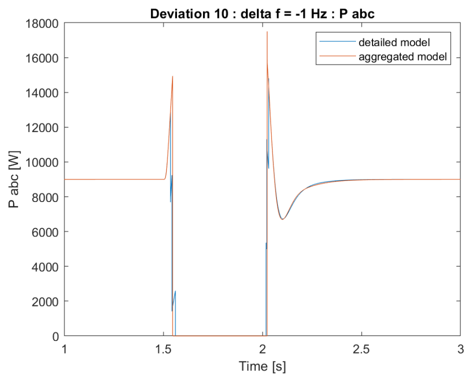

Power given for frequency deviation number 10

6.2 Appendix B

6.2.1 Results with the root mean square error

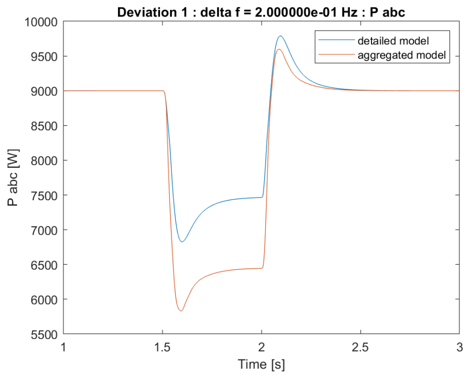

Power given for frequency deviation number 1

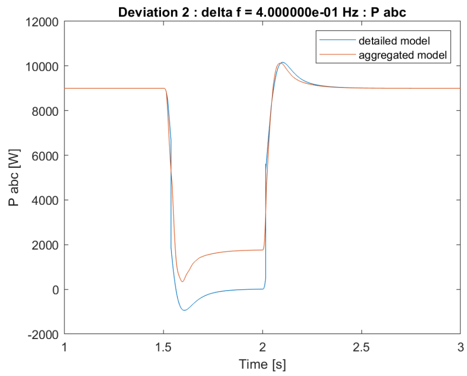

Power given for frequency deviation number 2

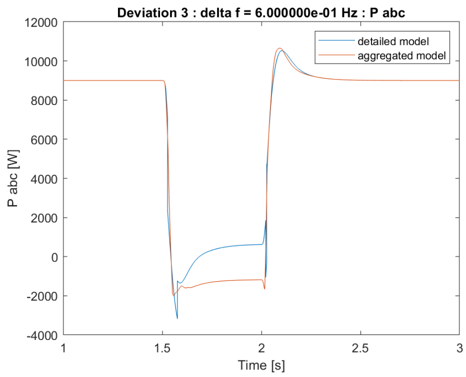

Power given for frequency deviation number 3

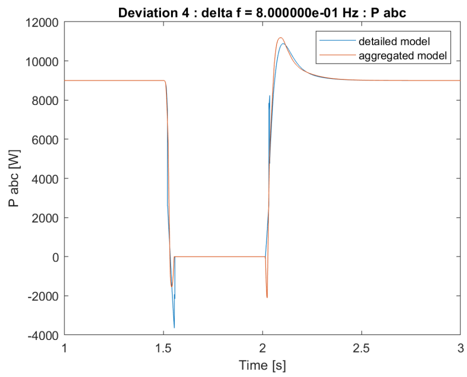

Power given for frequency deviation number 4

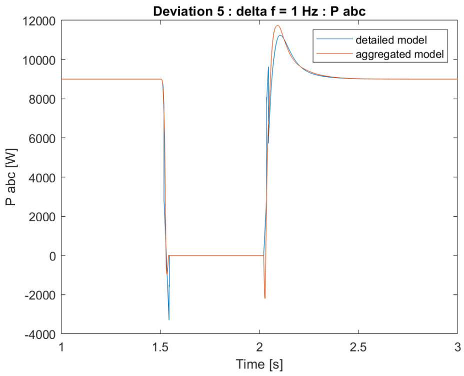

Power given for frequency deviation number 5

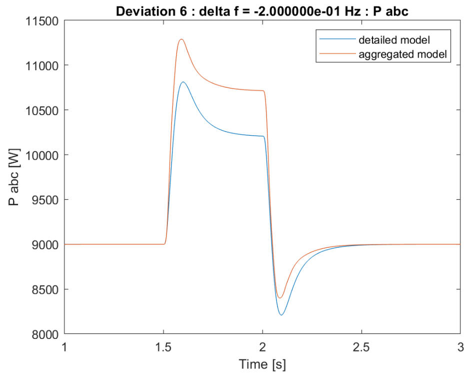

Power given for frequency deviation number 6

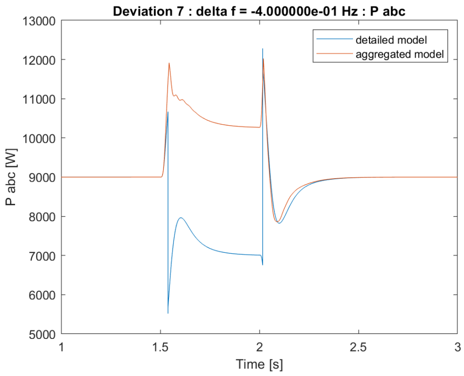

Power given for frequency deviation number 7

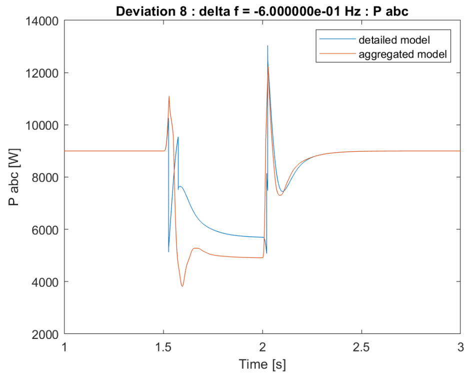

Power given for frequency deviation number 8

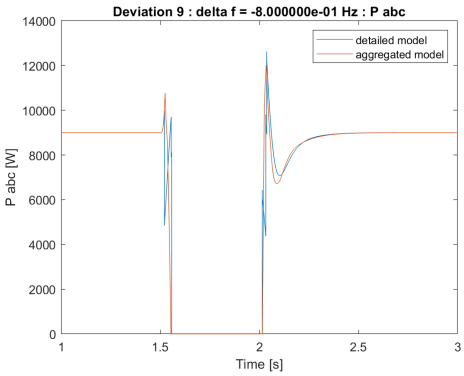

Power given for frequency deviation number 9

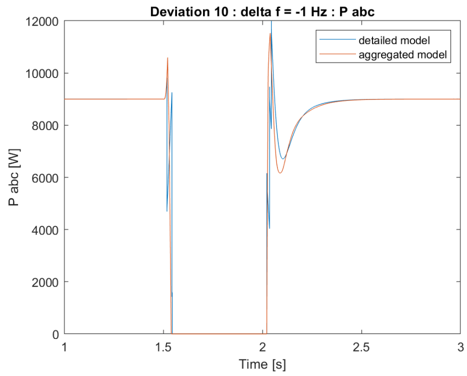

Power given for frequency deviation number 10

6.2.2 Results with the maximum error

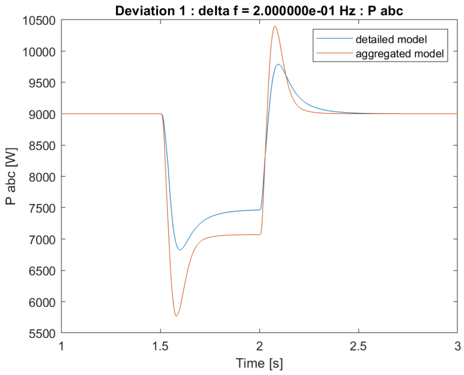

Power given for frequency deviation number 1

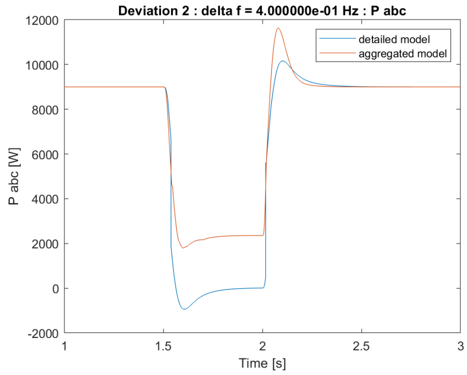

Power given for frequency deviation number 2

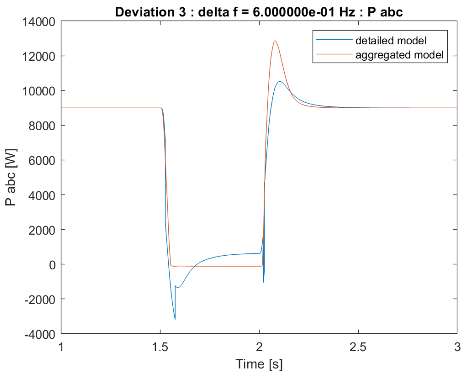

Power given for frequency deviation number 3

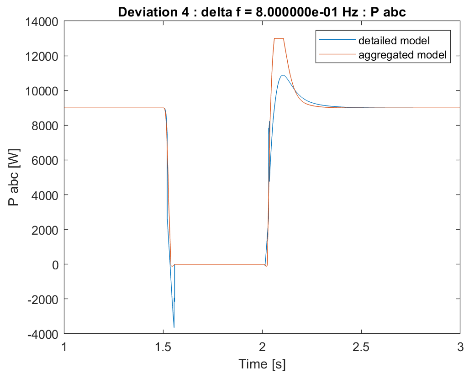

Power given for frequency deviation number 4

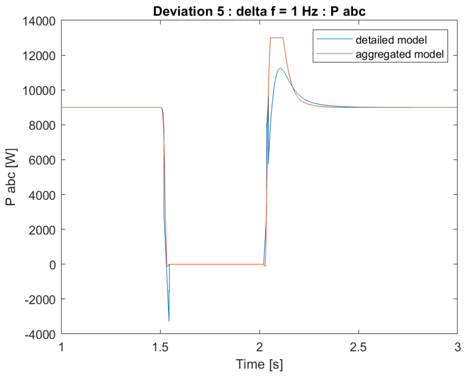

Power given for frequency deviation number 5

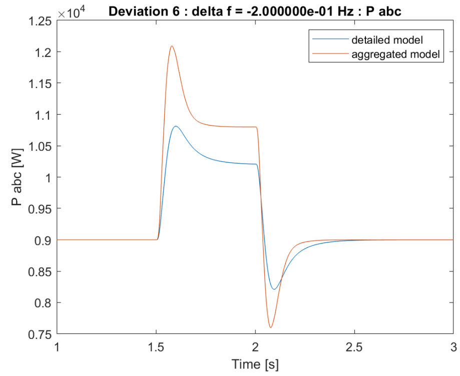

Power given for frequency deviation number 6

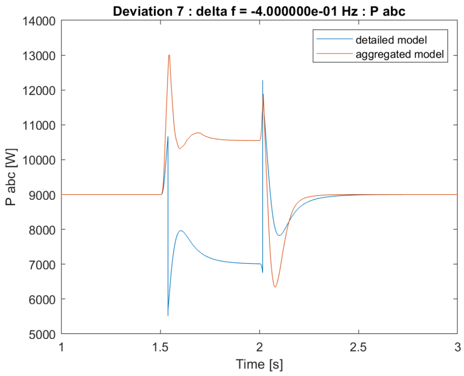

Power given for frequency deviation number 7

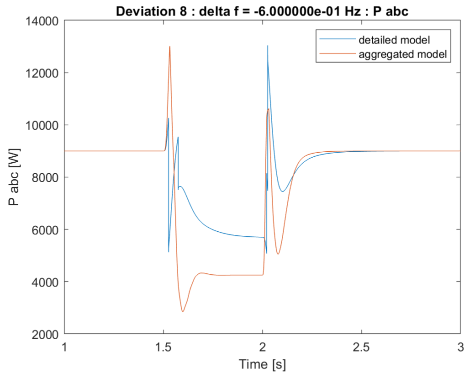

Power given for frequency deviation number 8

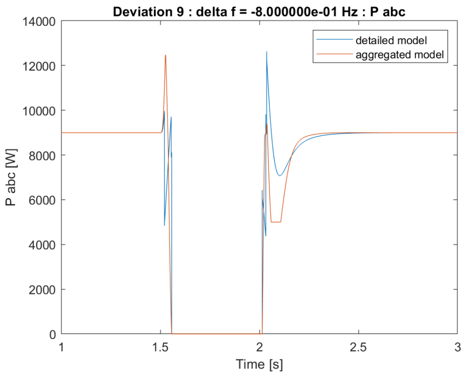

Power given for frequency deviation number 9

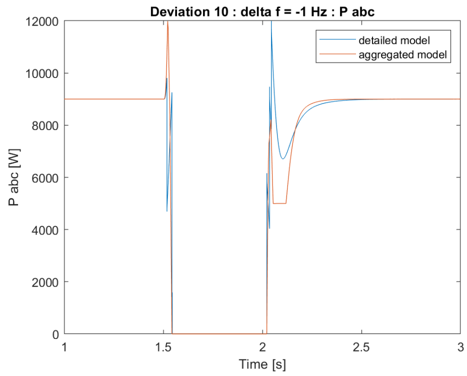

Power given for frequency deviation number 10

6.3 Appendix C

6.3.1 Results for training with all the parameters

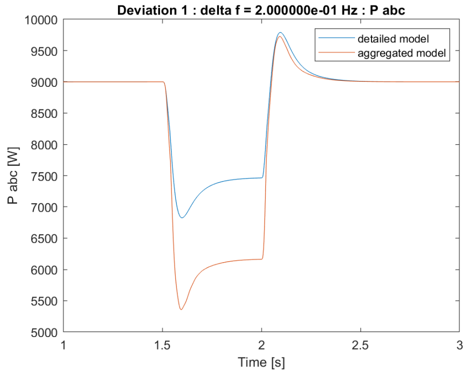

Power given for frequency deviation number 1

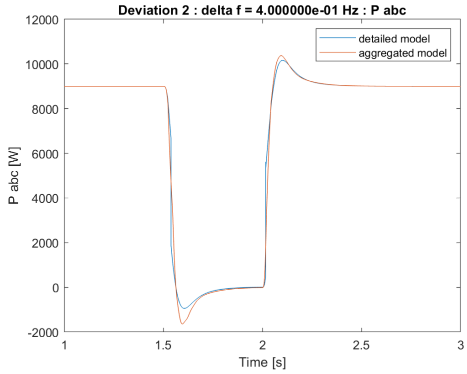

Power given for frequency deviation number 2

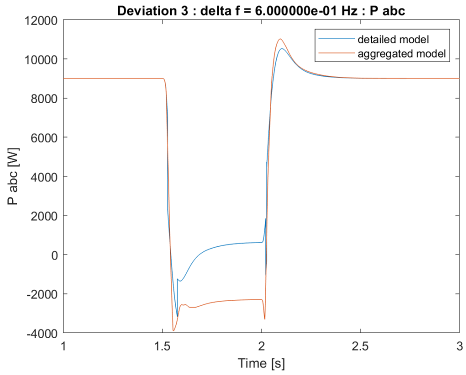

Power given for frequency deviation number 3

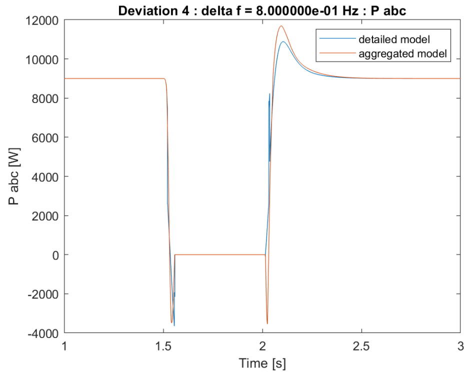

Power given for frequency deviation number 4

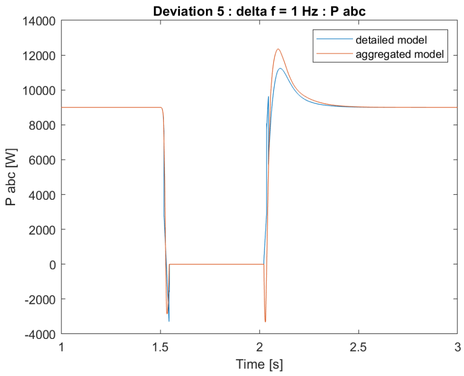

Power given for frequency deviation number 5

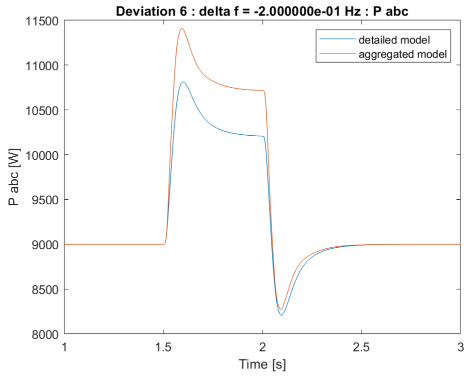

Power given for frequency deviation number 6

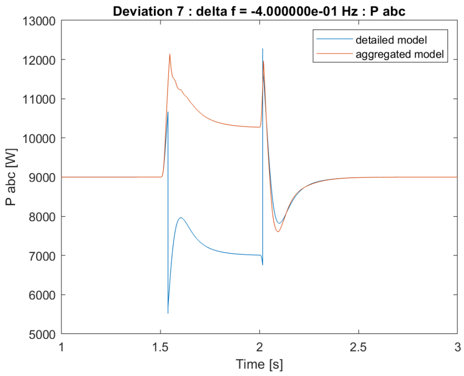

Power given for frequency deviation number 7

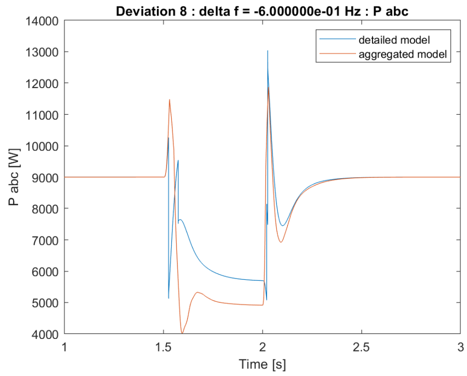

Power given for frequency deviation number 8

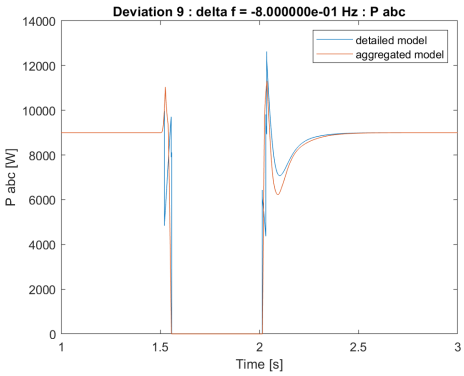

Power given for frequency deviation number 9

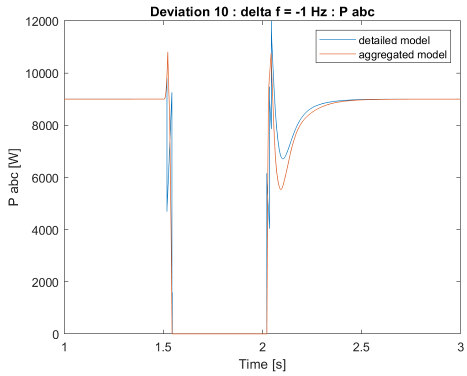

Power given for frequency deviation number 10

6.3.2 Results for training with only useful parameters

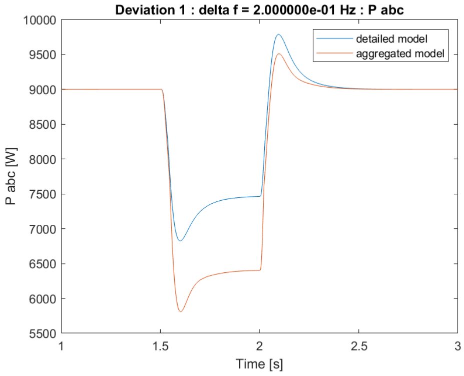

Power given for frequency deviation number 1

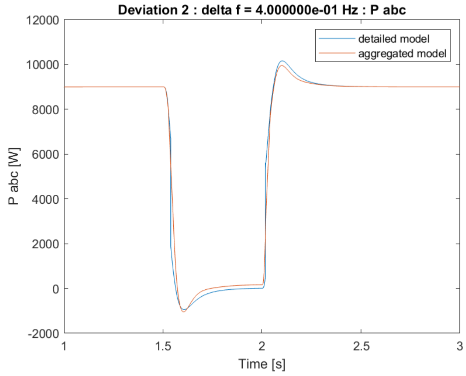

Power given for frequency deviation number 2

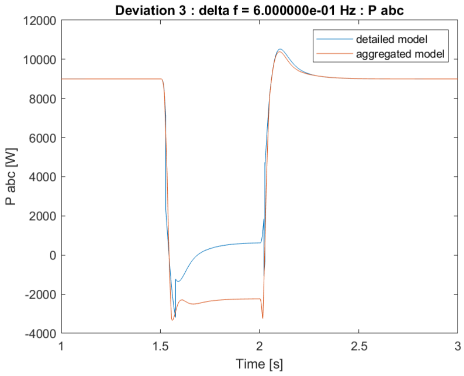

Power given for frequency deviation number 3

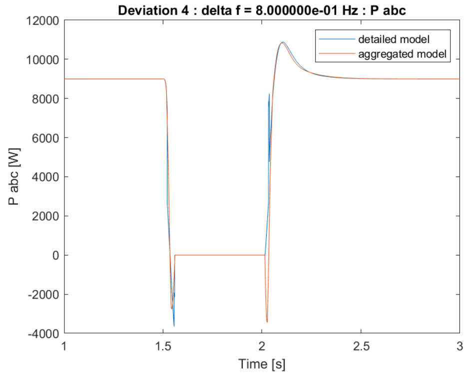

Power given for frequency deviation number 4

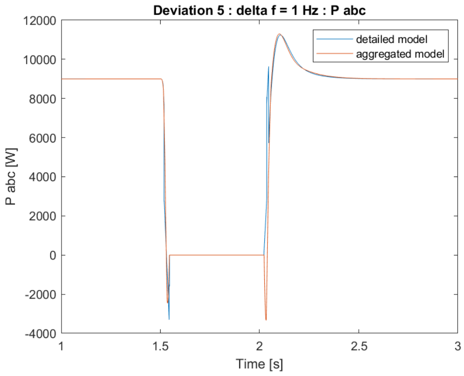

Power given for frequency deviation number 5

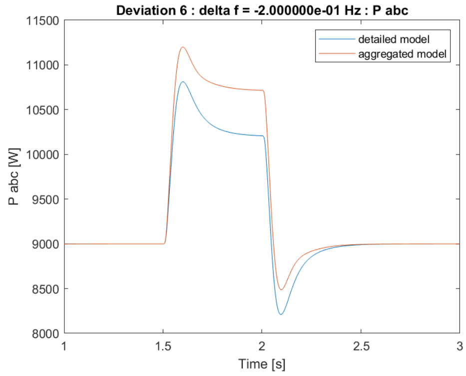

Power given for frequency deviation number 6

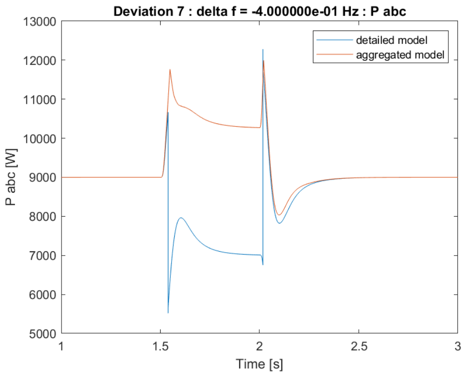

Power given for frequency deviation number 7

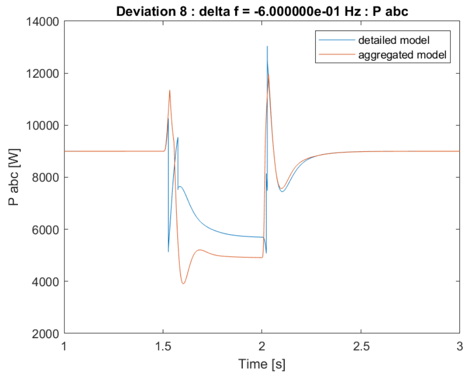

Power given for frequency deviation number 8

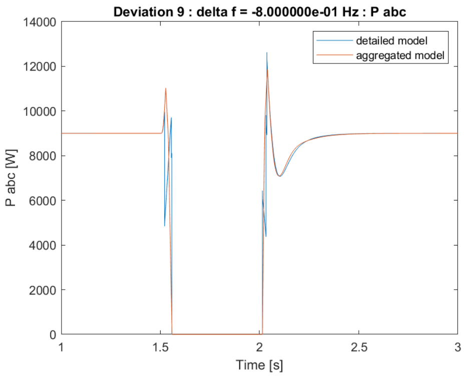

Power given for frequency deviation number 9

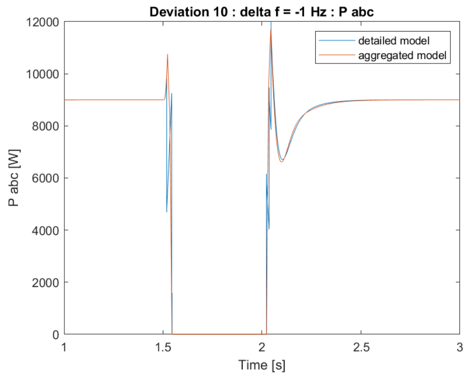

Power given for frequency deviation number 10

6.3.3 Results with extreme acceptable tolerance to frequency deviation

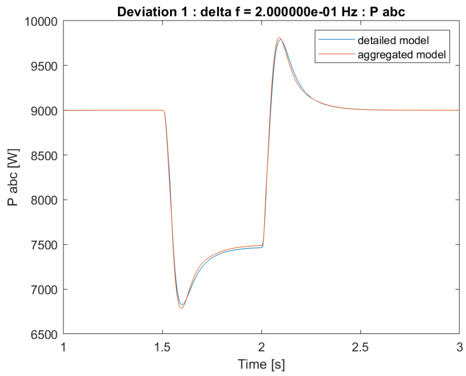

Power given for frequency deviation number 1

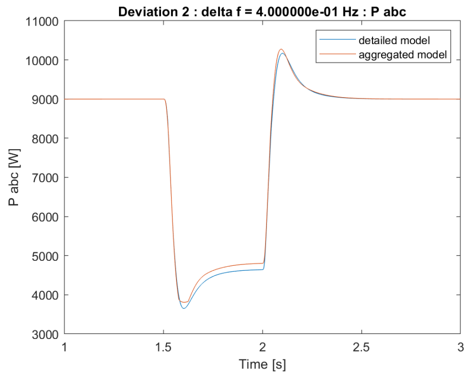

Power given for frequency deviation number 2

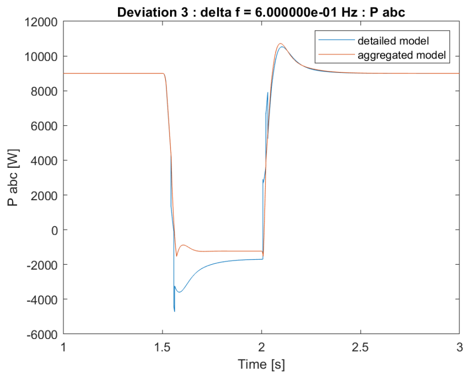

Power given for frequency deviation number 3

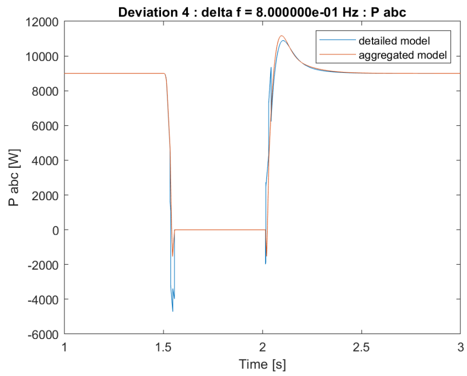

Power given for frequency deviation number 4

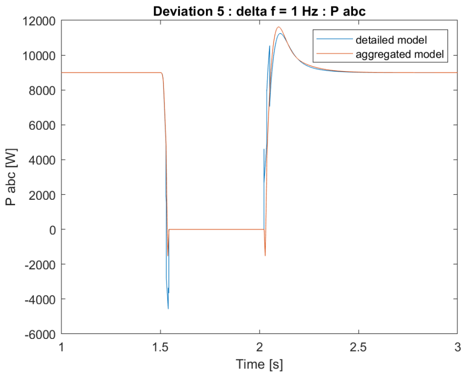

Power given for frequency deviation number 5

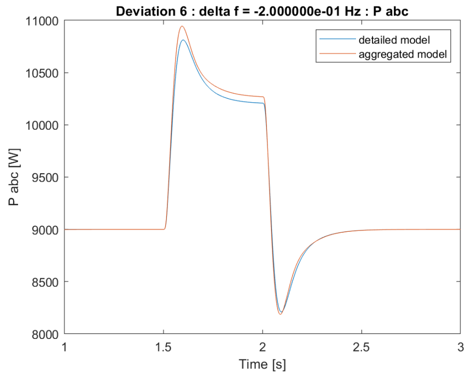

Power given for frequency deviation number 6

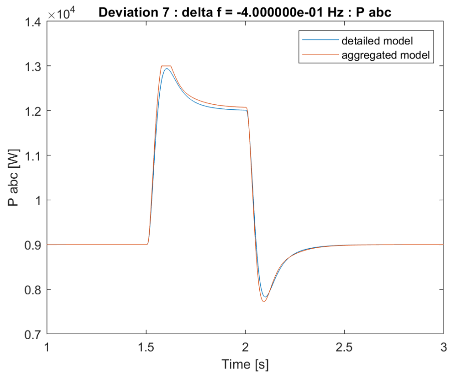

Power given for frequency deviation number 7

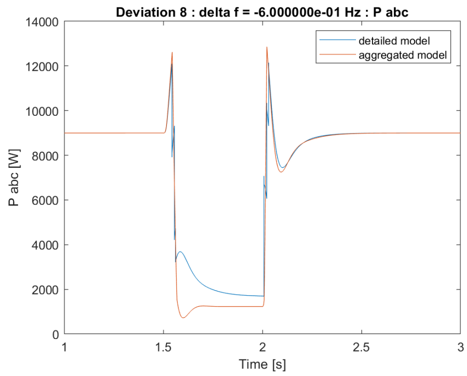

Power given for frequency deviation number 8

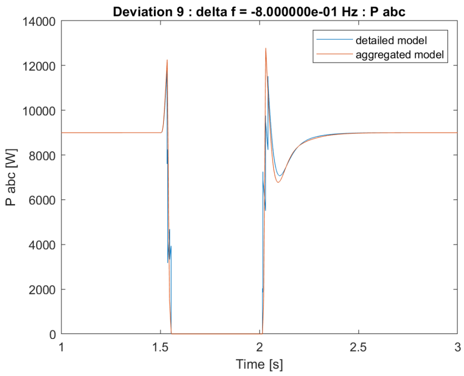

Power given for frequency deviation number 9

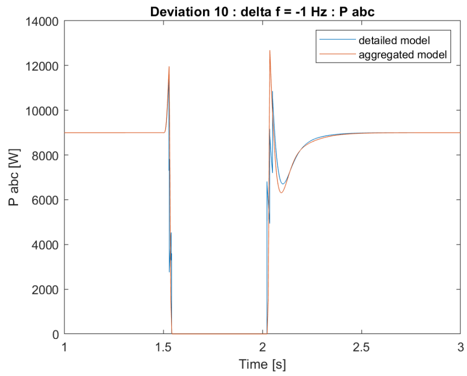

Power given for frequency deviation number 10

6.4 Appendix D

Detailed model of the grid with dynamic loads

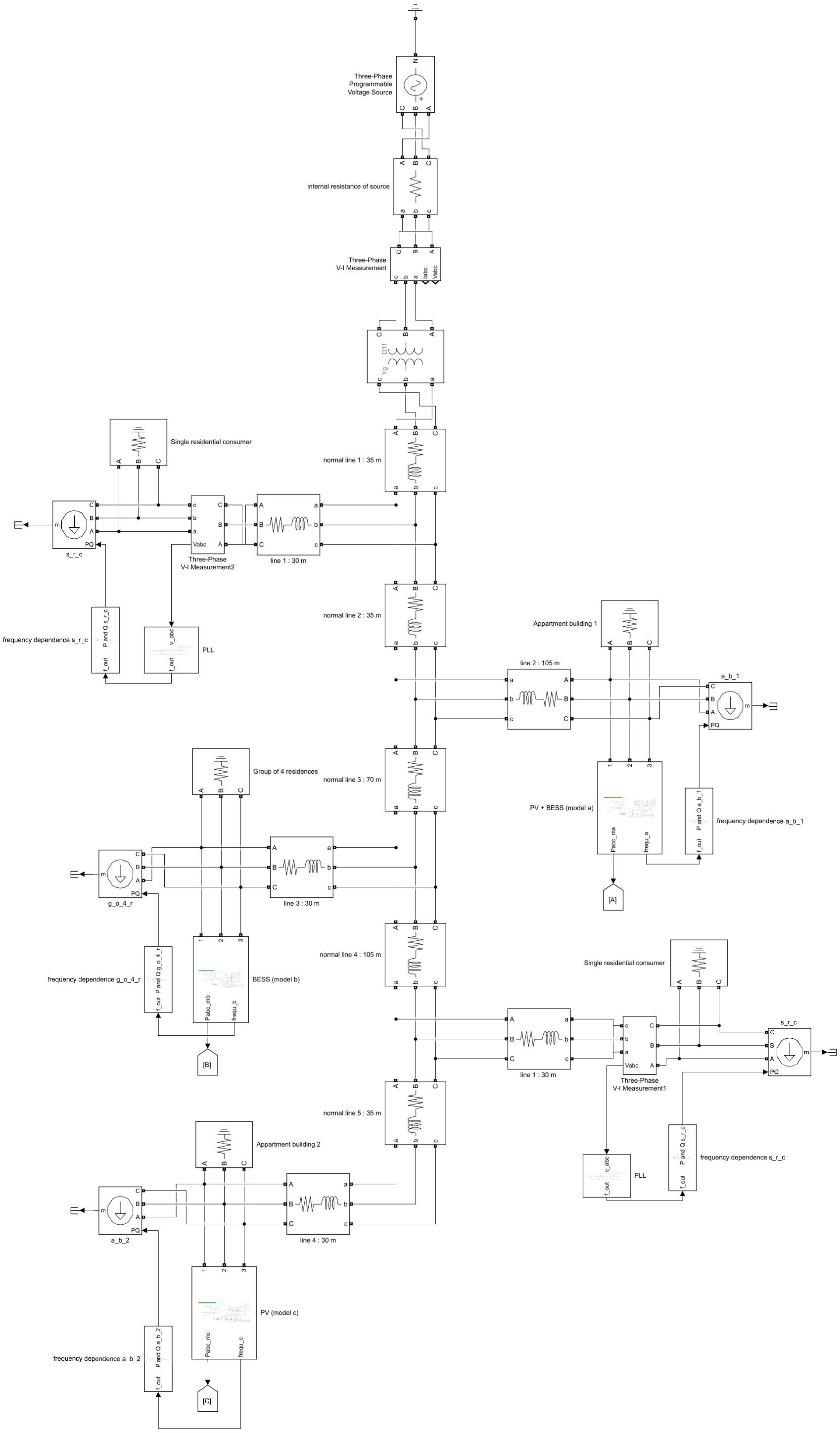

6.4.1 Results with dynamic loads

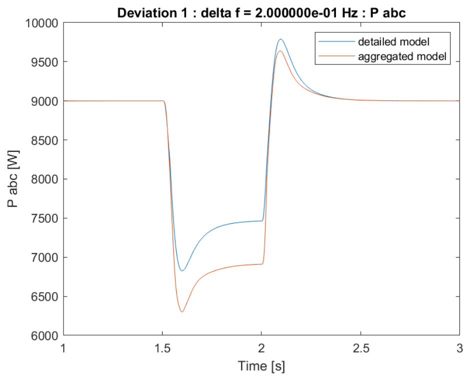

Power given for frequency deviation number 1

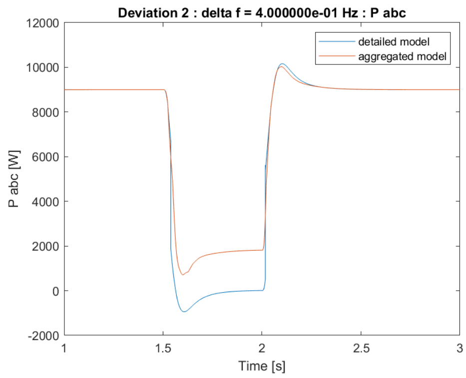

Power given for frequency deviation number 2

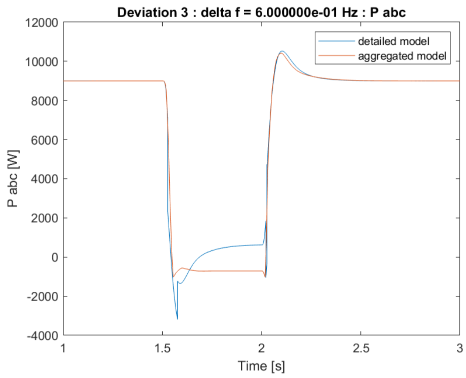

Power given for frequency deviation number 3

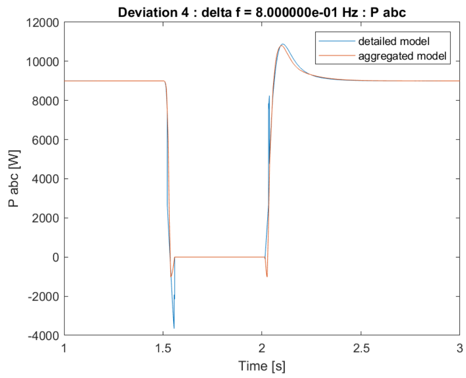

Power given for frequency deviation number 4

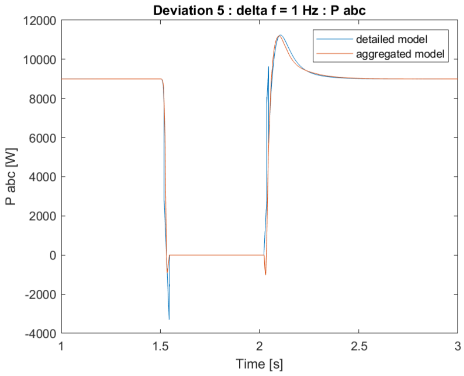

Power given for frequency deviation number 5

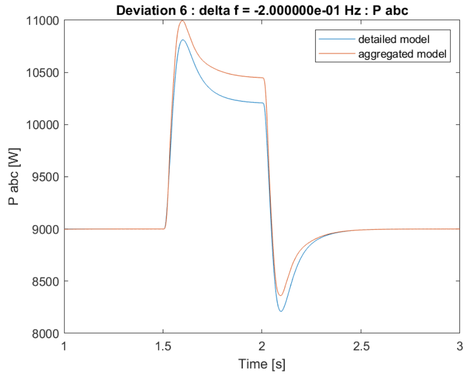

Power given for frequency deviation number 6

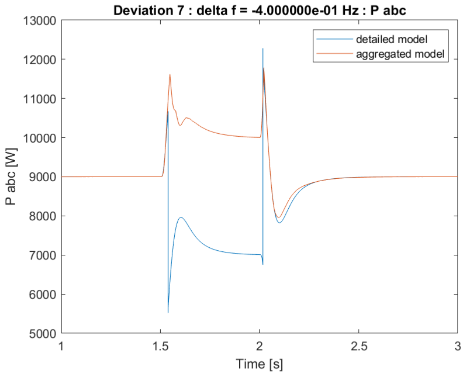

Power given for frequency deviation number 7

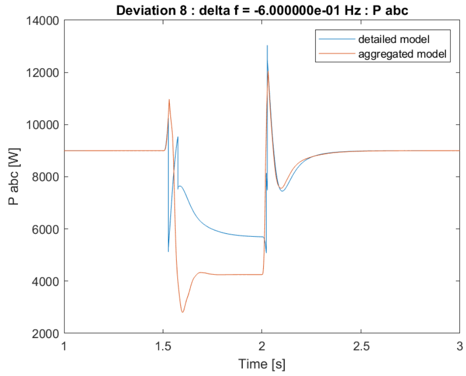

Power given for frequency deviation number 8

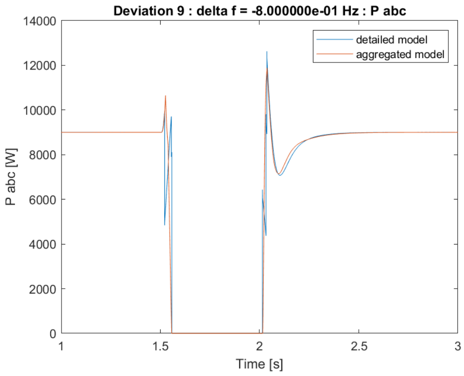

Power given for frequency deviation number 9

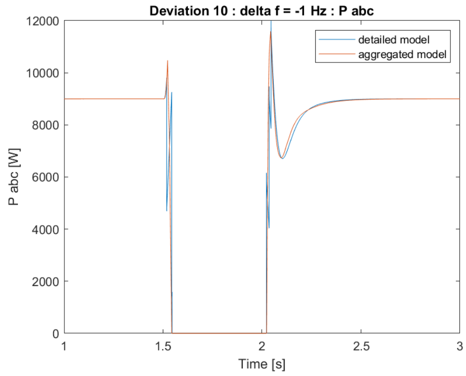

Power given for frequency deviation number 10

6.5 Appendix E

Detailed model of the more complex grid

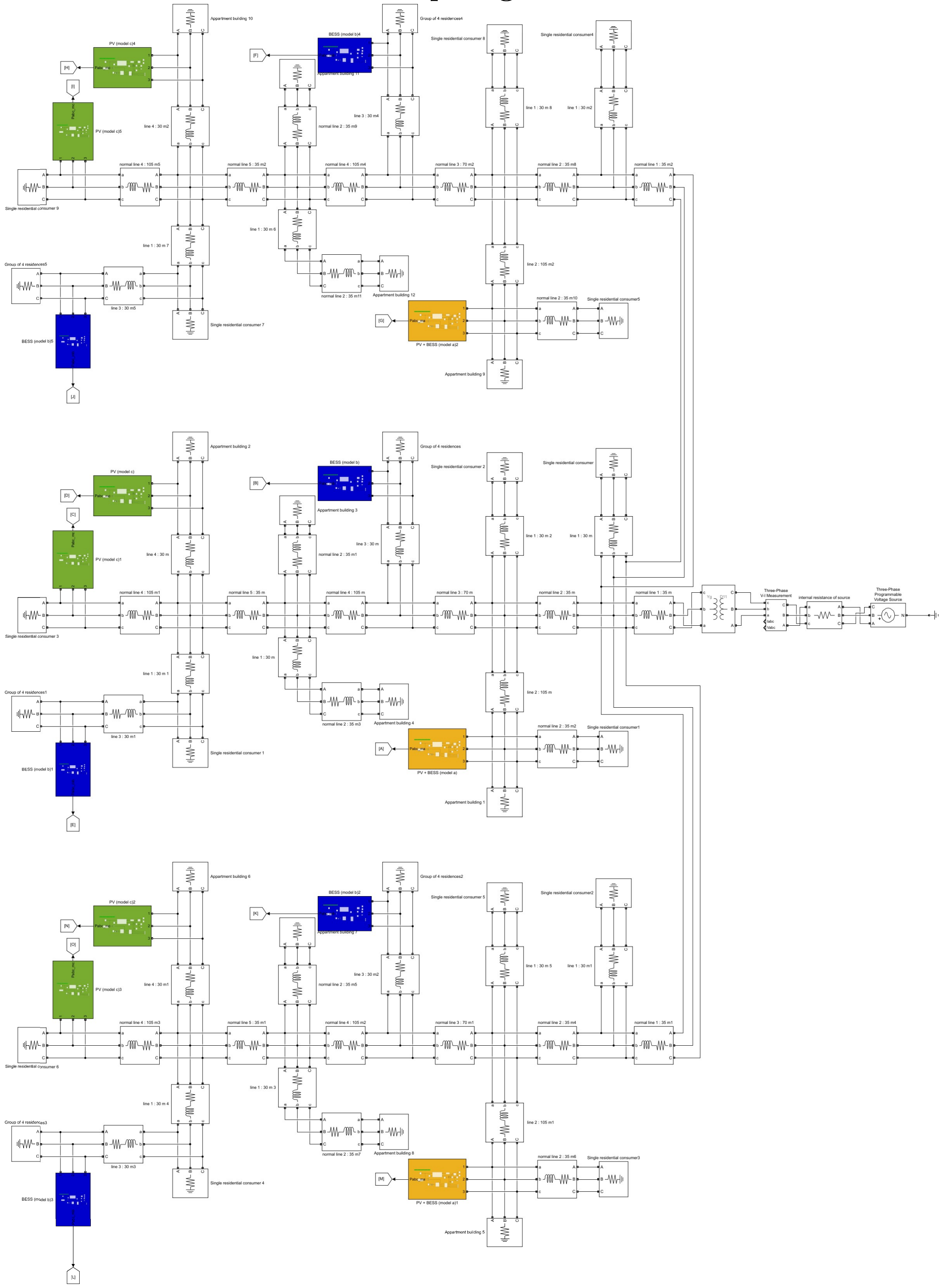

6.5.1 Results for a more complex grid

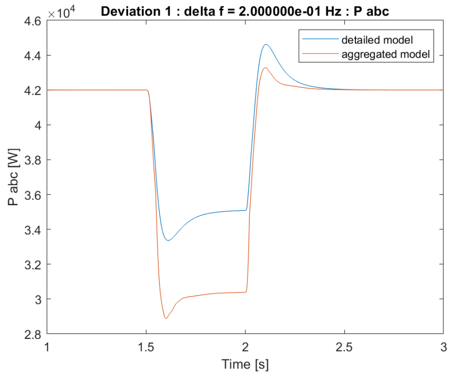

Power given for frequency deviation number 1

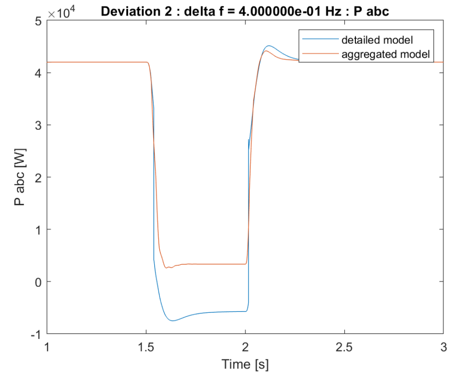

Power given for frequency deviation number 2

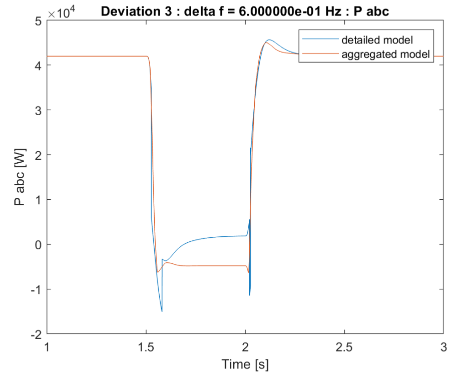

Power given for frequency deviation number 3

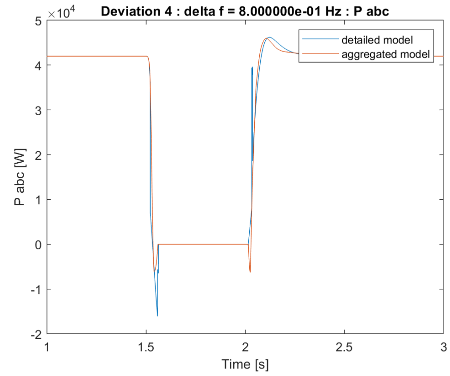

Power given for frequency deviation number 4

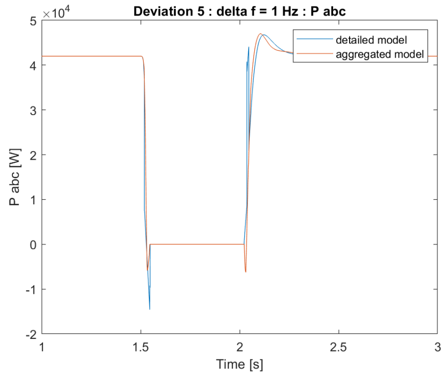

Power given for frequency deviation number 5

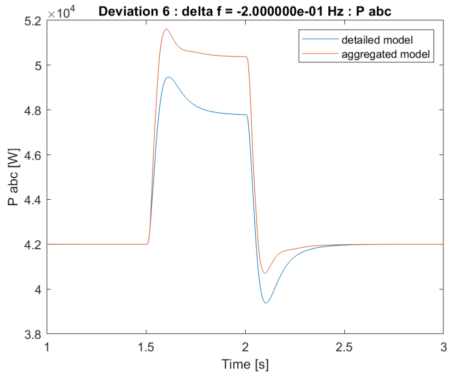

Power given for frequency deviation number 6

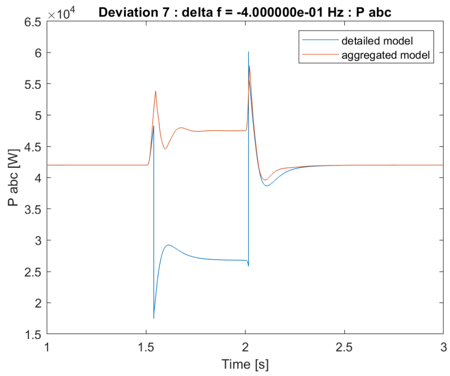

Power given for frequency deviation number 7

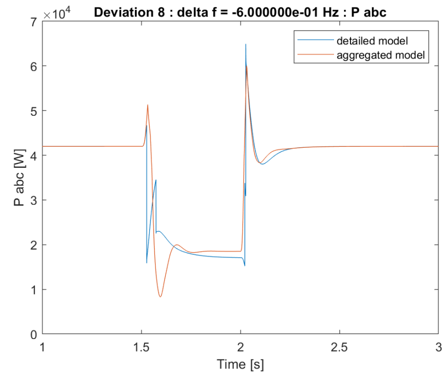

Power given for frequency deviation number 8

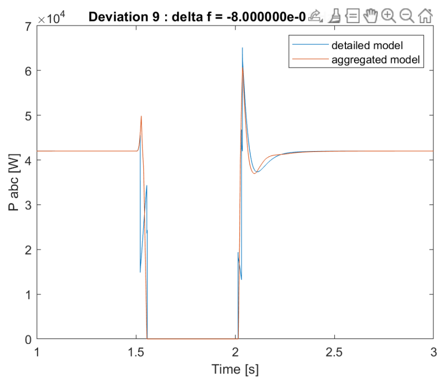

Power given for frequency deviation number 9

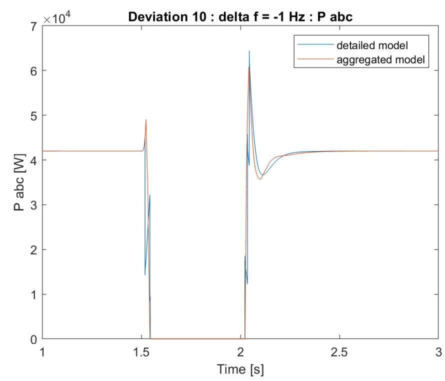

Power given for frequency deviation number 10

6.5.2 Results if all active components have the same frequency tolerance with a more complex grid

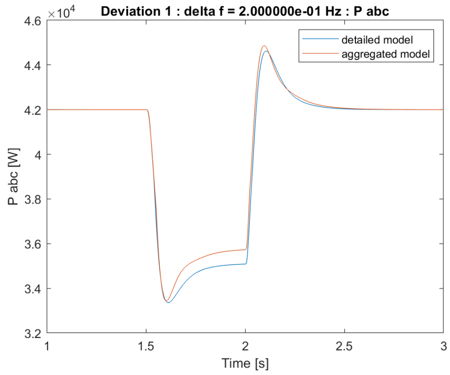

Power given for frequency deviation number 1

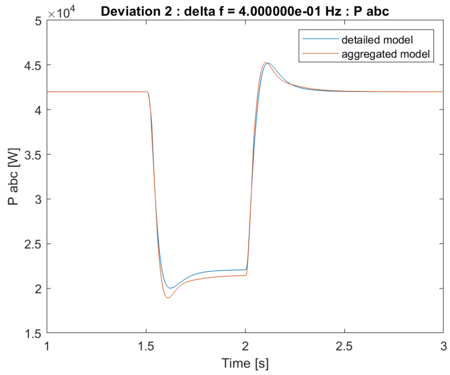

Power given for frequency deviation number 2

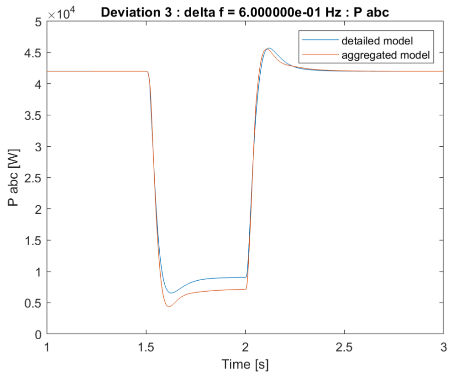

Power given for frequency deviation number 3

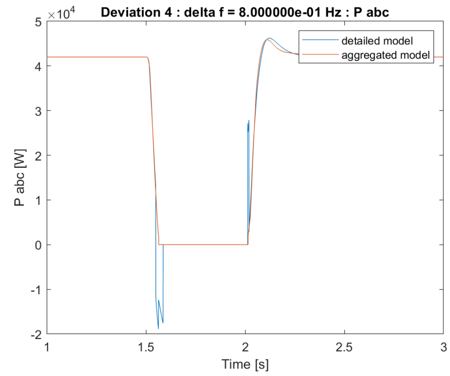

Power given for frequency deviation number 4

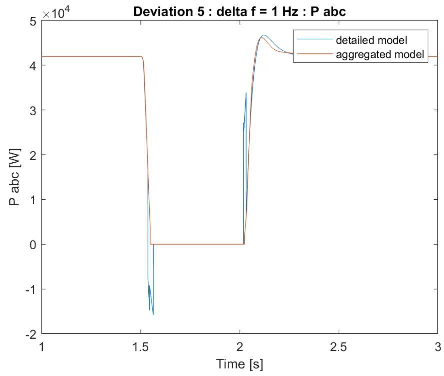

Power given for frequency deviation number 5

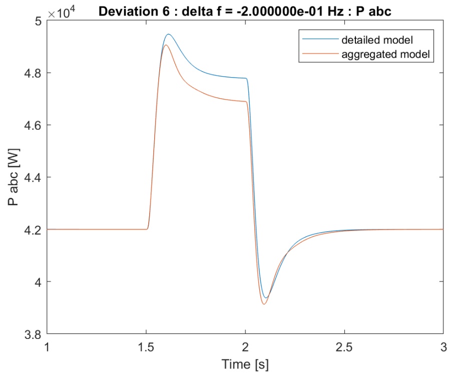

Power given for frequency deviation number 6

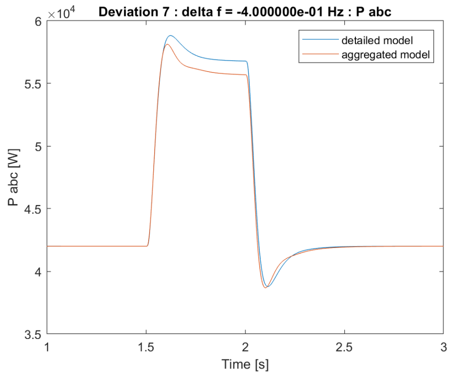

Power given for frequency deviation number 7

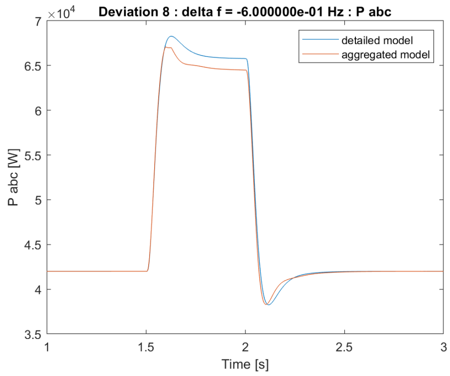

Power given for frequency deviation number 8

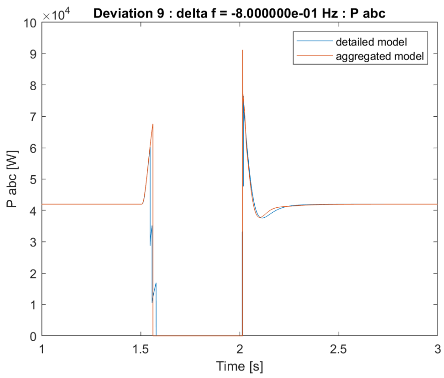

Power given for frequency deviation number 9

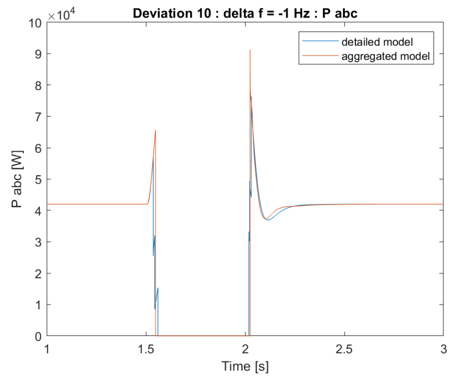

Power given for frequency deviation number 10

UNIVERSITÉ CATHOLIQUE DE LOUVAIN
École polytechnique de Louvain
Rue Archimède, 1 bte L6.11.01, 1348 Louvain-la-Neuve, Belgique | **www.uclouvain.be/epl**